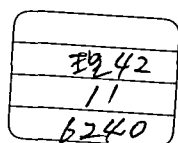| Title	STRUCTURE AND ELECTRICAL PROPERTIES OF SOLUBLE POLYDIACETYLENES
Author(s)	Se, Kazunori
Citation	大阪大学, 1983, 博士論文
Version Type	VoR
URL	https://hdl.handle.net/11094/24592
rights	
Note	

STRUCTURE AND ELECTRICAL PROPERTIES

OF

SOLUBLE POLYDIACETYLENES

A Doctoral Thesis Submitted to

The Faculty of Science, Osaka University

by

Kazunori Se

1983

CONTENTS

Chapter 1

INTRODUCTION

1-1. General Features of Highly Specialized Macromolecules

After vigorous pioneering work of Hermann Staudinger during 1930's, the macromolecular science has grown and been growing at a very rapid rate through early 1970's. Mark, Carothers, Ziegler, Natta, Flory, Szwarc and many others have contributed to the foundation of the modern science of macromolecules. With the progress in macromolecular science, macromolecular industries produced plastics, synthetic fibers, synthetic rubbers and numerous other macromolecular materials, which gave a good deal of wealth and happiness to mankind. We were in the age of chemistry. However, it appears to us that around the mid 70's, and since, the macromolecular science and industries reached their maturity or have been growing at a rather slow rate. Great efforts have been made to produce materials with more versatile utility of high performance and/or with new properties for special applications. Indeed, demand for developing highly specialized macromolecules is becoming more and more urgent. These special

function macromolecules must be those defined well in molecular design, be synthesized exactly, have a definite molecular architecture and show highly specialized physical properties.

In the present day we expect to develop various special functional macromolecules and to explore their applications in a variety of ways and purposes. There are four major goals for developing such functional materials. The first goal is to develop macromolecular membranes, which separate certain solutes from others in the mixture without accompanying a phase transition. The second one may be biomedical materials such as artificial organs. The third one is perfectly oriented macromolecular films having extremely high mechanical strength. The last one may be to develop functional materials in electrical and/or electronic applications. These four major groups of functional materials are interesting for us to study in the present day.

Among these varieties of functional materials, we concentrated our attention on the study on electrical properties of macromolecules, particularly with a hope of establishing the relationship between the electrical properties and characteristics of macromolecules.

1-2. Electrical Properties of Macromolecules

There are three areas of research in the field of the

electrical properties of macromolecules. The first area is related to (1) dielectric and related properties. Such a study is useful not only in developing non-conductive and low loss materials or dielectrics, but also in providing a powerful means of examining molecular dynamics such as the primary, side chain and local mode relaxation processes. [A1-A3] For this reason, studies on dielectric behavior form a desirable supplement to the studies on the molecular dynamics of macromolecular systems such as viscoelastic properties, nuclear magnetic relaxation, quasielastic scattering and many other relaxation phenomena.

The second area is related to (2) piezo- and pyro-electricity leading to explore new type of application of macromolecules as, for example, polymer electrets. [A4] This problem has been studied most extensively on poly-(vinylidene fluoride). [A4]

The last area is a relatively new field related to (3) electrical conductions in macromolecules. [A5-A7] The electric conductivities of macromolecular systems are very interesting on account of the following four aspects.

(i) The first aspect is that only conductive macro-molecules have possibility of becoming superconductors at room temperature, as suggested by Little. [A8] Superconduc-tion was first observed in metal at liquid helium temper-ature by Kammerlingh Onnes as early as in 1911. [A9] The phenomenon occurs when certain metals are cooled below

the characteristic transition temperature T_c. In this state currents flow without any resistance at all. Bardeen, Cooper and Schrieffer succeeded in explaining theoretically this phenomenon in 1957 using the model of Copper-electron pairs due to electron-phonon interactions.[A10] This theory called BCS theory predicted that the highest attainable T_c by any metals will be below about 40K. Experimental results showed that the T_c attained by all the superconductors based on metals and metal alloys are always below 20K. Little presented his theory on superconducting polymers based on the idea of electron pairs due to electron-exciton interactions in 1964.[A8] One of his most important conclusions was that a well defined macromolecule having a conjugated main chain such as polyene structure and polar side chains such as 1,1'-diethyl-4,4'-cyanine iodine might show superconduction at room temperature. All the attempts made so far for preparing such superconducting macromolecules were unfortunately unsuccessful. However, among several attempts in exploring organic superconductors, poly(sulfur-nitrogen)[A11] and certain charge-transfer complexes[A12] such as tetramethyltetraselenafulvalene (TMTSF) were found to become superconductors, although below liquid helium temperature.

(ii) The second feature is the anisotropy in electrical conductivity. Metals are three-dimensional conductors on account of their metallic bonds, extending in three

dimensions. Graphite is a two-dimensional conductor. Its plane consists of benzene-like conjugated bonds extending in two dimensions, and each planes are stacked by van der Walls interaction. Electrical conductivity in the plane is as much as 100 times larger than that in the direction perpendicular to the plane. On the other hand, macro-molecular conductors may be considered as one-dimensional conductors or linear-chain conductors [A13] on account of their conjugated backbones such as found in polyacetylene extending only in one dimension. Little's suggestion on the possibility of high temperature linear-chain conductors might be too optimistic. Nevertheless, the study on macro-molecular conductors itself is of interest as a subject of physics of low dimensional materials.

(iii) The third feature is easy processibility of macromolecules. Macromolecules may be molded into thin films or highly oriented fibrous specimens. Films made from macromolecular semiconductors may be utilized as solar cell materials and/or rechargeable organic batteries. Extremely thin films formed by casting dilute solution would permit an application as transistors and new types of sensing devices.

(iv) The last feature is the possibility of controlling the conductivity of macromolecular conductors in a very wide range by adequate chemical and physical means, such as demonstrated by Shirakawa et al. for polyacetylene by

chemical doping in 1978.[A14, A15] The range of electrical conductivity observed in varieties of materials covers 25 decades in magnitude. Such a wide range covered by the conductivity is perhaps the widest range of the property change, which cannot be found in any other material properties. Polyacetylene, originally an insulator, doped with halogens or AsF_5 was found to exhibit metallic conductivity as well as n-type and p-type semiconductivities. Figure 1-1 shows the range of conductivity of materials as compared with those of organic as well as macromolecular substances.

For these reasons mentioned above, we were motivated to study mainly the conductivity of macromolecules, although dielectric and piezo- and pyroelectric properties of macromolecules are also interesting and important.

1-3. Polydiacetylenes

A well known example as a conductive macromolecule is polyacetylene doped with halogens or AsF_5. Polyacetylene is one of the simplest organic macromolecules having conjugated π-electron backbones. However, because of the insolubility and infusibility of polyacetylene, it was difficult to characterize this macromolecule in regard to molecular weight and its distribution without some laborious

Conductivity $(\Omega^{-1}cm^{-1})$

Metal

10^6 — — GRAPHITE/AsF$_5$

Copper
Silver

Bismuth 10^4 — — $[CH(AsF_5)_{0.14}]_x$

$(SN)_x$

10^2 — — TTF/TCNQ

$(CH)_x AsF_5$

InSb 10^0 — — GRAPHITE

Germanium 10^{-2} — — Ionene TCNQ complex

Semi-
conductors 10^{-4} — —

Silicon 10^{-6} — — Trans(CH)$_x$

Cadmium
Sulphide 10^{-8} — —

10^{-10} — — Cis(CH)$_x$

10^{-12} — —

Insulators

Nylon

Diamond 10^{-14} — —

Sulfur 10^{-16} — — Teflon

polyester

10^{-18} — — polystyrene

Quartz
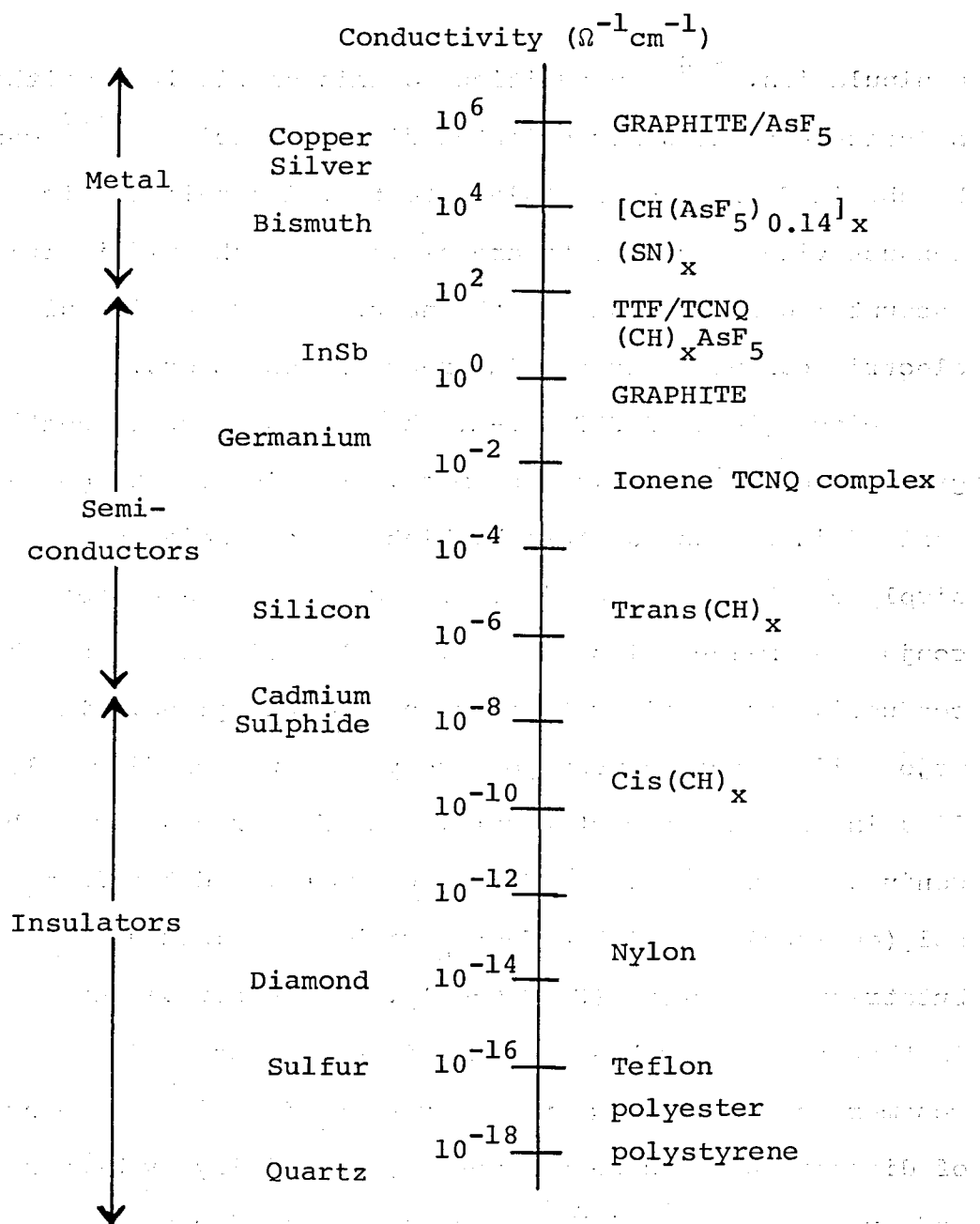
Figure 1-1. The conductivities of materials at room
temperature: chemical elements and common compounds in
the left hand side of this figure; graphite intercalation
compounds, charge transfer compounds and macromolecules
in the right hand side.

manipulation.[A16]   In addition to this difficulty, neither solvent-cast films nor oriented fibrous specimens [A17] can be obtained from polyacetylene to test its anisotropic conductivity.   Such facts are examples of the difficulties encountered in elucidating the nature and mechanism of electric conductivity of linear-chain conductors.

Diacetylenes $R-C\equiv C-C\equiv C-R$, where R is a substituent group, are a unique class of monomers which can be polymerized in the solid state by high energy radiation or simply by thermal annealing.   Polydiacetylenes possess conjugated main-chains, and may exhibit electric- and photo-conductivities similar to those of polyacetylene.   The major difference between polyacetylene and polydiacetylenes lies in the backbone structure.   The former possesses the conjugated ethene type $(CH=CH)_n$ backbone, and the latter poly(ene-yne) type $(CR-C\equiv C-CR)_n$ with an admixture of the butatriene structure $(CR=C=C=CR)_n$.   The other difference is that the latter has two substituent groups R in the monomer unit.   Although the polymerization of a large number of diacetylenes has been reported, especially by Wegner [A18] and by Baughman, [A19, A20]   most of the products were insoluble and infusible, and hence not feasible for molecular characterization.

Recently, Patel et al. succeeded in synthesizing several polydiacetylenes, in which

$$R = (CH_2)_n - O - \overset{\overset{O}{\|}}{C} - \overset{\overset{H}{|}}{N} - CH_2 - \overset{\overset{O}{\|}}{C} - O - (CH_2)_m - CH_3$$
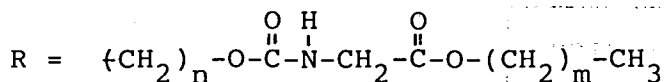
with n = 1-4 and m = 1 and 3. [A21, A22] They referred to

these new class of diacetylenes as nACMU (standing for n-methyl

alkoxy carbonyl methylurethane; the side chain) and the

polymer as poly(nACMU). [A21, A22]

Because the conjugated main chain is surrounded by

the bulky side groups, poly(nACMU) is fusible and soluble

in common organic solvents. Therefore, poly(nACMU)s could

be a convenient model of linear-chain conductors to study

the relationship between molecular characteristics and

electrical conductivity. Therefore, we selected them as

a working material for this study on linear-chain conductors.

1-4. Scope and Outline of This Dissertation

A key problem to be solved is undoubtedly to elucidate

the mechanisms of electric conduction and of enhancing

the conductivity of polymer conductors by doping. In order

to solve this problem we attempted first to elucidate the

relation between structure and conductivities.

Figure 1-2 shows a prospect of this research on

macromolecular conductors. As the first step in this study,

we choose a convenient model of linear-chain conductors,

```
  ┌──▶
  ├──▶  ┌─────────────────────┐
  ├──▶  │  1) DESIGN          │
  ├──▶  └─────────────────────┘
  │              │        a) Monomer
  │              │        b) Polymer
  │              ▼        c) Material
  │        ┌─────────────────────┐
  └────────│  2) STNTHESIS       │
           └─────────────────────┘
                  │        a) Monomer
                  │        b) Polymer
                  ▼        c) Film
                           d) Chemical Doping
           ┌─────────────────────┐
  ┌────────│  3) CHARACTERIZATION │
  │        └─────────────────────┘
  │              │        a) Molecular Characterization
  │              │           M_n, M_w, [η], et al.
  │              ▼        b) Material Characterization
  │                          X_c, T_g, X-ray, Raman, UV, et.al.
  │        ┌─────────────────────┐
  └────────│  4) CONDUCTIVITY     │
           └─────────────────────┘
                  │        a) Dependence on Applied Potential,
                  │           Time, Dopant Concentration and
                  │           Temperature
                  ▼        b) Ionic or Electronic Conduction
                           c) Mechanism of Conduction
           ┌─────────────────────┐
  └────────│  5) APPLICATION      │
           └─────────────────────┘
                           a) Semiconductor Devices
                           b) Sensors
```
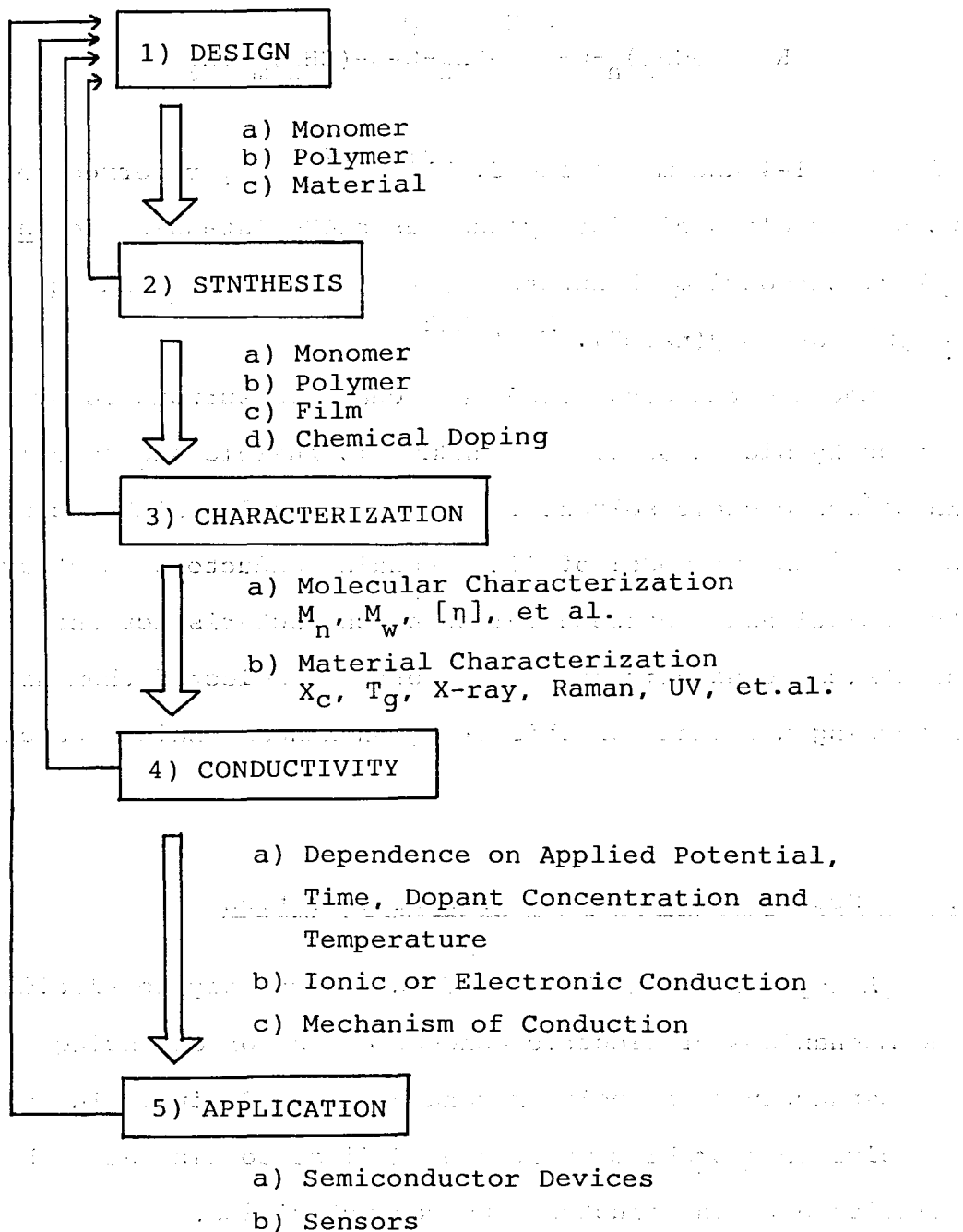
Figure 1-2. A prospect of the research procedure for polymer conductors.

which satisfy the requirements as much as possible to solve the given problems. This step, which involves the monomer, polymer and material designs, is of importance in starting a new research. We selected poly(nACMU)s as a model for the reasons mentioned in the previous sections.

As the second step in this study, we synthesized five different polydiacetylenes of poly(nACMU) type and subjected the products to molecular characterization.

As the third step, we carried out a structural study in the following two ways. One was solution-properties to reveal the conformations of an individual polymer chain. The other was bulk properties to elucidate the state of aggregation of the polymers. A structural analysis by X-ray diffraction was also conducted.

As the fourth step, we studied the conductivity of poly(nACMU)s in various forms such as solvent cast films, single crystals, partially oriented films, and KOH hydrolyzed specimens. It is important to estimate the material parameters which affect the conductivity and its activation energy. Taking the relation between the structure and electrical properties of poly(nACMU)s into account, we attempted to elucidate the mechanisms of the electric conduction.

As the last step, we examined the applicability of poly(nACMU)s as semiconductor devices such as rectification devices.

As shown in Figure 1-2, all these knowledges acquired would further stimulate the design and production of new materials, which in turn would enable us to reach deeper understanding on the relationships between structure and electrical properties. The understandings would eventually open up a new field of application of such materials.

This thesis consists of following six chapter. Chapter 1 is the Introduction. Chapter 2 is devoted to describe the preparation and characterization of some poly(nACMU)s. Our aim is to obtain well-defined or pure poly(nACMU) samples with negligible ammounts of impurities such as catalyst of polymerization. For this purpose, we used solid-state polymerization technique with ^{60}Co-γ irradiation.

Chapter 3 treats the phenomena of characteristic color changes exhibited by nACMU and poly(nACMU). Since the conjugated main chains of polydiacetylenes absorb visible light, poly(nACMU)s exhibit unique color changes in solution, reflecting the change in main-chain confor-mation. We study these phenomena in some detail. Chapter 4 treats the problem of complex formation on the bulk properties. Especially we paid our attention to study the difference in the bulk structure and properties before and after doping by measuring visible absorption spectra, Raman spec-tra, X-ray diffraction, differential scanning calorimetric thermograms, dynamic viscoelastic and dielectric spectra.

Chapter 5 treats the electrical properties of poly-
(nACMU)s having different substituent groups, molecular
weights and their distributions. Particularly, we studied
in this chapter the dependences of their electric conduc-
tivities on the molecular characteristics as well as on
the external variables such as applied potential, time,
dopant concentration and temperature. We attempted to
formulate the conductivity of doped poly(nACMU) system
by employing these parameters and to discover the predom-
inant parameter contributing to enhancement of the
conductivity. To this end, it is necessary to know whether
the conduction mechanism is ionic or electronic. Finally,
chapter 6 treats the application of poly(nACMU)s to semi-
conductor devices. We attempted to explore the possibility
of preparing photoconductive device, rectification device
and sensor from polydiacetylenes.

References

A1. McCrum, N. G.; Read, B. E.; Williams, G., "Anelastic
     and Dielectric Effects in Polymer Solid", John Wiley
     and Sons, Ltd., New York, 1967.

A2. Se. K.; Adachi,K.; Kotaka, T. Polymer J., 1981, 13,
     1009.

A3, Blythe, A. R.,; "Electrical Properties of Polymers",
     Cambridge Univ. Press., 1979.

A4. Turnhout, J., "Thermal Stimulated Discharge of Polymer
     Electrets", Elsevier Scientific Publ. Comp., New York,
     1975.

A5. Shirakawa, H.; Yamabe, T., Ed., "Gosei Kinzoku
     (Synthetic Metals)", Kagaku Dojin, Kyoto, 1980.

A6. Seanor, D. A., Ed., "Electrical Properties of
     Polymers", Academic Press, New York, 1982.

A7. Mikawa, H.; Kusabayashi, S., Ed., "Kobunshi Handotai
     (Polymer Semiconductors)", Kohdansha, Tokyo, 1977.

A8. Little, W. A. Phys. Rev., 1964, 134, 1416.; Davis, D.;
     Gutfreund, H.; Little. W. A. Phys. Rev. 1976, B13,
     4766.

A9. Onnes, H. K. Akad. van Wetenschappen (Amsterdam),
     1911, 14, 113; ibid, 818.

A10. Bardeen J.; Cooper, L. N.; Schrieffer, J. R. Phys.
     Rev. 1957, 108, 1175.

A11. Green. R. L.; Sreet, G. B.; Suter, L. T. Phys. Rev.
     Lett., 1975, 35, 577.

A12. Bechgaard, K.; Carneiro, K.; Olsen. M.; Rasmussen, F. B.; jacobsen, S. Phys. Rev. Lett., <u>1981</u>, 46, 852.

A13. Bernarioni, J.; Schneider, T., Ed., "Physics in one Dimension:, Proceeding of an International Conference. Fribourg, Switzerland, August 25-29, <u>1980</u>. (Spring-Verlag Berlin Heildeberg, New York, <u>1981</u>)

A14. Street. G. B.; Clarke, T. C., Ed., "IBM Symposium on Highly Conducting Polymers and Graphite", San Jose, March, <u>1979</u>. (Synthetic Metals, <u>1980</u>, 1, 99-347)

A15. Shirakawa, H.; Louis, E. J.; MacDiarmid, A. G.; Chiang, C. K.; Heeger, A. J. J. Chem. Soc., Chem. Comm., <u>1977</u>, 578.

A16. Shirakawa, H.; Sato. M.; Hamano, A.; Kawakami, S.; Soga, K.; Ikeda, S. Macromolecules, <u>1980</u>, 13, 457.

A17. Park, Y. W.; Druy, M. A.; Chiang, C. K.; MacDiarmid, A. G.; Heeger, A. J.; Shirakawa, H.; Ikeda, S. J. Polym. Sci., Polym. Lett. Ed., <u>1979</u>, 17, 203.

A18. Wegner, G. Makromol. Chem., <u>1971</u>, 145, 85; ibid, <u>1972</u>, 154, 35.

A19. Baughman, R. H.; Yee, K. C. J. Polym Sci., Macromolecular Rev., <u>1978</u>, 13, 219.

A20. Baughman, R. H. J. Polym. Sci., Polym. Ed., <u>1974</u>, 12, 1511.

A21. Patel, G. N. Polym. Prep., Am. Chem. Soc., Div. Polym. Chem., <u>1978</u>, 19, 154.

A22. Patel, G. N.; Walsh, E. K. J. Polym. Sci., Lett. Ed., <u>1979</u>, 17, 203.
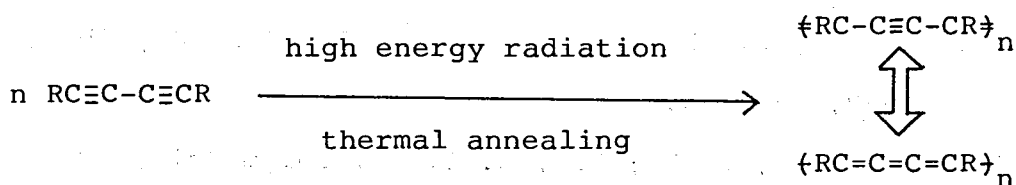
Chapter 2

PREPARATION AND CHARACTERIZATION OF

POLY(nACMU)S

2-1. Introduction

Diacetylenes, $RC\equiv C-C\equiv CR$, where R is a substituent
group, are a unique class of monomers which can be poly-
merized in the solid state by high energy radiation or
simply by thermal annealing.[B1-B3] The details of the
solid state polymerization of diacetylenes were revealed
mainly by Wegner,[B4, B5] who identified the polymerization
reaction as 1,4-addition shown as follows.

$$n\ RC\equiv C-C\equiv CR \quad \xrightarrow[\text{thermal annealing}]{\text{high energy radiation}} \quad \begin{array}{c} \leftarrow RC-C\equiv C-CR \rightarrow_n \\ \Updownarrow \\ \leftarrow RC=C=C=CR \rightarrow_n \end{array}$$

The structure of the backbone is a resonance admixture of
the acetylenic and the butatriene structures. A large
number of diacetylenes having different substituent groups
have been synthesized by a number of investigators.[B1-B6]

About half of the research-publications on diacetylenes

are concerned with the properties and polymerization of
2,4-hexadiyn-1,6-bis(p-toluene sulfonate), abbriviated as
PTS. [B7, B8] The PTS has become a model diacetylene of solid
state polymerization, because it yields the polymer single
crystal quantitatively by thermal polymerization. Poly-
(PTS) obtained from partially polymerized crystals with
the conversion less than 12% is completely soluble in
dimethylformamide (DMF), while poly(PTS) with the conversion
more 12% is entirely insoluble due to high molecular weights.
This fact is a fatal disadvantage of poly(PTS), when the
relation between the electrical properties and molecular
characteristics is to be studied.

Recently, Patel et al., succeeded in synthesizing
several soluble polydiacetylenes, [B9-B11] which have a
substituent R of the form:

$$R = -(CH_2)_n-O-\overset{O}{\overset{\|}{C}}-\overset{H}{\overset{|}{N}}-CH_2-\overset{O}{\overset{\|}{C}}-O(CH_2)_m-CH_3$$
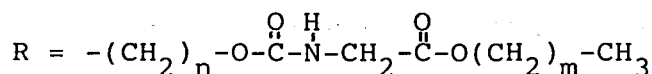
with n = 1-4 and m = 1 and 3. They referred to this new
class of diacetylenes as nACMU (standing for n-methyl alkoxy
carbonyl methyl urethane; the side chain) and the polymer as
poly(nACMU). As the first step in studying the physical
properties of linear-chain conductors, we synthesized five
different poly(nACMU)s.

Further, we attempted to examine the change in molec-
ular weight and its distribution during the solid state

polymerization by ^{60}Co γ-ray irradiation. Such an attempt

may be the first one ^{B12} in the polymerization of nACMUs.

All the polymer samples were tested on a gel permeation

chromatograph, and the intrinsic viscosities were also

determined.

2-2. Experimental Designs of Polymer Syntheses

We synthesized five different soluble polydiacetylenes
of poly(nACMU) type. They are:
poly[4,6-decadiyn-1,10-diol-bis(n-butoxy-carbonyl-methyl-
urethane)] or poly(3BCMU) with n = 3 and m = 3,
poly[4,6-decadiyn-1,10-diol-bis(ethoxy-carbonyl-methyl-
urethane)] or poly(3ECMU) with n = 3 and m = 1,
poly[3,5-octadiyn-1,8-diol-bis(n-butoxy-carbonyl-methyl-
urethane] or poly(2BCMU) with n = 2 and m = 3,
poly[3,5-octadiyn-1,8-diol-bis(ethoxy-carbonyl-methyl-
urethane)] or poly(2ECMU) with n = 2 and m = 1 and
poly[5,7-dodecadiyn-1,12-diol-bis(n-butoxy-carbonyl-methyl-
urethane)] or poly(4BCMU) with n = 4 and m = 3.
Five monomers were synthesized by usual techniques of
organic chemistry and the synthetic routes are shown in
Scheme 2-1, 2-2 and 2-3. The 3BCMU and 3ECMU monomers
were prepared through four steps. The 2BCMU and

2ECMU monomers were prepared through two steps. The
4BCMU monomers was prepared through five steps. The reac-
tion of oxidative coupling of the mono-ols and the reaction
of the diols with isocyanatoacetate are almost the same
for these different monomers. The other synthetic processes
are different from one another. The five monomers were
polymerized in the solid state by exposing the ^{60}Co γ-ray.
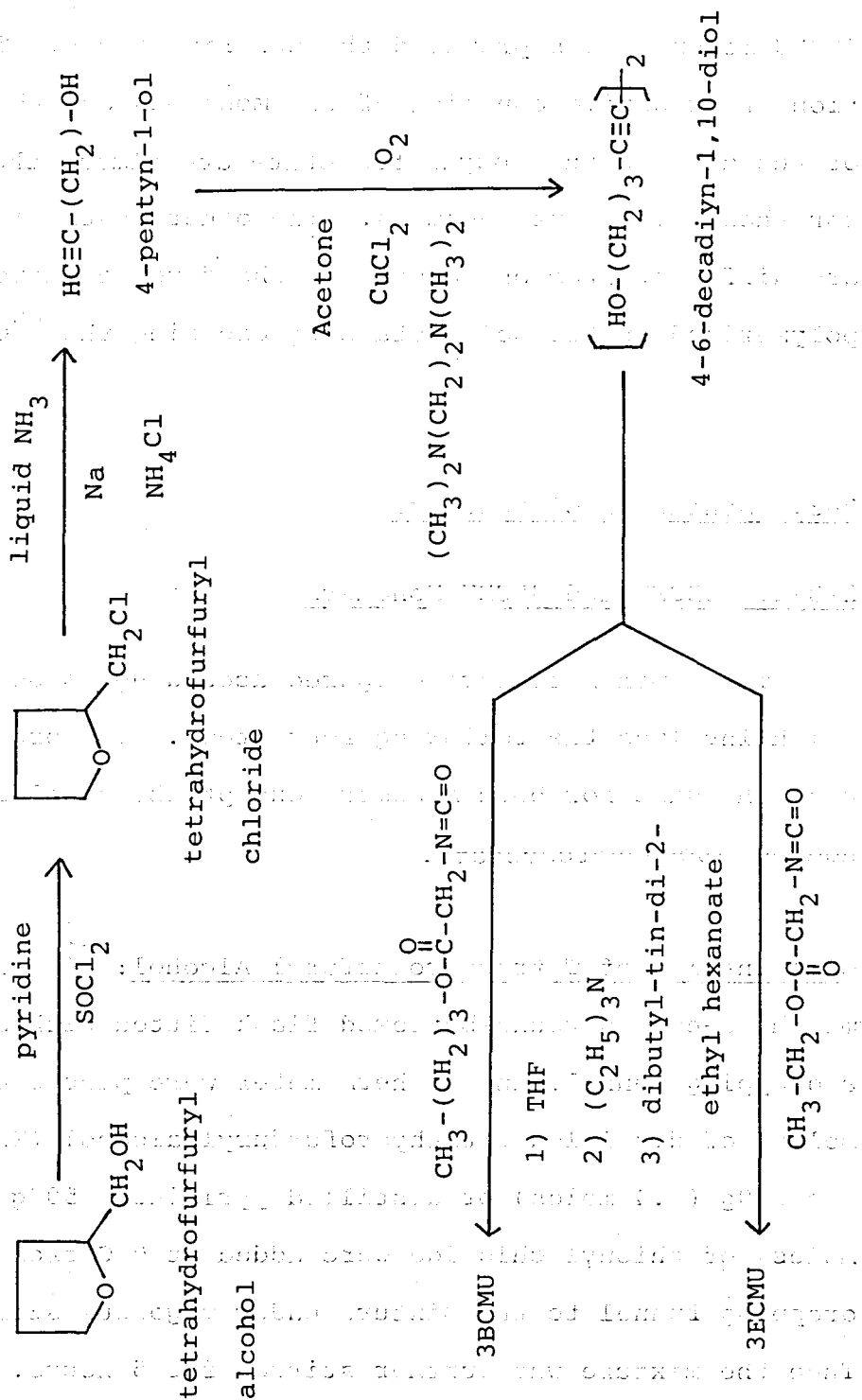

2-3. Syntheses of Monomers

2-3-1. 3BCMU and 3ECMU Monomers

These monomers were prepared according to Scheme 2-1,
which involves the following four steps. The procedures
were the same for both monomers except the final stage of
adding isocyanatoacetate.

Chlorination of Tetrahydrofurfuryl Alcohol:[B13] In a 2000
mL three-necked round-bottomed flask fitted with a stirrer,
a dropping funnel, and a thermometer were placed 410g (4.2
moles) of distilled tetrahydrofurfuryl alcohol (THF-OH)
and 350g (4.4 moles) of distilled pyridine. 500g (4.2
moles) of thionyl chloride were added at 0°C from the
dropping funnel to the mixture under vigorous stirring.
Then the mixture was further stirred for 5 hours. Tetra-
hydrofurfuryl chloride (THF-Cl) was extracted from the

Scheme 2-1. Routes of 3BCMU and 3ECMU Syntheses.

tetrahydrofurfuryl alcohol

CH_2OH

pyridine
$SOCl_2$

tetrahydrofurfuryl chloride

CH_2Cl

liquid NH_3

Na

NH_4Cl

$HC \equiv C-(CH_2)-OH$

4-pentyn-1-ol

Acetone

$CuCl_2$

$(CH_3)_2N(CH_2)_2N(CH_3)_2$

O_2

$[HO-(CH_2)_3-C \equiv C]_2$

4-6-decadiyn-1,10-diol

$CH_3-(CH_2)_3-O-\overset{O}{\overset{\|}{C}}-CH_2-N=C=O$

1) THF
2) $(C_2H_5)_3N$
3) dibutyl-tin-di-2-ethyl hexanoate

3BCMU

$CH_3-CH_2-O-\overset{O}{\overset{\|}{C}}-CH_2-N=C=O$

3ECMU

-20-

mixture with ether. After removing ether, the residue was distilled under reduced pressure and the fraction boiling at 57°C/25mmHg was collected. The yield of THF-Cl was 305g (70%).

Ring Opening of THF-Cl: [B13] 1500mL of anhydrous liquid ammonia were introduced through an inlet tube to a 3000mL three-necked flask, and 1g of hydrated ferric nitrate was added, following by 80g of freshly cut sodium at the temperature of -36°C. The mixture was stirred until all the sodium was converted to sodium amide. Then, 120g (1 mole) of THF-Cl was added from a dropping funnel for 30 minutes. The mixture was stirred for additional 2 hours, and 177g (3.3 moles) of solid ammonium chloride was added. After ammonia was evaporated, the product, 4-pentyn-1-ol, was extracted from the mixture with ether. After removing ether, the residue was distilled under reduced pressure and the fraction boiling at 66°C/20mmHg was recovered. The yield of 4-pentyn-1-ol was 63g (74%).

Oxidative Coupling: [B15] To a 1000mL three necked flask were added 500mL of acetone, 10g (0.1 mole) of copper(I) chloride and 14g (0.12 mole) of N,N,N',N'-tetramethylene diamine. 33.6g (0.4 mole) of 4-pentyn-1-ol were added from a dropping funnel to the reaction mixture into which oxygen was bubbling. After the addition was completed,

the reaction was continued for 3 hours. Then, acetone was evaporated, and 50mL of water containing 2mL of concentrated hydrochloric acid were added. The product, 4,6-decadiyn-1,10-diol (DD) was extracted from the mixture with ether. The ether was evaporated and the residual product was recrystallized from ethyl acetate. The melting point was 46°C. The yield of DD was 26.5g (79%).

Addition of Isocyanatoacetate: [B12, B16] For preparing 3BCMU, both n-butyl isocyanatoacetate (IA) and triethyl-amine (EA) were degassed and dried with CaH_2 in a high vacuum apparatus (10^{-5} torr) and then distilled to ampules with breakable seals. Tetrahydrofuran (THF) was purified by an anionic polymerization technique until the blue color characteristic to the sodium benzophenone complex appeared, and then distilled to another sodium mirror covered storage vessel with breakable-seals.

In a 1000mL round-bottomed flask fitted with a magnetic stirrer and a thermometer, 6.6g (0.04 mole) of DD and o.1g of dried dibutyl-tin-2-ethyl-hexanoate were introduced. Ampules of IA (13g, 0.08 mole) and EA (2mL) were connected to the reactor, which in turn was connected to the vacuum line and to the THF storage vessel, as shown in Figure 2-1. The whole apparatus was evacuated to 10^{-5} torr and was sealed off at the constriction (A) from the vacuum line. From the storage vessel (B) ca. 400mL of THF was distilled
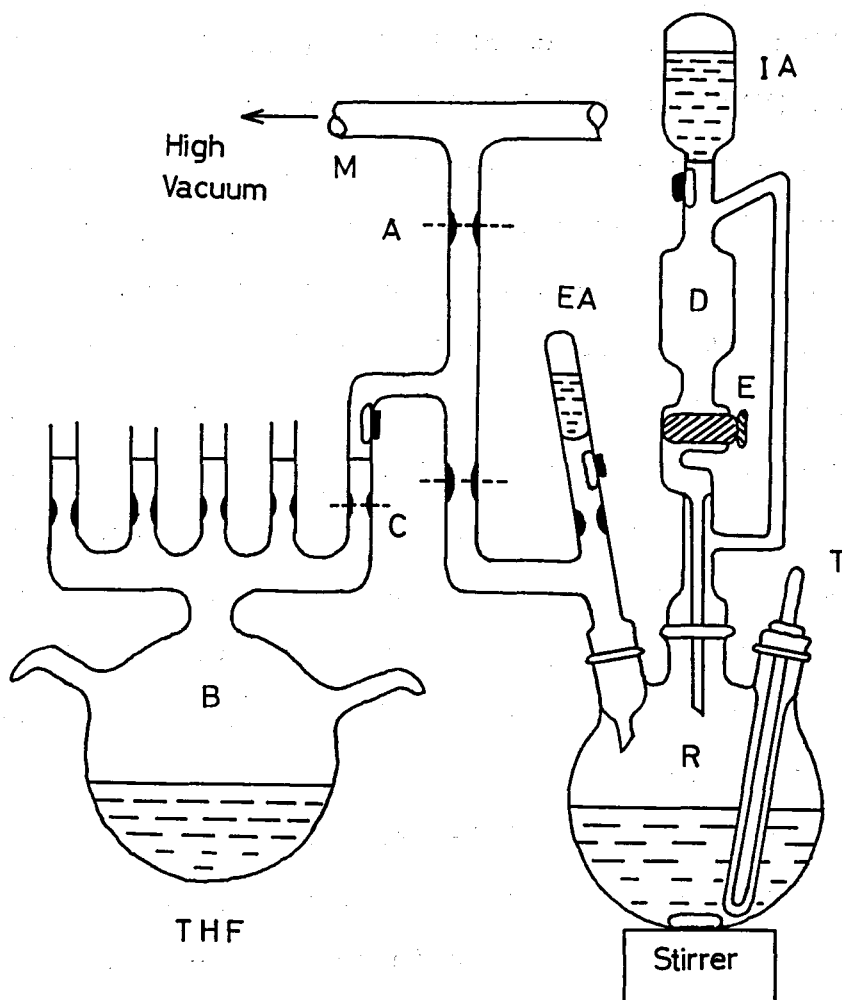
Figure 2-1. Reactor for nACMU monomer synthesis: (B) THF; (EA) triethyl amine; (IA) n-butyl or ethyl isocyanatoacetate; (M) high vacuum apparatus; (A) and (C) contrictions; (D) dropping funnel; (E) cock; (R) reactor; (T) a thermometer.

into the reactor (R). After the THF vessel (B) was removed

by sealing off at the constriction (C), the triethyl amine

catalyst (EA) was introduced into the reactor (R) by break-

ing the breakable-seal. The isocyanatoacetate (IA) was

introduced into a specially designed dropping funnel (D),

and then the IA was added through the dropping cock (E) to

the mixture (R) at 23°C, while vigorously stirring for

30 minutes. The temperature was monitored by the ther-

mometer (T). The mixture was stirred for 2 more hours,

and air was introduced to the reactor to terminate the

reaction. Then the resultant solution was poured into

1500mL n-hexane to precipitate the product, 3BCMU monomer.

The melting point of 3BCMU was 62°C. The yield of 3BCMU
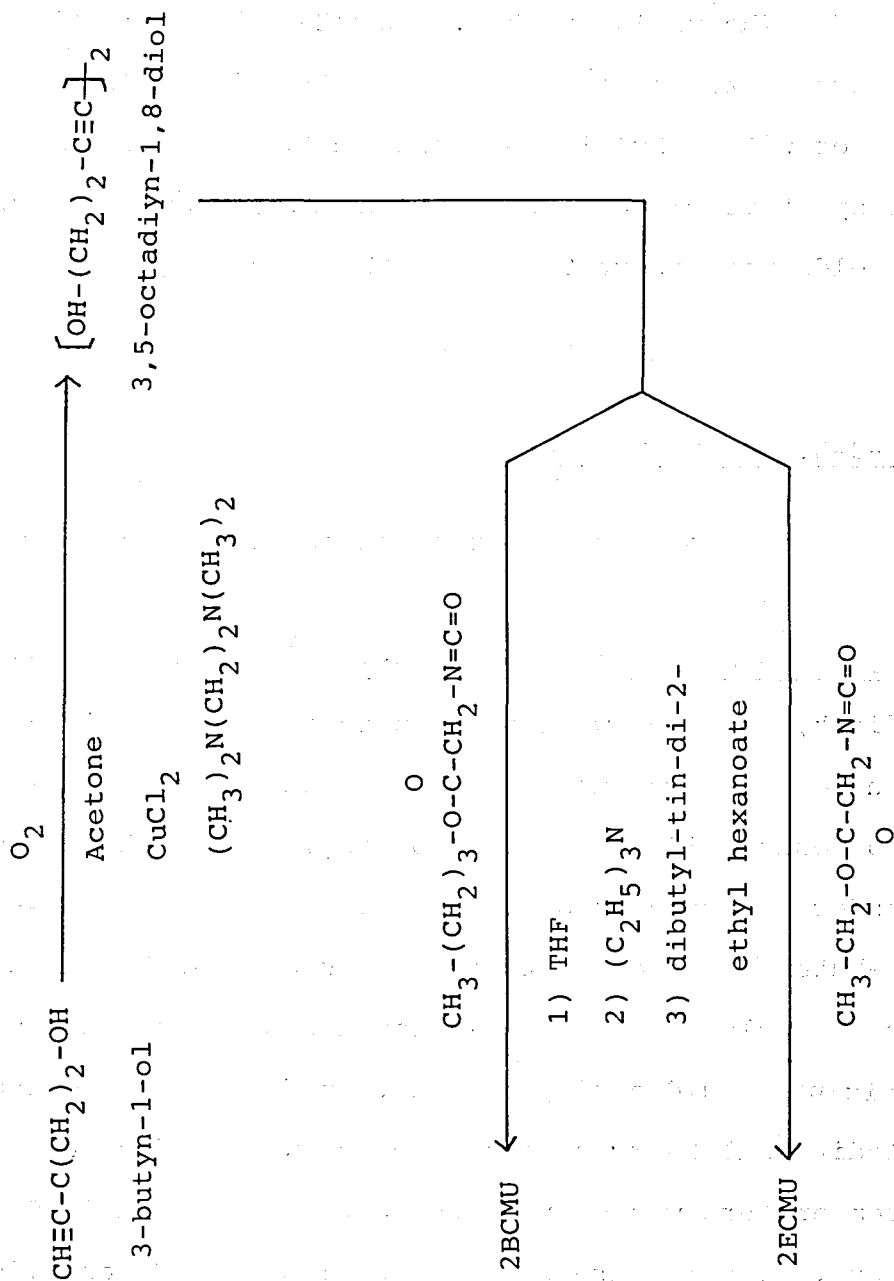
monomer was 19.6g (100%).

   4,6-decadiyn-1,10-diol-bis(ethoxy-carbonyl-methyl-

urethane) monomer (3ECMU) was prepared by the same manner

using ethylisocyanatoacetate instead of n-butyl IA. The

melting point of the product was 78°C. The yield was

again 100%.

2-3-2. 2BCMU and 2ECMU Monomers

These monomers were prepared according to Scheme 2-2.

Again the routes were the same except the final step.

   3-butyn-1-ol was purchased from Tokyo Kasei Co. 2BCMU

and 2ECMU monomers were prepared by the following two steps.

Scheme 2-2. Routes of 2BCMU and 2ECMU Syntheses.

$$CH\equiv C-C(CH_2)_2-OH \xrightarrow[\text{Acetone}]{O_2} \left[OH-(CH_2)_2-C\equiv C\right]_2$$

3-butyn-1-ol

$CuCl_2$

$(CH_3)_2N(CH_2)_2N(CH_3)_2$

3,5-octadiyn-1,8-diol

$$CH_3-(CH_2)_3-O-\overset{O}{\overset{\|}{C}}-CH_2-N=C=O$$

1) THF
2) $(C_2H_5)_3N$
3) dibutyl-tin-di-2-
   ethyl hexanoate

2BCMU

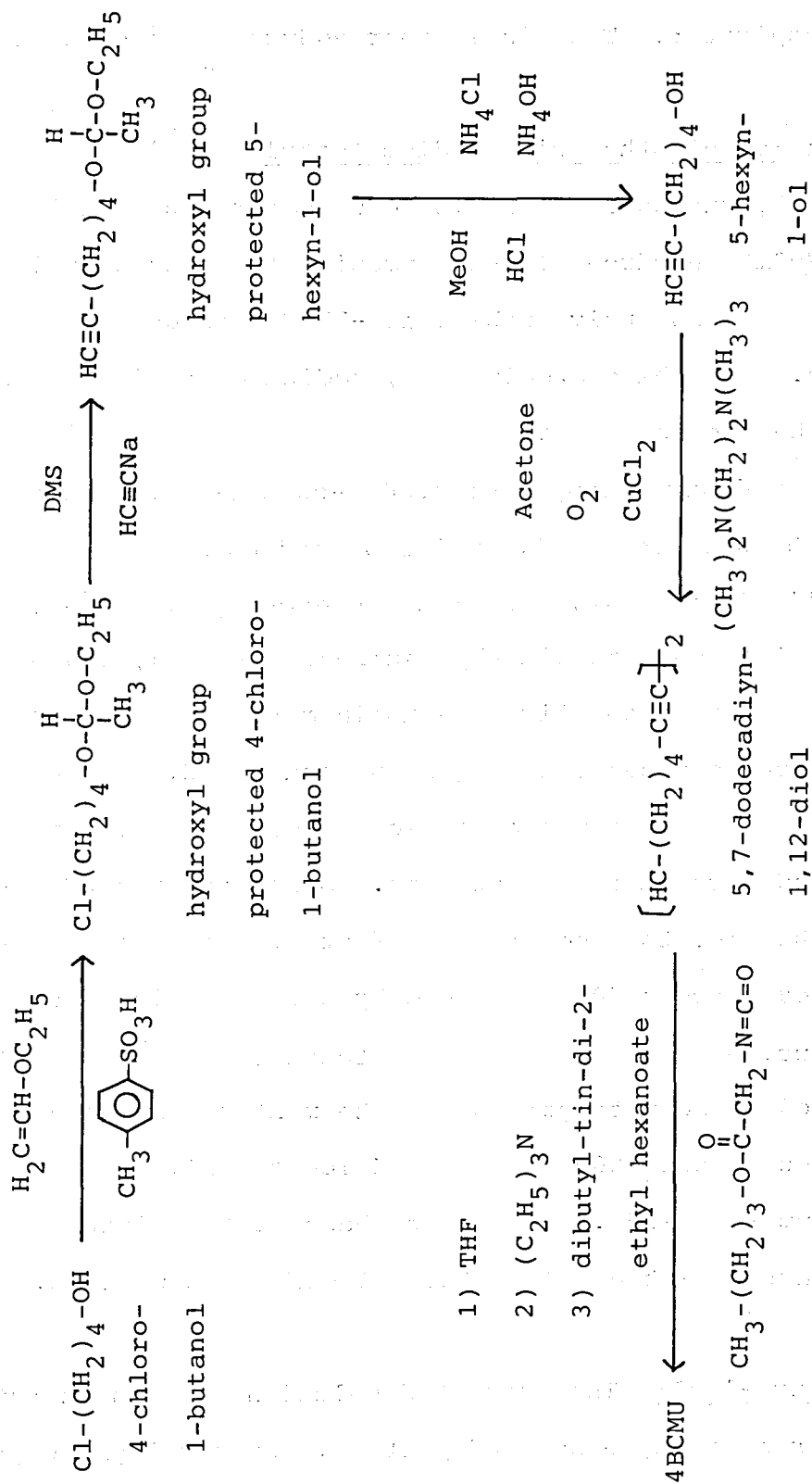$$CH_3-CH_2-O-\overset{O}{\overset{\|}{C}}-CH_2-N=C=O$$

2ECMU

(1) 3-butyn-1-ol was subjected to oxidative coupling by Hay's method to obtained 3,5-octadiyn-1,8-diol; mp was 41°C. The yield was 92%. (2) The diol was allowed to react in the same manner as 3BCMU and 3ECMU, with n-butyl IA or with ethyl IA to obtain 2BCMU and 2ECMU monomers, respectively: mp were 90.5 and 70.5, respectively. The yields were about 95% for both cases.

2-3-3. 4BCMU Monomer

This monomer was prepared according to Scheme 2-3.

Addition of Ethyl Vinyl Ether: [B17] A 500 mL three-necked flask, equipped with a dropping funnel, a stirrer and a thermometer was used. 100mg of the catalyst, p-toluene-sulfonic acid, was added to ethyl vinyl ether which was under stirring at 0°C. Immediately, 1 mole of 4-chloro-1-butanol was added to the mixture at such a rate that the heat evolution was small enough and the temperature of the mixture could easily be maintained between 5°C and 8°C. Additional 50 mg of the catalyst were added, and the temperature was maintained between 10°C and 15°C for 1 hour. The mixture was then cooled to 0°C, and vigorous stream of ammonia was passed into the solution for a few seconds. The excess of ethyl vinyl ether was removed by

Scheme 2-3. Route of 4BCMU Synthesis.

$H_2C=CH-OC_2H_5$

$Cl-(CH_2)_4-OH$ $\xrightarrow{\quad\quad}$ $Cl-(CH_2)_4-O-\overset{H}{\underset{CH_3}{C}}-O-C_2H_5$

4-chloro- $CH_3-\langle\bigcirc\rangle-SO_3H$

1-butanol   hydroxyl group

protected 4-chloro-

1-butanol

$\xrightarrow[HC\equiv CNa]{DMS}$ $HC\equiv C-(CH_2)_4-O-\overset{H}{\underset{CH_3}{C}}-O-C_2H_5$

hydroxyl group

protected 5-

hexyn-1-ol

$\xrightarrow[\substack{HCl \\ NH_4OH}]{\substack{MeOH \\ NH_4Cl}}$ $HC\equiv C-(CH_2)_4-OH$ 5-hexyn-

1-ol

1) THF

2) $(C_2H_5)_3N$

3) dibutyl-tin-di-2-

ethyl hexanoate

$\xrightarrow[\substack{O_2 \\ CuCl_2}]{Acetone}$ $\left[HC-(CH_2)_4-C\equiv C\right]_2$ 5,7-dodecadiyn-

1,12-diol

4BCMU $\longleftarrow$ $CH_3-(CH_2)_3-O-\overset{O}{\overset{\|}{C}}-CH_2-N=C=O$ $(CH_3)_2N(CH_2)_2N(CH_3)_3$

an aspirator. The vinyl ether adduct was stored at 0°C.

Reaction of Ether with Sodium Acetylide: [B17] 33g of
freshly cut sodium were introduced through an inlet tube
to 700mL anhydrous liquid ammonia, to which acetylene gas
was simultaneously bubbled at -35°C through other inlet
tube. The white precipitate, sodium acetylide was produced
in the liquid ammonia.

Hydroxyl group protected 4-chloro-1-butanol was added
to the solution of 1.4 moles of sodium acetylide in 700mL
of liquid ammonia. In order to exchange the solvent from
liquid ammonia to dimethyl sulfoxide (DMSO), 400mL of DMSO
were added to the liquid ammonia mixture. Then ammonia was
evaporated under stirring being continued. During the
evaporation of ammonia, a slow stream of acetylene was
passed through the inlet tube. Since the reaction was
exothermic, the temperature of stirred mixture was main-
tained between 60°C and 70°C by use of an ice bath. After
1 hour, acetylene stream was stopped, and the mixture was
cooled to room temperature. The mixture was then cautious-
ly poured onto 800g of crushed ice to kill the residual
sodium acetylide. The water phase of the mixture was
extracted with a 1:1 mixture of ether and pentane.

5-Hexyn-1-ol: The extracted solution was concentrated
after removing ether and pentane. Hydroxyl group protected

5-hexyn was mixed 200mL of methanol and 7mL of 36%

HCl.　After warming the mixture at 55°C for 30 min, the

excess of methanol was removed by an aspirator.　200mL of

concentrated NH_4Cl solution and 10mL of concentrated NH_4OH

were added to the mixture.　Extraction was carried out

with ether, and then the ether residue was concentrated

to obtain 5-hexyn-1-ol; bp = 72°C/10mmHg.　The total

yield from butanol to 5-hexyn-1-ol was 38%.

Oxidative Coupling: [B15]　5-hexyn-1-ol was subjected to

oxidative coupling by Hay's method to obtain 5,7-dodecadiyn-

1,12-diol; mp was 49°C.　The yield was 14%.　This step was

the most inefficient among all the synthetic processes.

It was found that the oxidative coupling of 5-hexyn-1-ol

is strongly affected by the solvent used.　In this study

acetone was used.　We repeated this reaction 8 times with

varying reaction-temperature and reaction-time.　However,

we could not find out any suitable condition.　Recently,

it was shown that use of isopropanol for oxidative

coupling is preferable to achieve high yield.

Addition of n-Butyl IA: [B12, B16]　The diol was reacted

with n-butyl IA to obtain 4BCMU monomer.　The mp was 72°C.

The yield was about 100%.　The experimental procedure was

the same for preparing 3BCMU mentioned above.

The intermediate and final products were identified by comparing their boiling points (bp) and melting points (mp) data with those of the literature values. All the substances were also checked by elemental analysis, infrared and nuclear magnetic resonance spectroscopies. The results were all satisfactory.

2-4. Solid State Polymerization

4BCMU monomer was polymerized with high polymer-conversion in comparison with other nACMU monomers. Therefore, poly(4BCMU) was studied as a model of the polymer single crystal, and other polymers were studied in the form of semicrystalline and/or amorphous films.

Powder-form monomers of 3BCMU, 3ECMU, 2BCMU, 2ECMU and 4BCMU were sealed in ampules after degassing under high vacuum (10^{-5} torr). The diacetylene monomers in ampules were exposed to ^{60}Co γ-irrdiation with varying doses from 0.09 to 45 Mrad at room temperature, and powder-form mixture of monomer and polymer crystallites were obtained. The unreacted monomers were removed by extracting with acetone. The poly(nACMU)s were dissolved in $CHCl_3$ and reprecipitated in excess hexane. Finally, the powder-form polydiacetylenes were recollected by drying under high vacuum.

The polymer samples were coded as poly(nACMU)/xMrad, where x denotes the total dose of ^{60}Co γ ray employed for the polymerization. Thus, the code poly(3BCMU)/45Mrad implies a poly(3BCMU) sample obtained by 45 Mrad exposure to the γ ray.

Needle-like and platelet-like single crystals of 4BCMU monomer (typical size; 6 x 1 x 0.2 and 3 x 2 x 0.2 mm^3, respectively) were grown from acetone/n-hexane solution by slowly evaporating the solvent. The single crystalline poly(4BCMU) monomer in high vacuum ampules (10^{-5} torr) was allowed to polymerize by irradiating it with 48 Mrad ^{60}Co γ ray at room temperature.

2-5. Molecular Characterization of Poly(nACMU)s

2-5-1. Methods

All the polymer samples were tested on a gel permeation chromatograph (GPC: Model 801A, Toyo Soda Mfg. Co.) to estimate their average molecular weights and molecular weight distributions. The carrier solvent was CHCl$_3$. Narrow distribution polystyrenes (TSK polystyrenes, Toyo Soda Mfg. Co.) were used as elution standards. Low-angle-laser-light-scattering (LALLS) measurements were made with an LALLS photometer (Model LS-8, Toyo Soda Mfg. Co.) at 633 nm on yellow colored CHCl$_3$ solutions at 25°C

Refractive index increments, dn/dc, of the same solutions

at 25°C were determined by a differential refractometer

(Model RF-600, G. N. Wood Mfg. Co.) with a 633 nm helium-

neon laser as the light source at professor Takahashi's

Laboratory of Mie University.

Intrinsic viscosities as a function of shear rate were

determined for some poly(3BCMU) samples in $CHCl_3$ and

$CHCl_3$/n-hexane mixtures at 30°C. Three conventional

Ubbelohde viscometers of different capillary sizes and a

four-bulb spiral capillary viscometer were used.

2-5-2. Results and Discussion

2-5-2-a. Poly(3BCMU)

Poly(3BCMU) is considered as a model specimen, because

it is easier to handle for laboratory work than any other

soluble polydiacetylenes. 3BCMU monomer and poly(3BCMU)

polymer conversions are higher than any other monomer and

polymer conversions. [B18] Hence, the polymerization process

of poly(3BCMU) was studied in greater detail with regard

to the relationship between molecular characteristics of

the products and the doses of ^{60}Co γ-ray exposure.

The polymer conversions at various doses were calculated

from the residual polymer found after careful extraction

of monomers with acetone. The conversions were also

checked by visible absorption spectroscopy and by differ-
ential scanning calorimetry (DSC). The results obtained
by these method agreed with one another reasonably well.

Figure 2-2 shows plots of polymer conversion vs total
dose or exposure time for poly(3BCMU). The curve consists
of two steps. The first step levels off at about 40%
conversion or at about 1 Mrad dose, and the second step
at about 60% conversion or above 45 Mrad dose.

Each of the polymerization mixtures was dissolved in
$CHCl_3$ for GPC test. The chromatograms showed two major
peaks corresponding to the unreacted monomer and the polymer.
Figure 2-3 shows the peaks for the polymers obtained at
various doses. The polymers obtained below 1 Mrad dose
or below 40% conversion show fairly sharp chromatograms
tailing to low molecular weight side. With polystyrene
elution standards, the PS-reduced weight-average molecular
weight M_w and polydispersity index (the ratio of the number
to weight-average molecular weight M_w/M_n) for all samples
were determined. The results are summarized in Table 2-1.

Patel et al. [B19] reported that the conversion in
synthesizing poly(3BCMU) increased steadily with increasing
radiation dose and that the polymers at various doses had
essentially similar average molecular weights and distri-
butions. The conversions obtained by Patel et al. are
about half or less than our values at low doses, but nearly
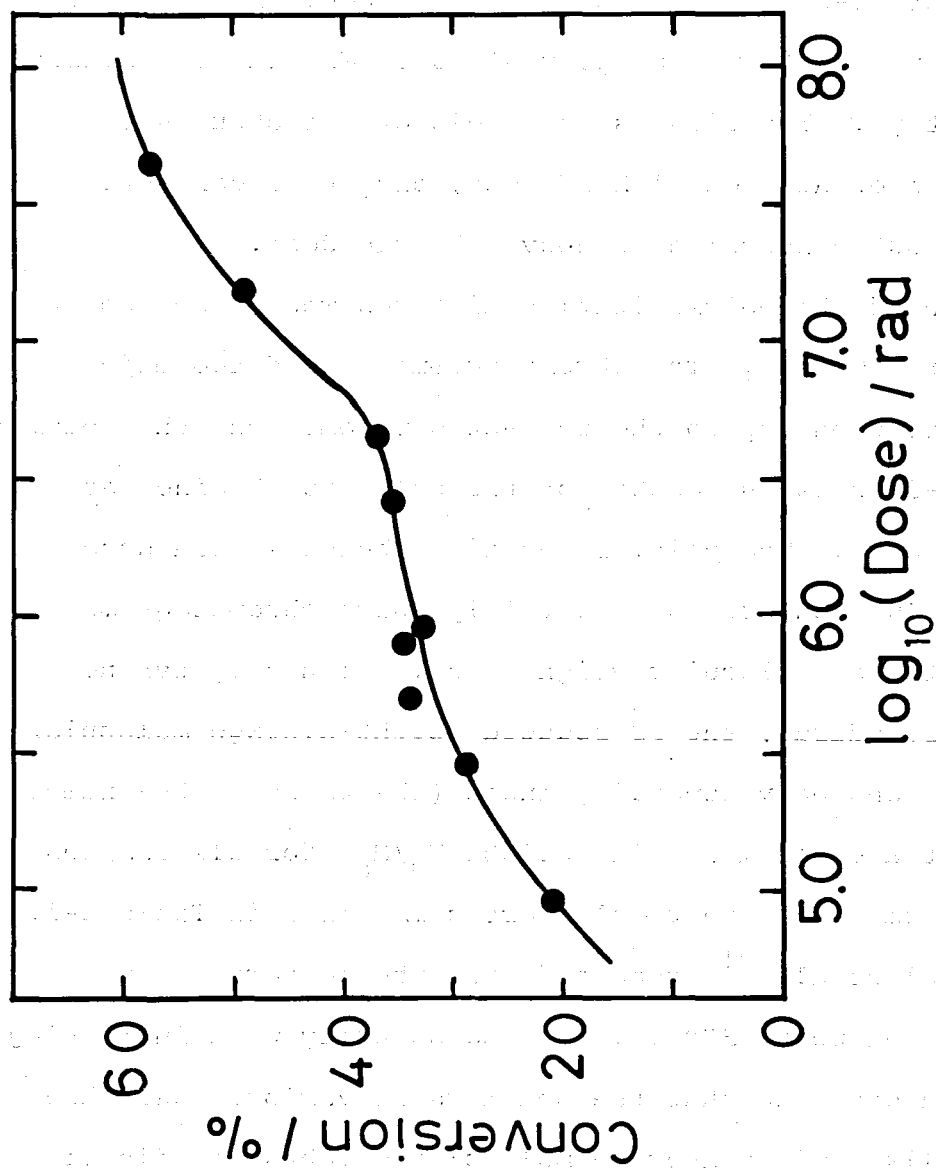the same as ours at high doses. Probably, in Patel's

Figure 2-2. Plots of polymer conversion versus ^{60}Co γ-ray dose for 3BCMU.
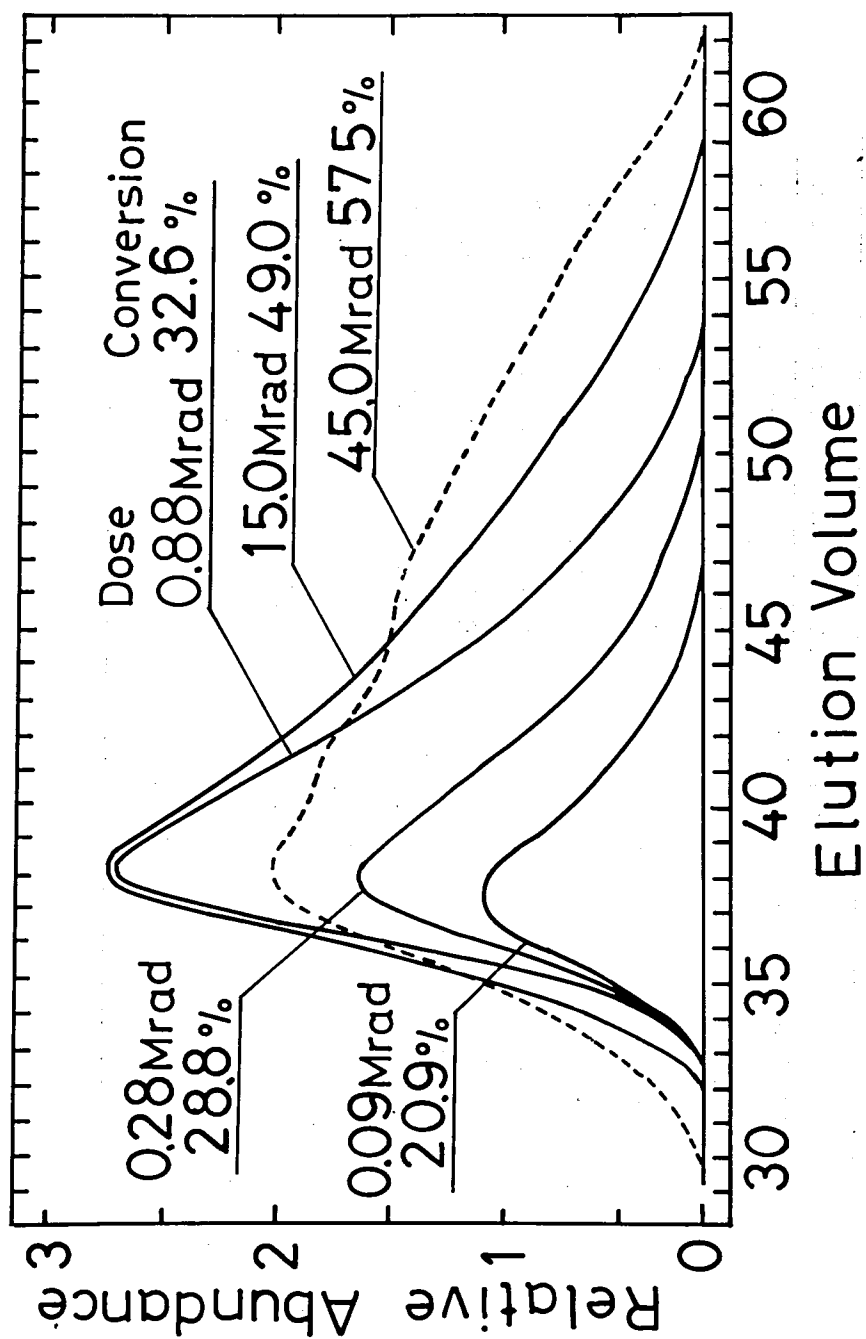
Figure 2-3. GPC chromatograms of poly(3BCMU) specimens obtained at different doses. The nummerical values represent dose levels and polymer yields.

Table 2-1. Polymer conversions and molecular characteristics of poly(3BCMU) samples polymerized at various dose leveles.

dose/Mrad	polymer conversion %	PS-reduced molecular weights		
		$10^{-6}M_n$	$10^{-6}M_w$	M_w/M_n
0.09	20.9	1.33	3.90	2.93
0.28	28.8	0.810	2.46	3.04
0.50	34.1	0.734	2.49	3.39
0.80	34.5	0.509	2.57	5.06
0.88	32.6	0.648	2.32	3.59
2.60	35.6	0.465	1.99	4.28
4.50	36.8	0.466	2.25	4.82
15.0	49.0	0.179	2.31	12.8
45.0	57.5	0.0802	3.18	39.7

experiment, the monomer was exposed to γ-ray in the air, in contrast to our experiment in which the monomer was vacuum-sealed.

In the early stage of the polymerization of 3BCMU, the reaction proceeds via 1,4 addition in the reactive monomer crystalline phase, yielding high-molecular weight and narrow distribution components. In the later stage, however, the monomer remaining in the mixed monomer-polymer crystalline phase undergoes polymerization. Some degradation of polymer chains also may take place by prolonged exposure to high energy radiation. These two factors seem to be responsible for the production of low-molecular weight components in the later stage of the reaction.

The 45 Mrad sample was further subjected to M_w determination by LALLS. The area of GPC chromatogram monitored by RI detector A^{RI} and that by LS detector A^{LS} are proportional to the polymer concentration c and to the product of the weight-average molecular weight M_w and c, respectively.

Therefore, the A^{RI}/A^{LS} ratio is given as followss:

$$\frac{A^{RI}}{A^{LS}} = \frac{1}{B} \frac{1}{M_w} (1 + 2 A_2 M_w c) \qquad (2-1)$$

where A_2 and B are the second virial coefficient and an apparatus constant, respectively.[20, 21] The B depends

on the experimental condition and on dn/dc of the polymer

solution as

$$B = B_s \ (dn/dc) \ / \ (dn/dc)_s \qquad\qquad (2\text{-}2)$$

where B_s is the value of B determined for a known standard,

say, polystyrene of known characteristics, and (dn/dc) and

(dn/dc)$_s$ are the refractive index increments of the unknown

solution and of the reference polymer solution, respectively.

Using several standard polystyrenes with known M_w, we

carried out the GPC-LALLS measurements to determine B_s of

the particular instrument. The ratio of the refractive

indices at 633 nm for poly(3BCMU) and polystyrene $CHCl_3$

solutions at 25°C, $(dn/dc)/(dn/dc)_s$ was determined by the

differential refractometer. By introducing these values

into Eq. 2-2, we determined the B for poly(3BCMU) in $CHCl_3$

solutions.

Figure 2-4 shows plots of A^{RI}/A^{LS} vs polymer concen-

tration c for poly(3BCMU)/45Mrad in $CHCl_3$ at 25°C. From

the intercept and slope of the plots, M_w and A_2 of poly-

(3BCMU)/45Mrad sample in $CHCl_3$ were determined to be 10.7

x 10^6 g mol^{-1} and 0.34 x 10^{-4} mol cm^3 g^{-2}, respectively.

This value of M_w is about 3.4 times as large as the PS

reduced GPC value. If the difference in monomer molecular
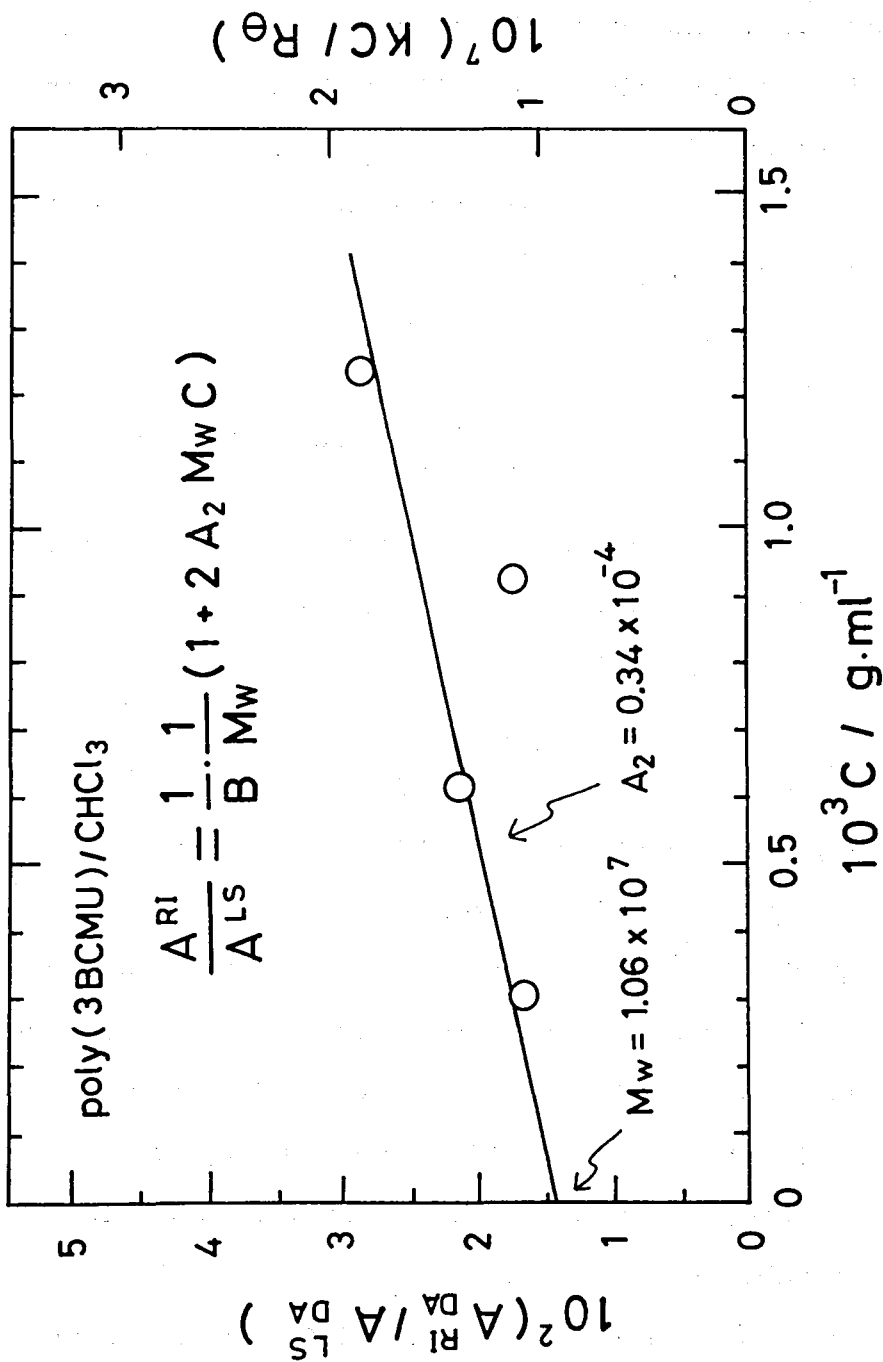
weight per unit contour length between PS and

Figure 2-4. Plot of $A_{DA}^{RI} / A_{DA}^{LS}$ versus polymer concentration c determined on GPC/LALLS system for $CHCl_3$ solution of poly(3BCMU)/45Mrad. The A^{RI} and A^{LS} are the areas under the RI and LS response curves.

poly(3BCMU) is taken into account, the GPC value should be multiplied by 2.51. However, the corrected GPC value is still about 35% smaller than the LALLS value. The difference may be attributed to the permeability limit and an imperfect resolving power of our GPC columns for high molecular weight components.

2-5-2-b. Poly(nACMU)s Other than Poly(3BCMU)

Poly(3ECMU) and poly(2BCMU) were obtained by the solid state polymerization exposing the powder form monomers to ^{60}Co γ-ray. The characteriatics are summarized in table 2-2.

2ECMU monomer was also exposed 45 Mrad dose of ^{60}Co γ-ray, but only a trace of poly(2ECMU) was obtained. It was light red-brown. The GPC chromatogram showed only a sharp single peak which corresponded to the 2ECMU monomer, although the solution showed yellow color due to the conjugated main chains of poly(2ECMU). However, the polymer can not be recollected by extracting the residues with acetone. Therefore, we concluded that 2ECMU monomer is hardly polymerizable by γ-ray irradiation.

Powder form and single crystalline 4BCMU monomers were polymerized by irradiating them with 48 Mrad ^{60}Co γ-ray. The polymer conversion determined by specific absorption

Table 2-2. Molecular characteristics of
poly(nACMU)s polymerized at 45Mrad dose.

Polymer	PS-reduced molecular weights		
	10^{-6}Mn	10^{-6}Mw	Mw/Mn
Poly(3BCMU)	0.080	3.2	40
Poly(3ECMU)	0.10	1.0	12
Poly(2BCMU)	0.066	0.89	13
Poly(2ECMU)	no polymerization		
Poly(4BCMU) powder-form	0.093	0.62	6.7
Poly(4BCMU) single crystal	0.15	0.98	6.5

at 470 nm of the $CHCl_3$ solution was 94% for single crystals and 74% for powder form samples. Thable 2-2 lists the PS-reduced molecular weights. Single crystalline sample has higher M_w and M_n than powder form ones. This finding is reasonable as compared to the results of poly(3BCMU). For poly(4BCMU), macroscopic polymer single crystals may be obtained not by the crystallization from dilute solutions but by the solid state polymerization of a monomer single crystal.[B22, B23] This possibility of preparing a polymer single crystal is one of the advantages of the solid state polymerization, although the molecular weight distribution tends to become broad due to the heterogeneous polymeriza-tion process.

There are three features in these samples. The first feature is that (1) the ratio of M_w and M_n are as large as 7 to 40. In case of homogeneous polymerization in solution, the ratio is usually around 2. In case of bulk polymeriza-tion such as radical polymerization of PS, the ratio may reach 2 to 4. On the other hand, the solid state polymeriza-tion of poly(nACMU)s usually produce highly polydisperse samples. This result is reasonable, since a trace amount of impurity and dislocations in crystal may hinder the 1-4 addition reaction of diacetylenes.

The second point is that (2) the M_w/M_n ratio of poly-(4BCMU) is half smaller than that of other soluble poly-(nACMU)s obtained at the same dose levels. This result

suggests that 4BCMU monomer crystal may have a highly regular monomer-arrangement to undergo the 1-4-addition than any other nACMU monomers.

The last point is that (3) the molecular weight of the single crystalline poly(4BCMU) is about 1.5 times larger than that of powder form poly(4BCMU)s. That is to say, an ideal solid state polymerization may have occurred in the macroscopic monomer single crystal rather than in monomer crystallites such as existing in powder-form specimens, because such a monomer single crystal contains little impurities and dislocations rather than the powder form monomers.

2-5-2-c. Shear Rate Dependence of Intrinsic Viscosity

The poly(3BCMU)s in solution are likely to assume an extended chain conformation because of its conjugated backbone, and its dimensions may differ in a good solvent $CHCl_3$ (yellow), and in a poor solvent, $CHCl_3$/n-hexane mixtures (blue or purple). In order to check this consideration, we made a study on intrinsic viscosity in the mixtures as a function of shear-rate. Particularly, we made an attempt to measure the viscosity of completely blue solutions with $CHCl_3$ content X (in mole fraction) < 0.55. However, it was found that these solutions always leave precipitates deposited on the capillary wall of the

viscometer after each experimental run. For this reason
the viscosity measurement was limited to a yellowish brown
solution with X = 0.70, which was apparently more stable
than the blue solution, and a yellow solution in $CHCl_3$.

For flexible macromolecules as well as rigid
ellipsoids, the dependence of $[\eta]$ on shear-rate has been
theoretically elucidated,[B24, B25] and tested by
experiments.[B26, B27] The available theories all may be
cast into a form

$$[\eta] = [\eta]_0 (1 - A\ \beta^2 + \text{higher terms in even}$$
$$\text{powers of } \beta) \qquad (2-3)$$

with

$$\beta = (M[\eta]_0 \eta_s / RT)\ \dot{\gamma} \qquad (2-4)$$

Where $[\eta]$ and $[\eta]_0$ are the intrinsic viscosities at an
apparent shear-rate $\dot{\gamma}$ and the limit of zero shear-rate,
respectively; A is a factor depending on the shape of the
polymer (e.g., the axial ratio for ellipsoids); β is the
reduced shear-rate defined by Eq.2-4, η_s is the solvent
viscosity, M is the solute molecular weight, and RT has
the usual meaning.

The value of $[\eta]$ was determined by the usual procedure using Ubbelohde type capillary viscometers and a four-bulb spiral capillary viscometer. The corresponding value of $\dot{\gamma}$ was calculated using the Hagen-Poiseulle law:

$$\dot{\gamma} = \frac{\rho gh\, a}{2\eta_s \ell} \tag{2-5}$$

Here a and ℓ are the radius and length of the capillary, respectively, h is the height of the midpoint between the upper and lower marks of the bulb above the meniscus of the liquid column; g is the acceleration due to gravity; and ρ is the solvent density. The values of $\dot{\gamma}$ for $CHCl_3$ at 30°C were 650, 950 and 1660 s^{-1} for the three Ubbelohde viscometers, and 53.6, 148.5, 256.4 and 357.3 s^{-1} for the four bulbs of the spiral capillary viscometer.

Figure 2-5 shows typical viscosity vs concentration plots for the poly(3BCMU) sample in $CHCl_3$ at 30°C. The insert in the figure compares the $[\eta]$ vs $\dot{\gamma}$ curve for the $CHCl_3$ solution with that for $CHCl_3$/n-hexane (X = 0.7) solution. From these data, the zero-shear intrinsic viscosities $[\eta]_0$ were estimated to be 236 and 254 $cm^3 g^{-1}$ for $CHCl_3$ and the mixture, respectively. It can be seen that $[\eta]_0$ and its decrease with an increase in $\dot{\gamma}$ are larger for the latter system than for the former one. This
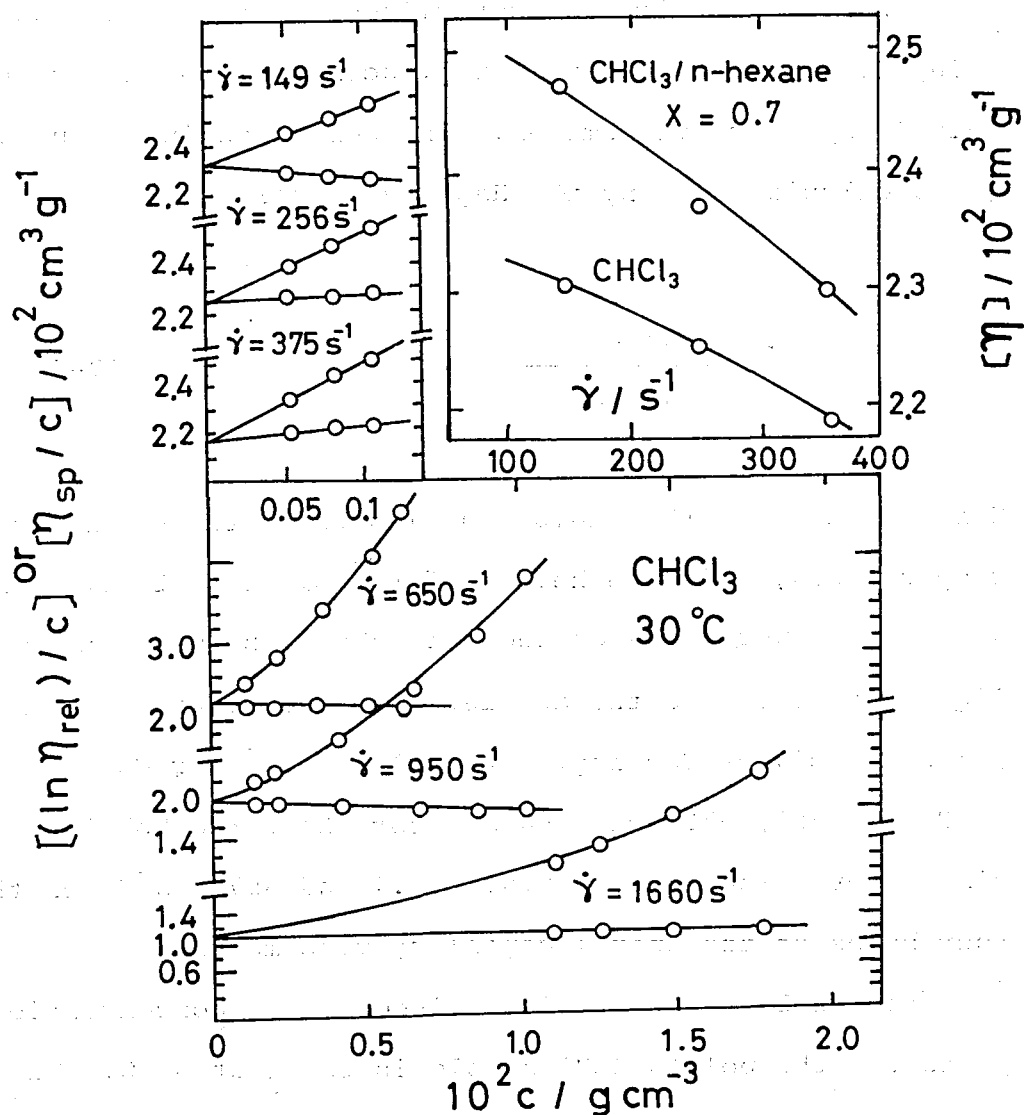
Figure 2-5. Viscosity-concentration plot for poly(3BCMU)/ 45Mrad in $CHCl_3$ at 30°C. The plots of η_{sp}/c and $\ln(\eta_r)/$ c are shown for the data obtained by three Ubbelohde viscometers and by three bulbs of the four-bulb viscometer. The shear-rates for $CHCl_3$ are indicated in the figure. The insert is the $[\eta]$ versus $\dot{\gamma}$ for $CHCl_3$ solution and $CHCl_3$/n-hexane(X = 0.7) solution.

tendency is opposite to that observed for solutions of ordinary flexible polymers, in which $[\eta]_0$ and non-Newtonian behavior are larger in good solvents than in poor solvents.

The $[\eta]$ of the poly(3BCMU) sample in $CHCl_3$ at finite $\dot{\gamma}$ are plotted as $[\eta]/[\eta]_0$ vs log β in Figure 2-6. For comparison, theoretical curves for prolate ellipsoids [B24, B25] and earlier experimental results on polystyrene solutions [B27] are also shown in the figure. The poly(3BCMU)/45Mrad data fall in the region of ellipsoids with very large axial ratios, suggesting that poly(3BCMU) in $CHCl_3$ assumes a highly extended conformation.

The data in the insert of Figure 2-5 shows that $[\eta]$ of the poly(3BCMU)/45Mrad exhibits larger shear-rate dependence in the $CHCl_3$/n-hexane mixture than in $CHCl_3$. Thus it seems that the conformation of this sample is more extended in a poor solvent, $CHCl_3$/n-hexane mixture, than in a good solvent $CHCl_3$, in contrast to the behavior of flexible polymers.

It is known that lyotropic liquid-crystalline solutions exhibit a characteristic rheological behavior when the phase changes from iostropic to anisotropic phases take place. [B28, B29] For example, at the phase transition usually called the A point, [B30] an abrupt change in viscosity occurs. Since poly(3BCMU)/45Mrad appears to assume a highly extended conformation, viscosity measurements were carried out to examine whether the
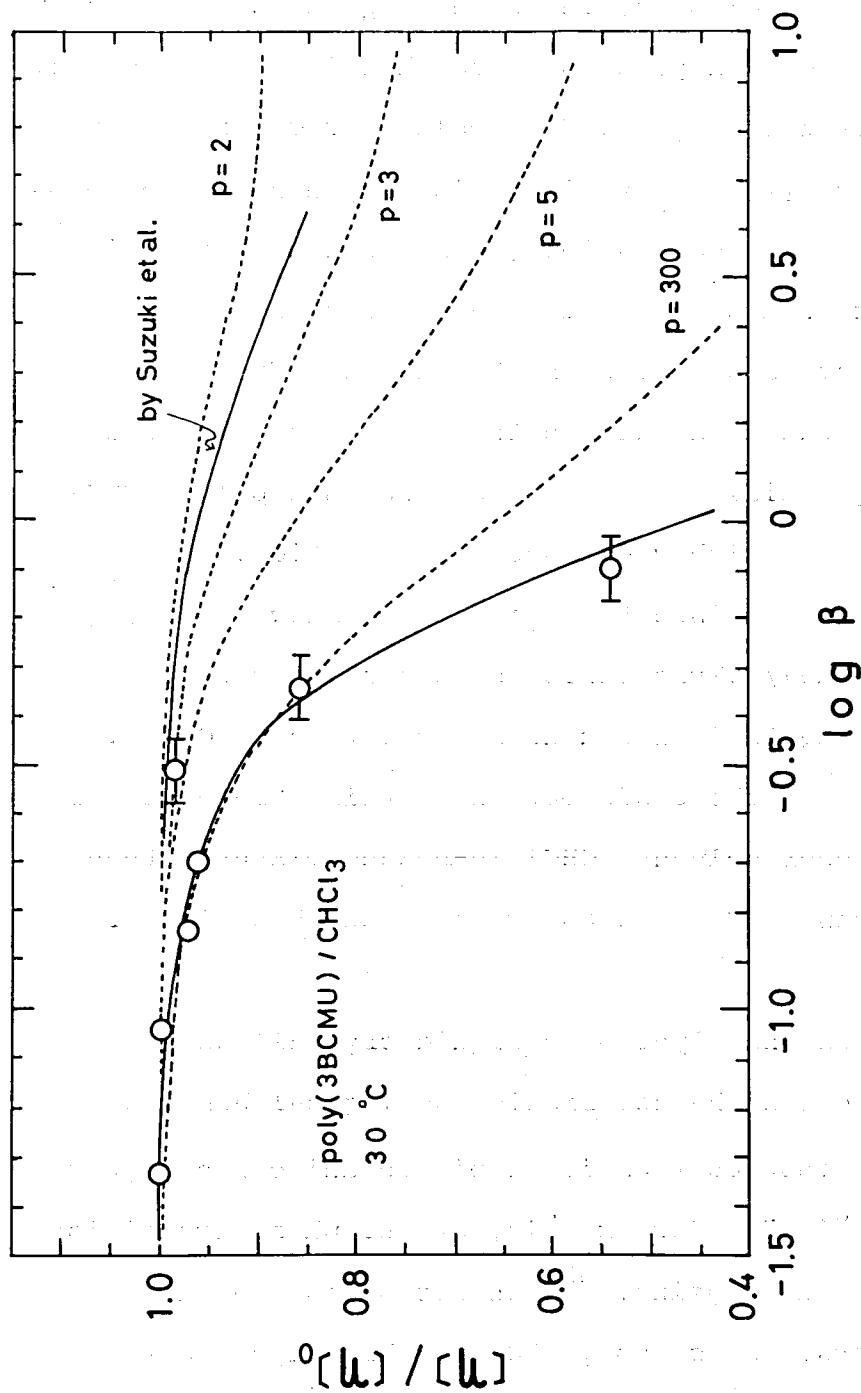
Figure 2-6. The non-newtonian intrinsic viscosity behavior of poly(3BCMU)/45Mrad in CHCl₃ at 30°C. The ratios of $[\eta]$ at $\dot\gamma$ and $[\eta]_0$ at $\dot\gamma \to 0$ are plotted against reduced shear-rate $\beta = (M[\eta]_0\eta_s / RT)\cdot\dot\gamma$. Theoretical curves for prolate ellipsoids with various axial ratios are indicated by the broken lines. The solid curve indicates the data for polystyrene solutions obtained by Suzuki at al. B27

expected liquid crystalline behavior appears in the η_r (relative viscosity) vs c for poly(3BCMU)/45Mrad sample in CHCl$_3$ at 30°C. For the solutions of c below 3.16 wt%, η_r increased in proportion to $c^{2.5}$ and reached 63 at the 3.16 wt% solution. For those of c between 3.16 and 5.37 wt%, η_r was proportional to $c^{7.5}$. Above 5.37 wt% the polymer was not dissolved completely in CHCl$_3$. If the break at c = 3.16 wt% on the log η_r vs log c curve corresponds to the A point for this system, a sudden drop in η_r should be seen at or in the vicinity of this point. However, for the solutions with c below 5.37 wt% no such drop in viscosity was observed.

According to Flory, [B31] the polymer volume fraction v_2 at the A point of a solution of rodlike macromolecules is given by

$$v_2 \simeq (8/p)(1 - 2/p) \qquad\qquad (2\text{-}6)$$

where p is the axial ratio of the rod. For the poly(3BCMU)/ 45Mrad sample, the axial ratio p may be estimated to be as large as 300 from the data in Figure 2-6. Assuming the specific volume of the polymer to be 1 cm^3/g and substituting p = 300 into Eq. 2-6, we obtain $v_2 \simeq 2.65$ %, which is somewhat lower than the volume fraction at the break point. Furthermore, within the solubility limit no

evidence was obtained for the liquid crystal formation of poly(3BCMU). These findings appear to be due partly to a partial flexibility of the polymer chain and partly to the tendency of aggregate formation in solutions.

Another interesting observation on moderately concentrated ($c > 4$ wt%) solutions of poly(3BCMU)/45Mrad in $CHCl_3$ was that they exhibited a significant Weissenberg effect.[B32] This fact also suggests that the poly(3BCMU) chain assumes a highly extended (but not rigid rodlike) conformation in $CHCl_3$.

2-6. Conclusion

Monomers of five different (nACMU)s were prepared in this study. From these monomers except 2ECMU, the polymers were obtained by the solid state polymerization with ^{60}Co γ-ray irradiation of 45 Mrad dose. The partially polymerized poly(nACMU)s obtained show a black-golden color, corresponding to the exsistence of conjugated main chains. PS-reduced molecular weights, M_n and M_w, of the poly-(nACMU)s from GPC measurements were about 0.1×10^6 and 1×10^6, respectively. The samples have sufficiently high molecular weight to form tough films. Their single crystals of poly(4BCMU) were also obtained. Its typical size was $3 \times 2 \times 0.2$ mm^3.

Poly(3BCMU) samples obtained at low doses have fairly

high molecular weight and narrow distribution and those at

high doses relatively low molecular weight and broad dis-

tribution. We found that the molecular weight and its

distribution of poly(3BCMU) may vary with dose levels in

the solid state polymerization.

Non-Newtonian intrinsic viscosities of poly(3BCMU)/

45Mrad solutions in $CHCl_3$ and in $CHCl_3$/n-hexane mixture

were compared. The result suggested that the polydi-

acetylene chains may assume a more extended conformation

in poor solvents rather than in good solvents.

References

B1. Baughman, R. H. J. polym. Sci., Polym. Phys. Ed.,
     1974, 12, 1511.

B2. Baughman, R. H.; Yee, K. C. J. Polym. Sci.,
     Macromolecular Rev., 1978, 13, 219.

B3. Enkelmann, V. Macromol. Chem., 1978, 179, 2811.

B4. Wegner, G. Macromol. Chem., 1971, 145, 85; ibid.,
     1972, 154, 35.

B5. Tieke, B.; Lieser, G.; Wegner, G. J. Polym. Sci.,
     Polym. Chem. Ed., 1979, 17, 1631.

B6. Miller, G. G.; Patel, G. N. J. Appl. Polym. Sci.,
     1979, 24, 883.

B7. Chance, R. R.; Patel, G. N. J. Polym. Sci., Polym.
     Phys. Ed., 1978, 16, 859.

B8. McGhie, A. R.; Kalyanaraman, P. S.; Garito, A. F. Mol.
     Cryst. Liq., Crys., 1979, 50, 287.

B9. Pater, G. N.; Chance, R. R.; Witt, J. D. J. Chem.
     Phys., 1979, 70, 4387.

B10. Patel, G. N.; Khanna, Y. P.; Ivory, D. M.; Sowa, J. M.;
     Chance, R. R. J. Polym. Sci., Polym. Phys. Ed.,
     1979, 17, 899.

B11. Patel, G. N.; Chance, R. R.; Turi, E. A.; Khanna, Y. P.
     J. Am. Chem. Soc., 1978, 6644.

B12. Se, K.; Ohnuma, H.; Kotaka, T. Polymer J., 1982,
     14, 895.

B13. Org. Synthesis coll., vol. 3, 1955, 698.

B14. Org. Synthesis coll., vol. 3, 1955, 778.

B15. Hay, A. S. J. Org. Chem., 1962, 27, 3320.

B16. Paterl, G. N. Polym. Prep., Am. Chem. Soc., Div.
Polym. Chem., 1978, 19, 154.

B17. Brandsma. L., "Preparative Acetylenic Chemistry",
Elsevier Publishing Co., Amsterdam, 1971.

B18. Se, K.; Ohnuma, H.; Kotaka, T. Macromolecules, 1983,
16, in press.

B19. Patel, G. N.; Walsh, E. K. J. Polym. Sci., Polym.
Lett. Ed., 1979, 17, 203.

B20. Ouano, A. C.; Kate, W. J. Polym. Sci., Polym. Chem.
Ed., 1974, 12, 1151.

B21. Cantow, H. J.; Siefert, E.; Kurn, R. Chem. Eng.
Technol., 1966, 38, 1032.

B22. Mikulski, C. M.; Russo, P. J.; Saran, M. S.;
MacDiarmid, A. G.; Garito, A. F.; Heeger, A. J.
J. Am. Chem. Soc., 1975, 97, 6358.

B23. Chance, R. R.; Patel, G. N.; Witt, J. D. J. Chem.
Phys., 1979, 71,206.

B24. Saito, N. J. Phys. Soc., 1951, 6, 197.

B25. Scherga, H. A. J. Chem. Phys., 1955, 23, 1526.

B26. See, for example; Yang, J. T. J. Am. Chem, Soc.,
1958, 81, 1783; ibid, 1959, 82, 1902.

B27. Kotaka, T.; Suzuki, H.; Inagaki, H. J. Chem. Phys.,
1966, 45, 2770; ibid, 1969, 51, 1279.

B28. Papkov, S. P.; KiLichikhin, V. G.; Kalmykova, v. D.

J. Poly. Sci., Polym. Phys. Ed., <u>1974</u>, 12, 1753.

B29. Gray, G. W., "Molecular Structure and Properties of Liquid Crystal", Academic Press, New York, <u>1962</u>.

B30. Robinson, C. Trans. Faraday. Soc., <u>1956</u>, 52, 571.

B31. Flory, P. J. Proc. R. Soc., London Ser. A, <u>1956</u>, 234, 73.

B32. Ferry, J. D. "Viscoelastic Properties of Polymers", John Willey and Sons, New York, <u>1970</u>.

Chapter 3

CHARACTERISTIC COLOR CHANGES OF POLY(nACMU)S

3-1. Introduction

Polydiacetylenes have the highly conjugated

backbones. [C1, C2] This feature of poly(nACMU)s together

with their solubility and fusibility allows us to observe

visually the process of polymerization, chemical reactions,

and physical transitions such as melting, dissolution, and

hydrolyzation, through color changes due to the conforma-

tional transitions of the polymer chains. [C3-C6]

The conjugated main chains of polydiacetylenes absorb

light in the visible portion of the spectrum. On the other

hand, diacetylene monomers have two non-conjugated triple

bonds, which do not absorb visible light. Therefore, as

the polymerization proceeds, the colorless monomer eventually

changes to black polydiacetylene with metallic luster.

This color change was the first example by which one saw

the process of polymerization by eye. [C7, C9] The highly

conjugated backbones of poly(3BCMU) usually assume planar

conformation stabilized by the hydrogen bonds between the

urethane moieties in the neighboring side chains.

Breaking of the hydrogen bonds either by melting the crystallites or by dissolving the polymer in a good solvent tends the polymer backbones to assume nonplanar conformation. The effective conjugation length is relatively long in the planar backbones, which absorb long wavelength light and hence look blue. On the other hand, the effective conjugation length is rather short in nonplanar backbones, which therefore absorb only short wavelength light and look yellow. These characteristic color changes will be discussed in this chapter.

Because 3BCMU monomer and poly(3BCMU) underwent most striking color changes during these visual processes, we employed them as the model system in this study. Poly(3BCMU) is soluble in usual organic solvents and gives colored solutions. [C10, C11] Their color depends on the solvent quality such as the ratio of good versus poor solvent in the mixture. The change in color corresponds to that in the effective length of conjugation extending along the chain backbone, which is affected by the conformation of poly(3BCMU) chains in the solution. [C9] Hence, the phenomenon of the characteristic color change in solution was examined in detail to establish phase diagrams for the conformational transitions in poly(3BCMU) solution. Effects of temperature and molecular weight on this phenomemon were also studied. Further spectroscopic studies were carried out to elucidate the details of the color change

by employing UV absorption and Raman spectroscopy.

Two ester groups in the side chain of poly(3BCMU) can be easily hydrolyzed, and the polymer becomes soluble in aqueous media. The potassiun salt of KOH hydrolyzed poly-(3BCMU), abbreviated as poly(3KAU), also exhibits a similar characteristic color change by varying pH. This behavior was also examined.

3-2 Experimental Procedures

Materials: A few drops of 3BCMU/acetone solution were used to demonstrate color changes on a filter paper due to polymerization, melting and recrystallization in partially polymerized polymer/monomer solid solution.

To establish phase diagrams of poly(3BCMU) in $CHCl_3$/n-hexane mixture, we employed 45 Mrad and 0.09 Mrad samples.

For the visualization of the color changes in aqueous media, we hydrolyzed poly(3BCMU)/45 Mrad sample to obtain potassium salt of poly[4,6-decadiyn-1,10-diol bis(carboxyl methyl urethane)] abbreviated as poly(3KAU), which has the substituent R of the form: $R = -(CH_2)_3O-CONH-CH_2-COO^- K^+$.
To approximately 30 mL of poly(3BCMU)/$CHCl_3$ solution, we added a few mL of 6N KOH/CH_3OH solution and stirred the mixture at room temperature for 20 minutes. The degree of saponification was not determined quantitatively. However, by comparing the solubility of these two polymers,

we concluded that poly(3BCMU) was saponified substantially to poly(3KAU). The hydrolyzed materials was soluble in water but not in $CHCl_3$, while poly(3BCMU) was opposite.

Methods: The polymerization of 3BCMU on a filter paper was carried out using a 245 nm wavelength UV lamp. For crystalline melting in polymer/monomer solid solution on the filter paper, a jet dryer was employed.

Phase diagrams on 0.09 and 45 Mrad samples in $CHCl_3$/ n-hexane mixture were determined by visual observation of the color changes. For determining absorption spectra of the solutions, a JASCO spectrophotometer (Model UVDEC-5A, Nihon Bunko Co.) was employed. Raman spectra of the solutions were obtained by a JASCO R-500 double beam monochrometer with plane polarized light of 514.5 nm length from an argon-ion laser source.

3-3. Results and Discussion

3-3-1. Demonstration of Color Changes

Color changes in solid: The polymerization of 3BCMU crystallites on a filter paper by UV irradiation proceeds in 1,4-addition to form polymer/monomer solid solution, accompanying development of color. Partially polymerized and fully polymerized polymer/monomer mixtures exhibit

another color changes by heating and cooling. These visual processes are demonstrated in photographs 1. A few drops of 3BCMU/acetone solution were placed on a piece of filter paper and dried by breeze of a drier. Thin colorless coating of 3BCMU on the filter paper was obtained as shown in photograph 1-a. Upon irradiating the filter paper with the UV lamp, blue color of poly(3BCMU) appeared immediately, and intensified and turned to deep purple color after another one minute exposure, as seen in photographs 1-b and -c, respectively. Further exposure completed the polymerization, and the color turned metallic black gold. This color development corresponds to formation of poly(3BCMU) with increasing yield by prolonged UV irradiation.

When this blue filter paper with partially polymerized 3BCMU (photograph 1-b) was heated by a drier, the color changed to red-purple, and then to yellow upon further heating to higher temperature, as shown in photograph 1-e. The color change from purple to yellow corresponds to the melting of poly(3BCMU) crystallites.

Color Changes in Solution: Crystalline poly(3BCMU)/45 Mrad sample looked like coal inlaid with gold as shown in photograph 2-d. The powder form sample as well as the partially polymerized sample on a filter paper were soluble in $CHCl_3$ and gave orange-colored solution, as shown in photograph 2-b. By slowly evaporating the solvent, a film with metallic gold luster as shown in photograph 2-a was
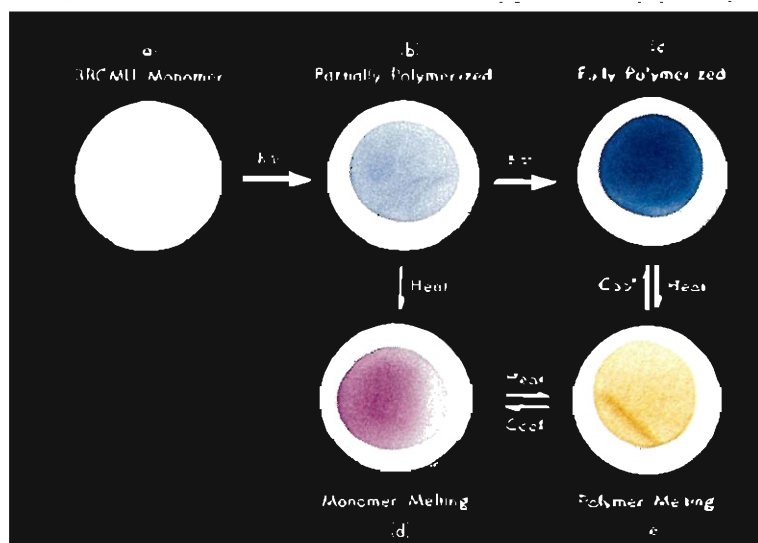
photograph 1.   Color changes on filter paper·demonstrate
the processes of polymerization of 3BCMU monomer and
melting/recrystallization of poly(3BCMU)/3BCMU solid
solution: (a) colorless monomer crystal; (b) partial
polymerization by 254nm UV irradiation; (c) further
polymerization by prolonged exposure to the UV irradi-
ation (d) color changes in the mixture of polymer/monomer
crystal by heating; (e) color changes in melting of poly-
mer crystal.
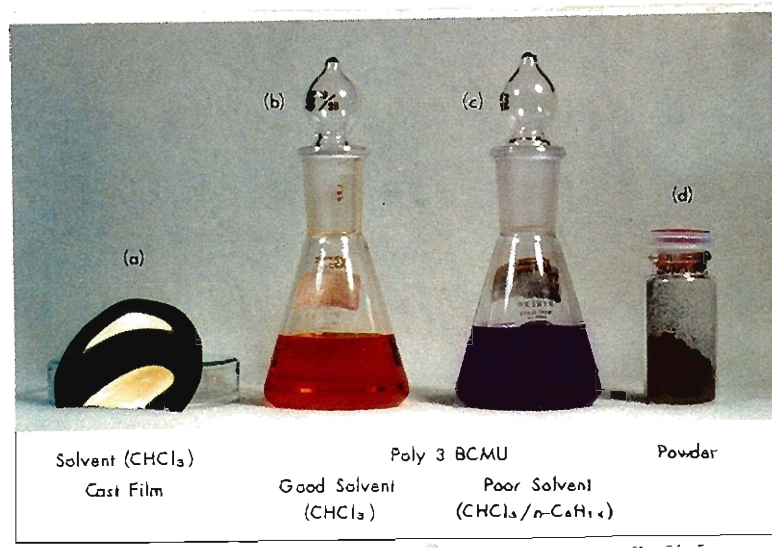
Photograph 2. Poly(3BCMU) in solutions and in the solid state: (a) $CHCl_3$ as-cast film; (b) $CHCl_3$ solution; (c) $CHCl_3$/n-hexane mixture; (d) powder-form poly(3BCMU) specimen polymerized by ^{60}Co γ-ray.
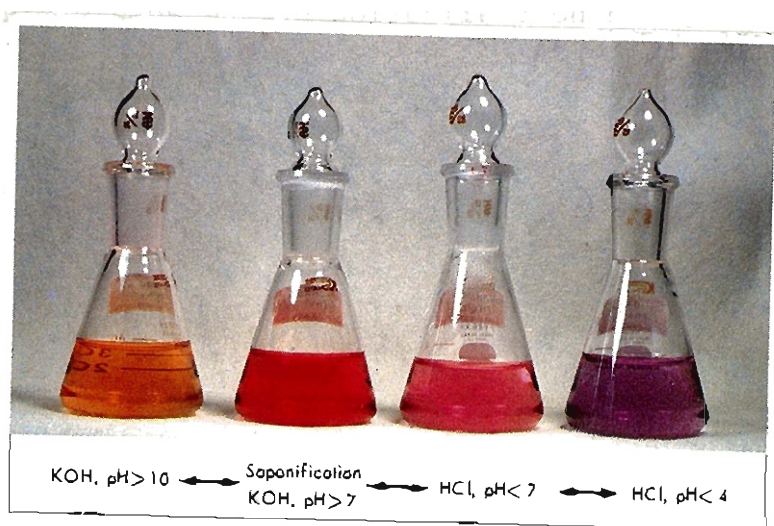
Photograph 3. Color changes in poly(3KAU) aqueous solution with pH: (a) alkaline solution, pH > 10; (b) mild alkaline solution, pH > 7; (c) mild acidic solution, pH < 7; (d) acidic solution, pH < 4.

obtained. Addition of a poor solvent, n-hexane, to orange
colored poly(3BCMU)/CHCl$_3$ solution changed its color to
purple, as shown in photograph 2-c.

Potassium salt of poly(3KAU) dissolved in water gave
red-yellow solution above pH = 7, as shown in photograph
3-b. When the pH was raised above 10 by adding KOH, the
solution color changed to yellow, as shown in photograph
3-a. On the contrary, when the pH was lowered, it changed
to pink solution (photograph 3-c) and eventually turned to
blue colored solution as shown in photograph 3-d. Finally,
in acidic solution with pH below 4 purple precipitates
emerged. Obviously, these color changes correspond to the
nonplanar to planar conformational transition of the chain
backbones by the neutralization of the acidic side chains.

3-3-2. Phase Diagrams for Color Changes

3-3-2-a. Phase Diagrams

Poly(3BCMU) is soluble in common organic solvent such
as CHCl$_3$, N-methyl-2-pyrroridones, m-cresol, dichloroacetate,
and dimethylformamide. Among these solvent, CHCl$_3$ is the
best solvent which dissolves poly(3BCMU) up to nearly 5 %
at room temperature. n-Alkanes and alcohols, on the
contrary, are nonsolvent. We selected CHCl$_3$ as the good
solvent and n-hexane as the nonsolvent.

By titrating poly(3BCMU) CHCl$_3$ solution with n-hexane

and back titrating the solution with CHCl$_3$, we established

phase diagrams as a function of polymer concentration c

and solvent composition X.   Figure 3-1 shows the phase

diagrams obtained for poly(3BCMU)/45 Mrad and 0.09 Mrad

samples at 22 °C and 0 °C.   The dashed line indicates a

typical route of titration and back titration.   For example,

poly(3BCMU)/ 45 Mrad in CHCl$_3$ with the concentration of

10^{-3} mol l^{-1} (the point a in Figure 3-1) showed orange

color.   Addition of n-hexane to the solution made its

color change from orange to blue abruptly at the mole

fraction of CHCl$_3$ X$_C$ = 0.68 (at the point of b).   By

further addition of n-hexane blue precipitates of the

polymer appeared at the point c (X$_C$ = 0.43).   On the

contrary, addition of CHCl$_3$ to the solution at the point

d (X$_C$ = 0.35) made the precipitates dissolve at the point

e to yield blue solution.   Further addition of CHCl$_3$ changed

the color of the solution from blue to yellow at the point

f, different from the b.   The transitions between these

different colors were reversible.   These reversible color

changes were also very sharp so that the transitions could

detected accurately by visual observation with naked eyes.

For pure CHCl$_3$ solution with polymer concentration above

10^{-2} mol l^{-1}, dark blue precipitates appeared by addition

of only one drop of n-hexane.   The space between the two

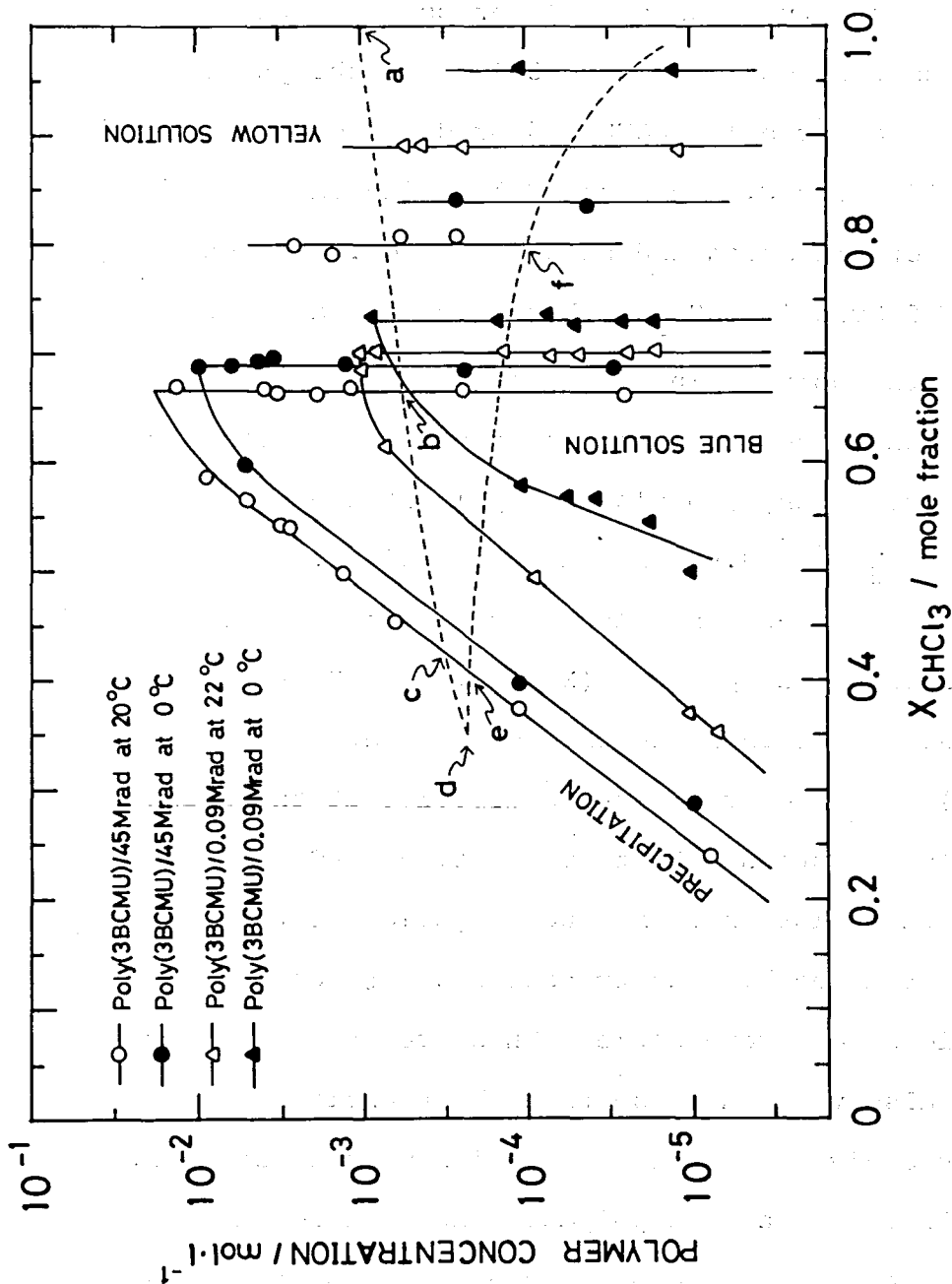vertical lines between b (X$_C$ = 0.66) and f (X$_C$ = 0.80)

Figure 3-1. Phase diagrams for poly(3BCMU)/45Mrad (circles) and poly(3BCMU)/0.09Mrad (triangles) in $CHCl_3$/n-hexane mixture. The closed and open marks (circles and triangles) represent the results obtained at 20°C and 0°C, respectively. The vertical lines around X_{CHCl_3} = 0.65-0.75 and slanting lines are obtained by titration with n-hexane. The vertical lines around X_{CHCl_3} = 0.80-0.95 represents the results from back titration of blue solutions with $CHCl_3$. The dashed curve represents one of the routes of forward and backward titrations.

-64-

indicates the transition region.

The phase diagrams obtained have the following features: (i) The solvent compositions X_c and X_c' (in the mole fraction of $CHCl_3$), at which the yellow-to-blue and the blue-to-yellow transition take place, respectively, do not coincide, and always $X_c < X_c'$. (ii) Neither X_c nor X_c' depends on the polymer concentration. However, (iii) the transition from precipitation to dissolution takes place reversibly at the same composition X_p, which depends on the polymer concentration. Besides these features already pointed out by Patel et al., [C13] the present results indicate some additional features such as follows: (iv) By lowering the temperature from 20°C or 22°C to 0°C, the phase boundaries shifted to the good solvent side. Particularily, the shift of X_c' for the 0.09 Mrad sample was substantial. Comparison of the phase diagrams of the two samples shows that (v) the diagram of the 0.09 Mrad sample is located in the better solvent side than that of 45 Mrad one, but that the difference between the X_c of the two samples is not as large as either that between their X_c' or that between their X_p.

3-3-2-b. Absorption Spectra

Figure 3-2 shows typical absorption spectra of
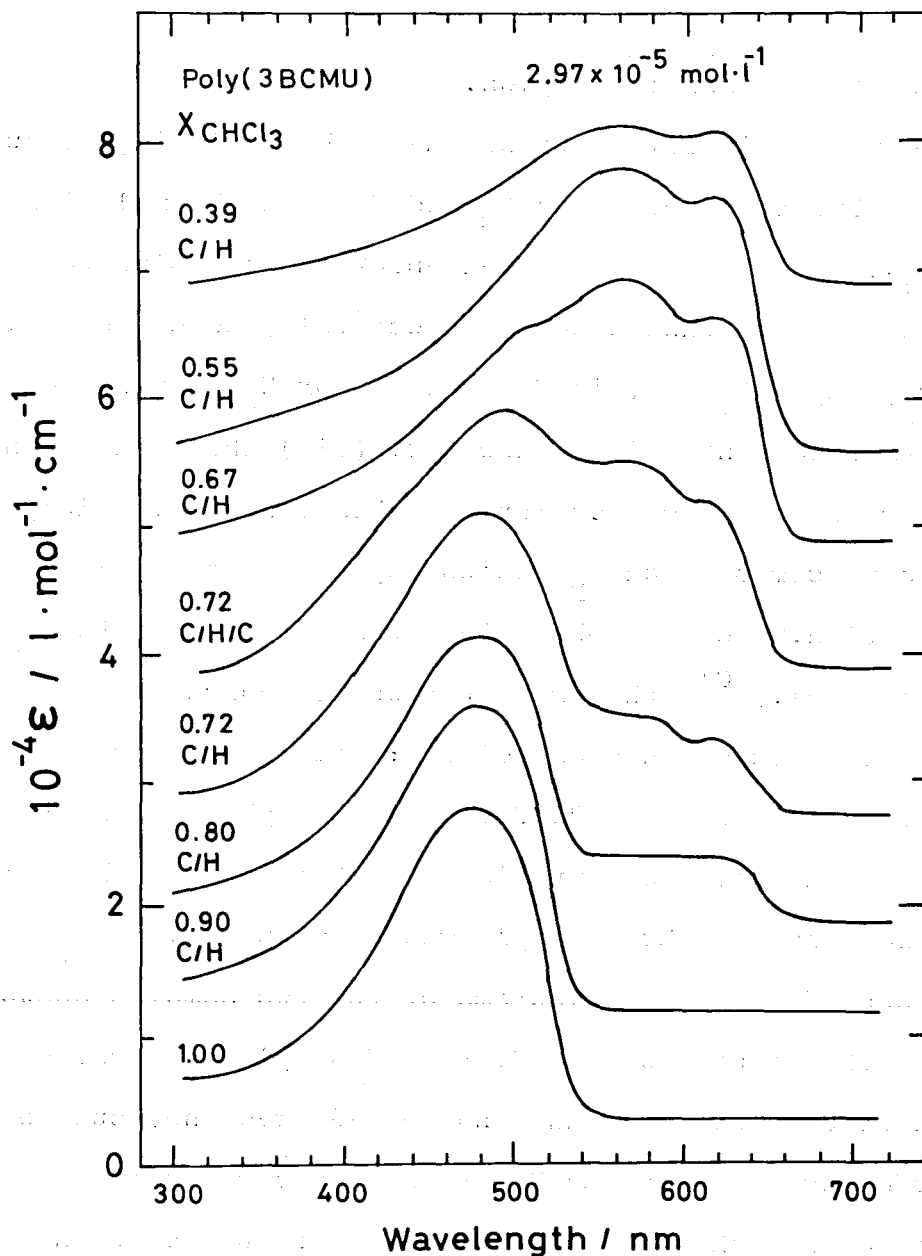
Figure 3-2. Visible absorption spectra of solutions of poly(3BCMU)/45Mrad for various mole fraction of $CHCl_3$ in n-hexane at 16°C. The spectra are progressively offset by arbitrary amount. The polymer concentration is 2.97 x 10^{-5} mol l^{-1}. C/H/C implies that the solution in $CHCl_3$/n-hexane was back titrated with $CHCl_3$ until X_{CHCl_3} = 0.72.

poly(3BCMU)/45Mrad sample in $CHCl_3$/n-hexane mixtures during the processes of titration and back titration. The spectra of the solutions of concentrations between X_c and $X_{c'}$ changed gradually with increasing annealing time. Figure 3-3 shows that the spectrum of a visibly yellow solution of the 45 Mrad sample obtained by adding n-hexane to the $CHCl_3$ solution to X = 0.75 underwent a blue shift although the solution remained visibly yellow after 480 hours annealing. The spectrum of the visible blue solution of the same sample of X = 0.75 (X_c' = 0.80) obtained by back titrating the mixture of X = 0.66 with $CHCl_3$ also showed a blue shift. These blue shifts suggest that at X = 0.75 the blue-colored solution is more stable than the yellow colored one. However, the change was so slow that it was impossible to estimate the time required for these solutions to reach equilibrium. Actually, it was beyond our estimation whether such an equilibrium exists.

From Fourier transform infrared spectra, Patel et al., [C14] suggested that the color changes arise from the planar-nonplanar conformational transition of the poly (nACMU) backbone and that the planar, fully conjugated conformation be stabilized by intramolecular hydrogen bonding of urethane moieties on the adjacent substituent groups. The planar-conformation is schematically illustrated. in Figure 3-4. The disruption of the planarity or the shortening of the conjugation length l_e of the backbone is
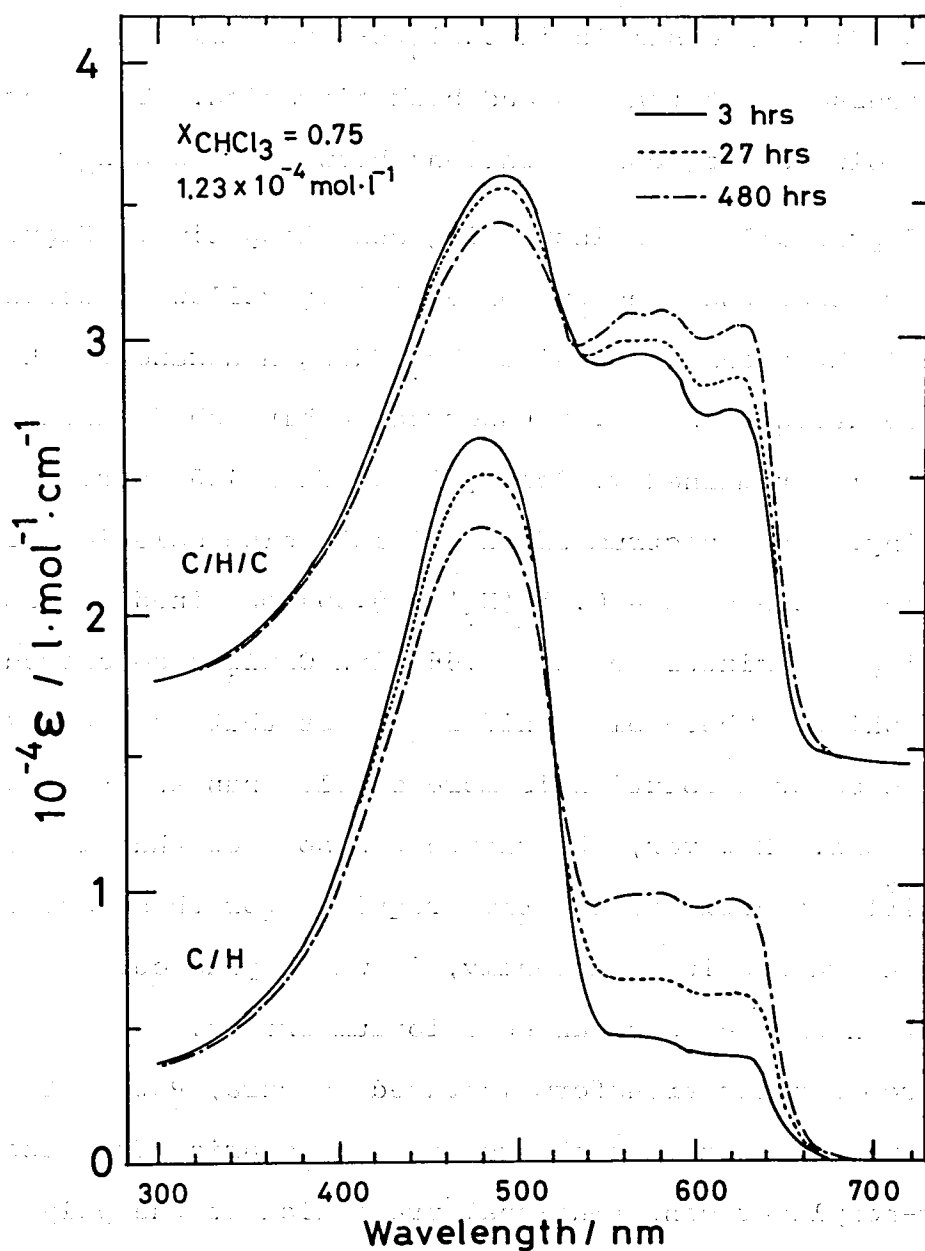
Figure 3-3. Change of spectra with time of two solutions of poly(3BCMU)/45Mrad with X_{CHCl_3} = 0.75: One coded as c/h was obtained by titrating $CHCl_3$ solution with n-hexane, while the other C/H/C by back titrating $CHCl_3$/n-hexane solution with $CHCl_3$.
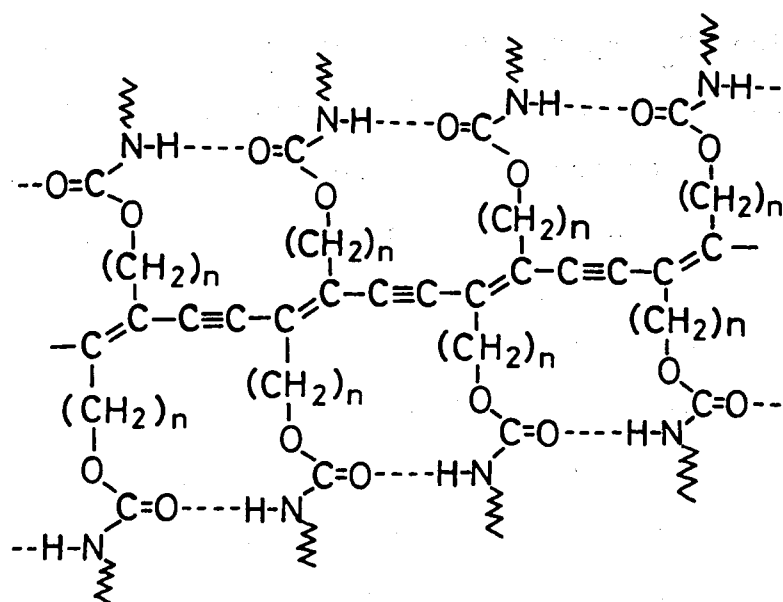
Figure 3-4. Planar, hydrogen-bonded conformation of poly(nACMU)s/poly(ene-yne) isomer as suggested by Patel et al. [C14] The dashed lines between N-H and O=C indicate hydrogen bonds.

compensated for by an increase in entropy of the substituent groups due to the breaking of hydrogen bonds in the $CHCl_3$ solution. On the other hand, the decrease in entropy of the side groups enhances the planarity of the backbone, and gives rise to an increase in the critical solvent compositions X_c and X_c' (i. e., shift to the $CHCl_3$ rich side). The values X_c and X_c' summarized in Table 3-1 indicates that as the temperature is lowered, i. e., the contribution of entropy is decreased, both X_c and X_c' increase, especially the latter substantially.

On the basis of a modified free electron theory of Kuhn, [C15] Patel [C9, C13] calculated the effective conjugation length l_e from the wavelength of the visible absorption peak. For the yellow solution with the absorption peak at 475 nm, l_e was estimated to be 6 to 7 repeat units or 12 to 14 conjugated multiple bonds. For blue solutions l_e exceeded 30 repeat units.

3-3-2-c. Raman Spectra

Raman spectra were determined on 0.297 $\mu mol\ dm^{-3}$ solutions. Figure 3-5 shows typical results. The spectrum of the yellow solution excited by 514.5 nm radiation exhibits two strong bands due to the resonance Raman effect. [C16] According to Baughman et al., [C17, C18] the band at 2125 cm^{-1} may be assigned to $-C{\equiv}C-$ vibration and

Table 3-1. Critical solvent compositions for
the color transition in poly(3BCMU) solutions. [a]

Code	Temp/°C	X_C	X'_C
45Mrad	20	0.66	0.80
45Mrad	0	0.68	0.84
0.09Mrad	22	0.70	0.89
0.09Mrad	0	0.73	0.96

a) X_C and X'_C, indicating the mole fraction of $CHCl_3$
at the color transition points, determined by the
titration of $CHCl_3$ solution with n-hexane and of
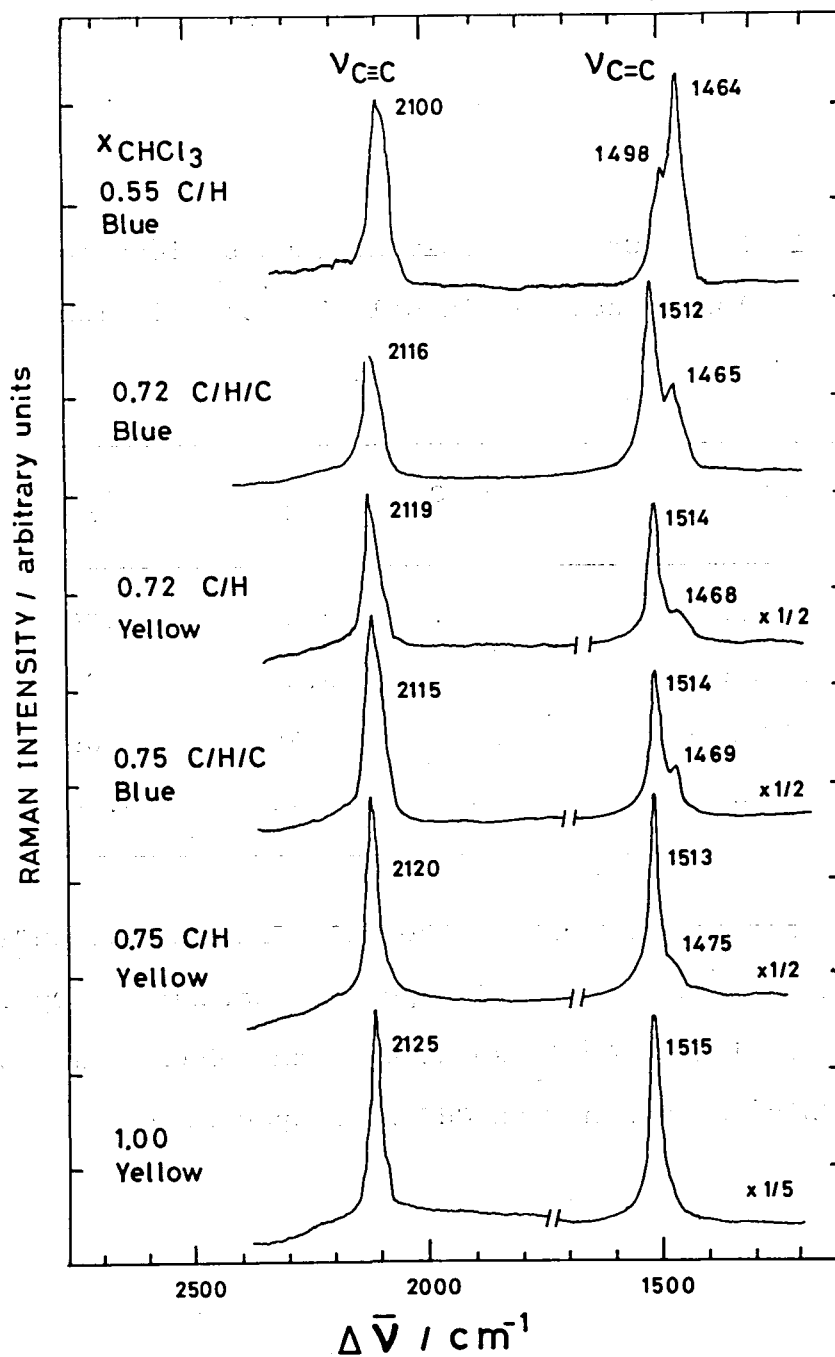a blue solution with $CHCl_3$, respectively.

Figure 3-5. Raman spectra of 0.297 mol dm^{-3} solutions of poly(3BCMU)/45Mrad at 25°C in CHCl$_3$ and in CHCl$_3$/ n-hexane mixture.

the one at 1515 cm^{-1} to -C=C- vibration. For the blue

solution of X_c = 0.55, the -C≡C- band shifts to 2100 cm^{-1}

and the -C=C- and to 1464 cm^{-1}, accompanied with a small

band at 1498 cm^{-1}. It should be noted that visibly blue

and yellow solutions obtained at the same solvent

compositions (X_c = 0.72 and 0.75) exhibit somewhat different

Raman spectra. This difference suggests that, in the

solutions between X_c and X_c', the intramolecular hydrogen

bonds between adjacent urethane moieties, which influences

the planarity of the molecule, are unstable.

Probably, electron delocalization in conjugated

backbone chains is responsible for the above-mentioned

lowering of -C≡C- and -C=C- vibration frequencies as well

as for the yellow-to-blue color transition. In order to

evaluate the difference in the concentration of delocalized

electrons, we carried out an electron spin resonance (ESR)

measurement using a Japan Electron Optics Lab. Model

JES-FE 1X apparatus provided with a 100 kHz modulator.

However, no significant difference was detected between

the ESR spectra of the two solutions. Therefore, the color

changes result from changes in the effective conjugated

length, not from changes in the number of delocalized

electrons.

3-4. Conclusion

The process of polymerization was observed as the development of blue color. The conformational changes of poly(3BCMU) due to melting or dissolution were observed as color changes between yellow and blue with naked eyes. These drastic color changes were demonstrated in this chapter.

Phase diagrams for the changes in color of poly(3BCMU)/ 45Mrad and poly(3BCMU)/0.09Mrad samples in $CHCl_3$ and $CHCl_3$/ n-hexane were compared. The critical solvent compositions ($CHCl_3$ content) X_c and X_c' at which yellow-to-blue or blue-to-yellow changes, respectively, occurred were independent of polymer concentration but varied with molecular weight and temperature. Visible absorption spectra and Raman spectra were compared for yellow $CHCl_3$ and blue $CHCl_3$/n-hexane solutions of poly(3BCMU)/45Mrad samples. The spectra of poly(3BCMU) solutions between X_c and X_c' gradually changed to blue light side with increasing annealing time. Intramolecular hydrogen bonds between adjacent urethane moieties were found to be unstable in the solution between X_c and X_c'.

Conjugation lenghts of poly(3BCMU) chain in the yellow and in the blue solutions were estimated to be 6 to 7 repeat units and 30 repeat units, respectively. However, the concentration of delocalized electrons in the

backbones appears to be the same for both yellow and blue

solutions.

References

C1.   Wegner, G.   J. Polym. Sci., 1971, B9, 133.

C2.   Baughman, R. H.; Yee, K. C.   J. Polym. Sci.,
Macromolecular Rev., 1978, 13. 219.

C3.   Patel, G. N.; Chance, R. R.; Witt, J. D. Polym. Prepr.,
Am. Chem. Soc., 1978, 19, 160.

C4.   Patel, G. N.. Polym. Prep., Am. Chem. Soc., 1979, 20,
452.

C5.   Patel, G. N.   Chem. and Eng. News, Aug., 4, 1980, 24.

C6.   Kotaka, T.; Se, K.; Ohnuma, H.; Patel, G. N.   Kagaku,
1982, 36. 811.

C7.   Patel, G. N.   J. Polym. Sci., Polym. Lett. Ed., 1978,
16, 607.

C8.   Se, K.; Ohnuma, H.; Kotaka, T.   Polymer J., 1982, 14,
895.

C9.   Patel, G. N.; Chance, R. R.; Wott, J. D.
J. Chem. Phys., 1979, 70, 4387.

C10. Patel, G. N.; Witt, J. D.; Khanna, Y. P.
J. Polym. Sci., Polym. Phys. Ed., 1980, 18, 1383.

C11. Chance, R. R.   Macromolecules, 1980, 13, 396.

C12. Bhattachrjee, H. R.; Prezios, A. F.; Patel, G. N.
J. Chem. Phys., 1980, 73, 1478.

C13. Patel, G. N.; Chance, R. R.; Witt, J. D.
J. Polym. Sci., Polym. Lett. Ed., 1978, 16, 1478.

C14. Chance, R. R.; Patel, G. N.; Witt, J. D.
J. Chem. Phys., 1979, 71, 206.

C15. Kuhn, H. Frotschi. Chem. Org. Naturstaffe, <u>1958</u>, 16,

169.; ibid, <u>1959</u>, 17, 404.

C16. Bernstein, H. J., Resonance Raman Spectra: in

"Advance in Raman Spectroscopy", Mathieu, J. P., Ed.,

Heyden, <u>1973</u>.

C17. Melverger, A. J.; Baughman, R. H. J. Polym. Sci.,

Polym. Phys. Ed., <u>1973</u>, 11, 603.

C18. Baughman, R. H.; Witt. J. D.; Yee, K. C. J. Chem.

Phys., <u>1974</u>, 60, 4755.

Chapter 4

STRUCTURE OF PURE AND DOPED POLY(nACMU)S

4-1. Introduction

It has been known that the doping with electron
acceptors such as iodine and AsF_5 makes polyacetylene and
other polymers having conjugated main chains change
from insulators to semiconductors and/or metallic
conductors.[D1-D4] Similar effects of doping on the
conductivities are anticipated for polydiacetylenes. In
order to elucidate this phenomenon we must carry out the
structural analyses as well as measurements of electric
and electronic properties of poly(nACMU)s employed as the
model of linear chain conductors [D5, D6] in this study.

Structural analyses involve the following three areas.
The first area is related to the microscopic structure
observed by spectroscopic techniques such as Raman
scattering and visible absorption. From such studies we
would obtain information on the intermolecular interaction
between the conjugated main chains and dopants. The second
area is related to the crystalline region. We would obtain
answers to such questions whether poly(nACMU) films are

crystalline or amorphous, and whether dopants enter into the crystalline or amorphous regions. The tools to do this may be the differential scanning calorimetry and X-ray diffraction analysis. The last area is related to the amorphous region. The glass transition temperature is a significant parameter related to the amorphous region. Hence, dynamic mechanical and dielectric spectroscopies would be helpful.

All different experimental techniques mentioned above supplement with one another to reveal the complex structures of pure and doped polydiacetylenes.

4-2. Experimental Procedures

4-2-1. Materials

<u>As-Cast Films</u>: Poly(3BCMU), poly(3ECMU), poly(2BCMU) and poly(4BCMU) samples were used for this study. Films of 0.2-0.3 mm thick were cast from 2 % (w/v) $CHCl_3$ solution of the purified polydiacetylenes. The solvent was allowed to evaporate slowly at room temperature over a period of 80 hours. The films of poly(3BCMU), poly(3ECMU), poly(2BCMU) black purple luster, metallic black red luster and metallic red luster, respectively. These films were further dried at room temperature in vacuum of 10^{-3} torr for about 100 hours to completely remove the residual solvent.

Single Crystals and Oriented Films: Needle-like and plate-like single crystals of poly(4BCMU) were obtained by in situ polymerization of 4BCMU monomer single crystals by ^{60}Co γ-ray irradiation. The polymer conversion was about 94 %. Their typical sizes were 6 x 1 x 0.2 mm^3 and 3 x 2 x 0.2 mm^3. Although films of poly(4BCMU) showed a metallic red color, single crystals of poly(4BCMU) were metallic black gold.

Partially oriented films of poly(3BCMU) were obtained by the following procedures: An as-cast film of 0.05 mm thick sandwiched between two teflon sheets was clamped by a stretching device. And the film together with the teflon sheets was stretched to a certain elongation ratio near the melting point of poly(3BCMU).

4-2-2. Doping With Iodine.

The solvent cast and melt-stretched films of poly(nACMU)s were easily doped with iodine, a strong electron-accepter simply by exposing them to iodine vapor in a desiccator evacuated in advance under vacuum of 10^{-3} torr. In some cases, the conductivity was measured simultaneously with iodine-doping in a special home-made glass cell. This technique will be described in the next chapter. The specimens doped with iodine were relatively

stable even in air, where iodine was lost very slowly.
However, AsF_5 was very unstable and toxic and had to be
handled under vacuum. Therefore, in this study only iodine
was used as the dopant, although AsF_5 is a much more
effective dopant. The dopant concentration was varied from
1 to 60 weight % by adjusting the doping time from 1 minute to
30 hours, as shown in Figure 4-1. The amount of iodine absorb-
ed were determined by measuring the weight increases of the
specimens. The dopant concentration Y was expressed as
the number of moles of I_3^- ions per one mole of the nACMU
unit by the reason we will mention later. Therefore we
express the doped films as $poly[nACMU(I_3)_Y]$.

4-2-3. Methods

Raman Spectroscopy: Raman spectra were obtained with a
triple monochrometer Raman spectrometer (Nihon Bunko Co.,
Model R750). The 514,5 nm line from Ar^+ ion laser was
used as the excitation source. The measurements were
carried out at room temperature and at liquid nitrogen
temperature. The temperature was monitored by a copper
constantan thermocouple. Above 7 x 3 x 0.2 mm^3 films
were sealed in the glass tubes to keep the dopant
concentration constant and to prevent frost.
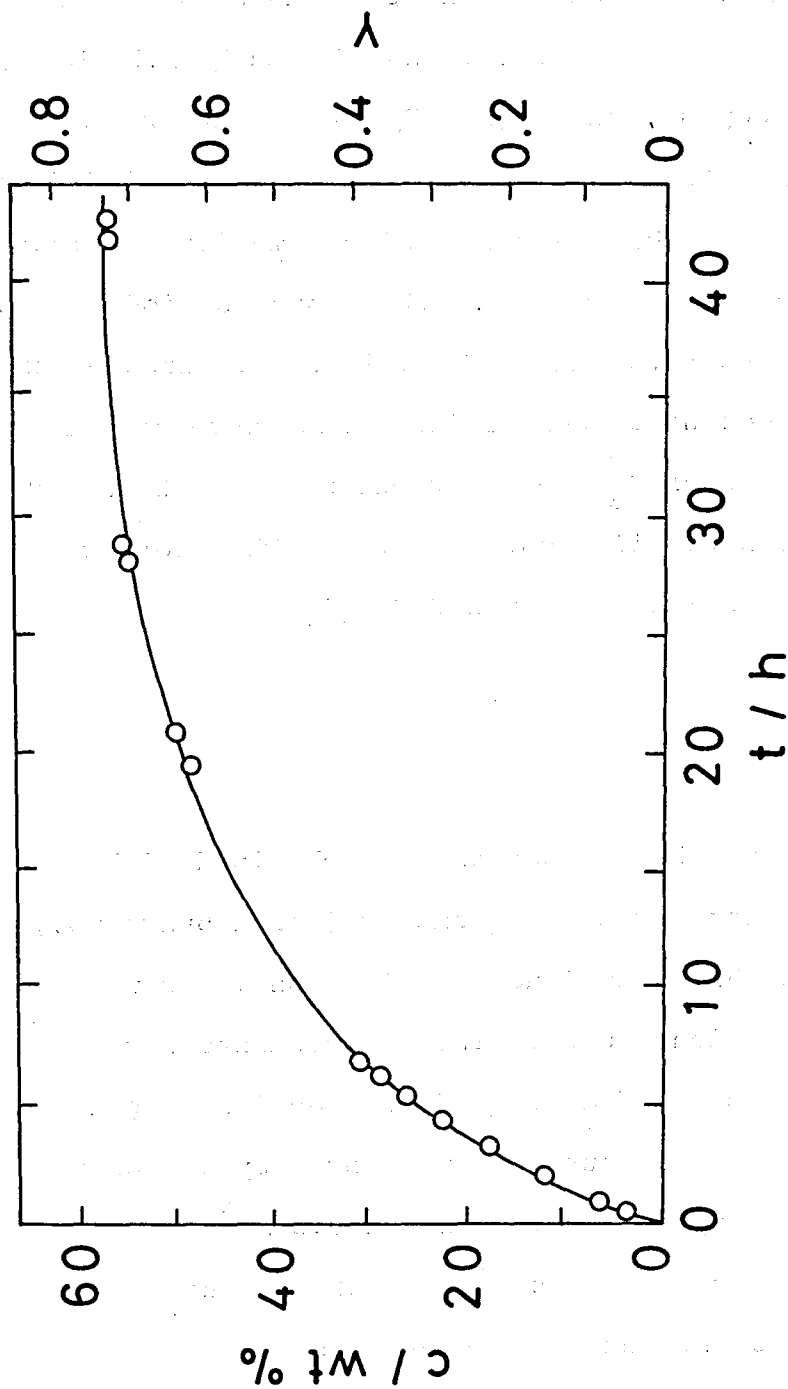
Figure 4-1. Absorption curve of iodine by poly(3BCMU)/45Mrad at room temperature. The vapor pressure of iodine at this temperature is 0.3 mmHg. The Y is the mole ratio of I_3^- per 3BCMU monomer.

Visible Absorption Spectroscopy: Visible absorption spectra of thin films were obtained by a Shimadzu UV-360 spectrophotometer. Thin films of about $30 \times 20 \times 0.002$ mm^3 were prepared from 2×10^{-3} wt% $CHCl_3$ solution by casting on a glass plate and evaporating the solvent. The measurements were carried out at room temperature.

Differential Scanning Calorimetry: Differential scanning calorimetry was carried out on a DSC apparatus (Rigaku Denki Co., Model 8055) with heating rate of 10 K min^{-1}. About 10 mg sample was compressed into an Al pan by a mini-molder. These specimens were used in this study.

X-ray Diffraction: X-ray diffraction patterns were obtained by a cylindrical camera of 3.5 cm radius. The radiation used was CuK $_\alpha$ line monochromatized by Ni filter. Samples of powder-form, as-cast film-form, partially oriented film-form and single crystal-form were measured at room temperature. The exposure time was about 1 hour.

Infrared Spectroscopic Analysis: Measurements of infrared spectra were carried out by JASCO grating infrared spectrophotometers (DC-402 G and A-3, Nihon Bunko Co.) at room temperature. Stretched thin films of about $20 \times 25 \times 0.02$ mm^3 were used as specimens.

<u>Dynamic Mechanical Measurement</u>: Dynamic mechanical measurements were made on a Rheovibron DDV-11 (Toyo-Baldwin Co.) at 110Hz. About 20 x 5 x 0.2 mm^3 films were used. The temperature was monitored by a copper constantan thermocouple. The heating rate was about 1 K min^{-1}. Measurements were made in a box under nitrogen atmosphere to prevent frosting on the samples.

<u>Complex Dielectric Permittivity</u>: Complex dielectric permittivity was measured with a transformer bridge (General Radio Model 1615) in the range of 0.01-100 kHz. A specimen of 25 mm diameter and 0.2 mm thickness was inserted in an improved three-electrode cell with an air-tight brass container. The container was then filled with helium and the measurement was carried out at the heating rate of 0.4 K min^{-1}. The temperature was monitored by a copper constantan thermocouple.

<u>4-3. Results and Discussion</u>

<u>4-3-1. Raman Spectra</u>

We obtained spectra at room temperature and at liquid nitrogen temperature for pure and doped poly(3BCMU)/0.09Mrad films. As shown in Figure 4-2, Raman spectrum of the pure (undoped) specimen at room temperature has two strong bands
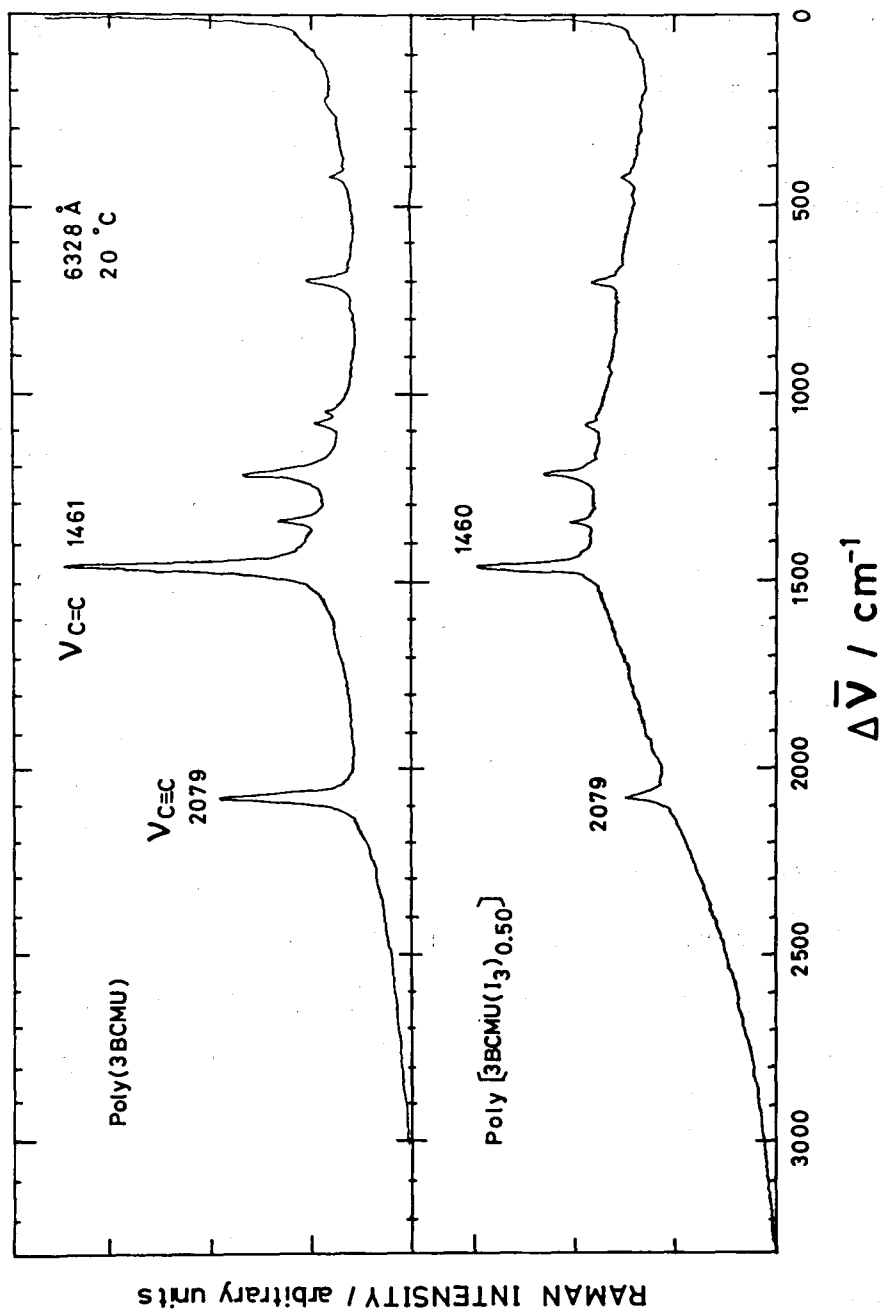
Figure 4-2. Raman spectra of poly(3BCMU) (upper curve) and poly[3BCMU(I$_3$)$_{0.50}$] (lower curve).

due to the resonance Raman Effect.[D7]   On the basis of the

results reported on polydiacetylenes [D8, D9] one absorption

at 2079 cm^{-1} may be assigned to $C \equiv C$ vibration and the other

at 1461 cm^{-1} to $C \equiv C$ vibration. The doped specimen also

exhibited the same two bands as those of the pure specimen.

However, the doped specimen exhibited rather high background

intensity. This increment in the background intensity may

be regarded either as the fluorescent background [D7] due

to some impurities, or as that due to charge transfer

complex [D10] between conjugated main chains and dopant ions.

Figure 4-3 shows Raman spectra in the range of small

wave number obtained at liquid nitrogen temperature. The

doped specimen (Y = 0.52) shows additional bands in the

range of wave number below 400 cm^{-1}. Comparing these results

with those reported for iodine doped polyacetylene,[D11, D12]

we concluded that one absorption at 105 cm^{-1} was due to

the I_3^- vibration and the other at 160 cm^{-1} to I_5^-

vibration. Moreover, we observed their overtones with the

intensities less than those of the fundamental absorptions.

The results clearly indicate the existence of I_3^- and I_5^-

ions in the iodine doped specimens.

4-3-2. Absorption Spectra

A $CHCl_3$ cast film of 0.002 mm thickness mounted on a
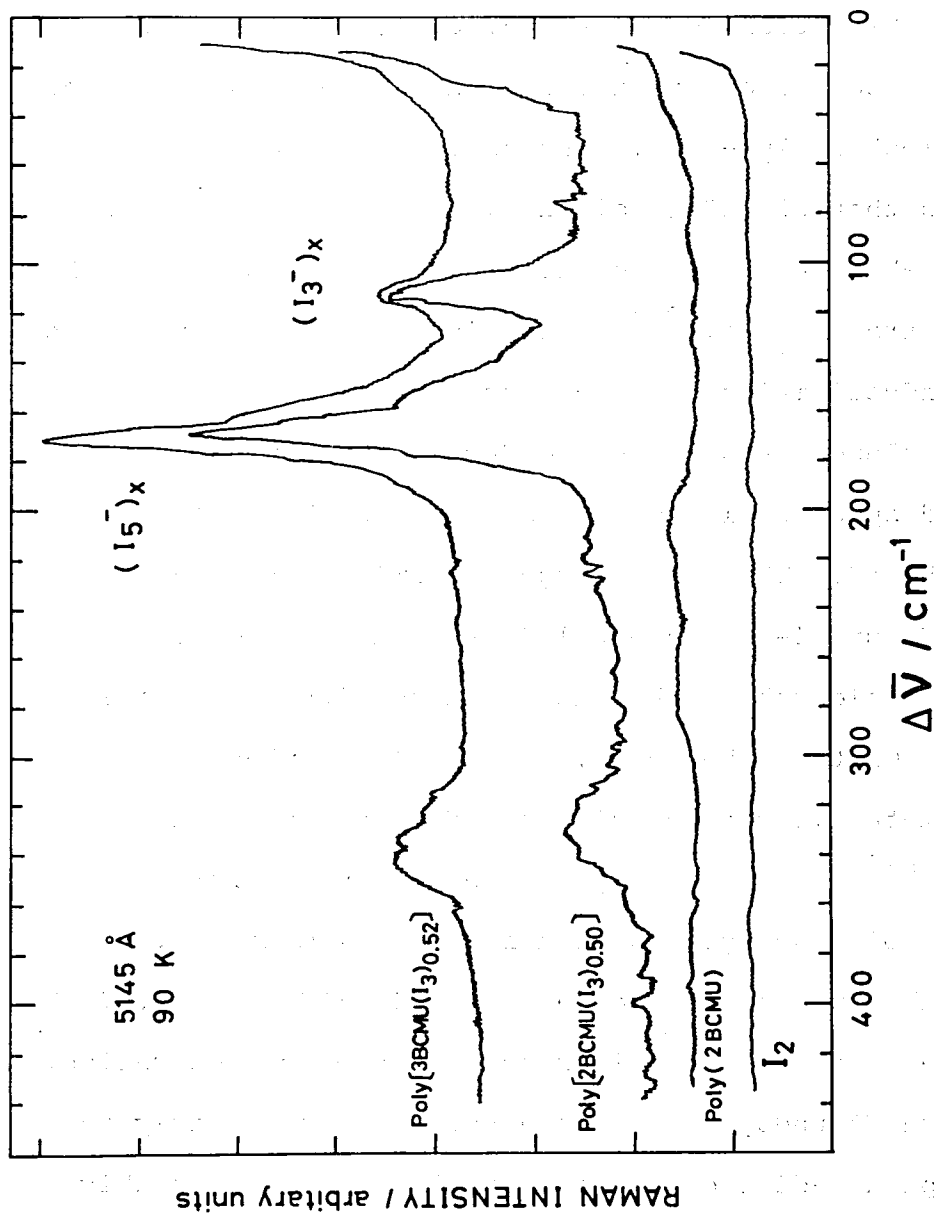
Figure 4-3. Low frequency region of Raman spectra at 90 K of iodine in pure and doped poly(3BCMU) and poly(2BCMU) samples.

glass plate was used to determine the visible absorption
spectrum of the solid film. As shown in Figure 4-4, the
visible spectrum of pure (or undoped) poly(3BCMU) film has
two broad absorption peaks at 1.97 eV (629 nm) and 2.21 eV
(561 nm). Because of the absorption at the long wavelength,
the film looked blue-gold. The spectrum was essentially
similar to that of $CHCl_3$ solution. [D11] These absorptions
are presumable due to the photo-excitation processes such
as $\pi \rightarrow \pi^*$ transitions. [D13] According to the band theories
of semiconductivities, [D14] the excitation of electrons
from the valence band to the conduction band usually results
in a broad spectrum increasing steeply in the longer
wavelength end. The band energy determined from the spectra
shown in Figure 4-4 is about 1.8 eV. This value coincides
with the wavelength at the maximum intensity of the solar
spectrum. On the other hand, doped polyacetylene
exhibits metallic conductivity and does not have such a
band gap. [D14] This fact might be an advangage for
utilizing polydiacetylenes as a solar cell material.

The absorption coefficients of poly(3BCMU) at 1.97 eV
and 2.21 eV increase with increasing dopant concentration.
The spectra of undoped and doped specimens are nearly the
same except an additional peak for the latter presumably
due to I_3^- ions. [D15] These results may be interpreted as
follows; (1) The increase in the absorption coefficients
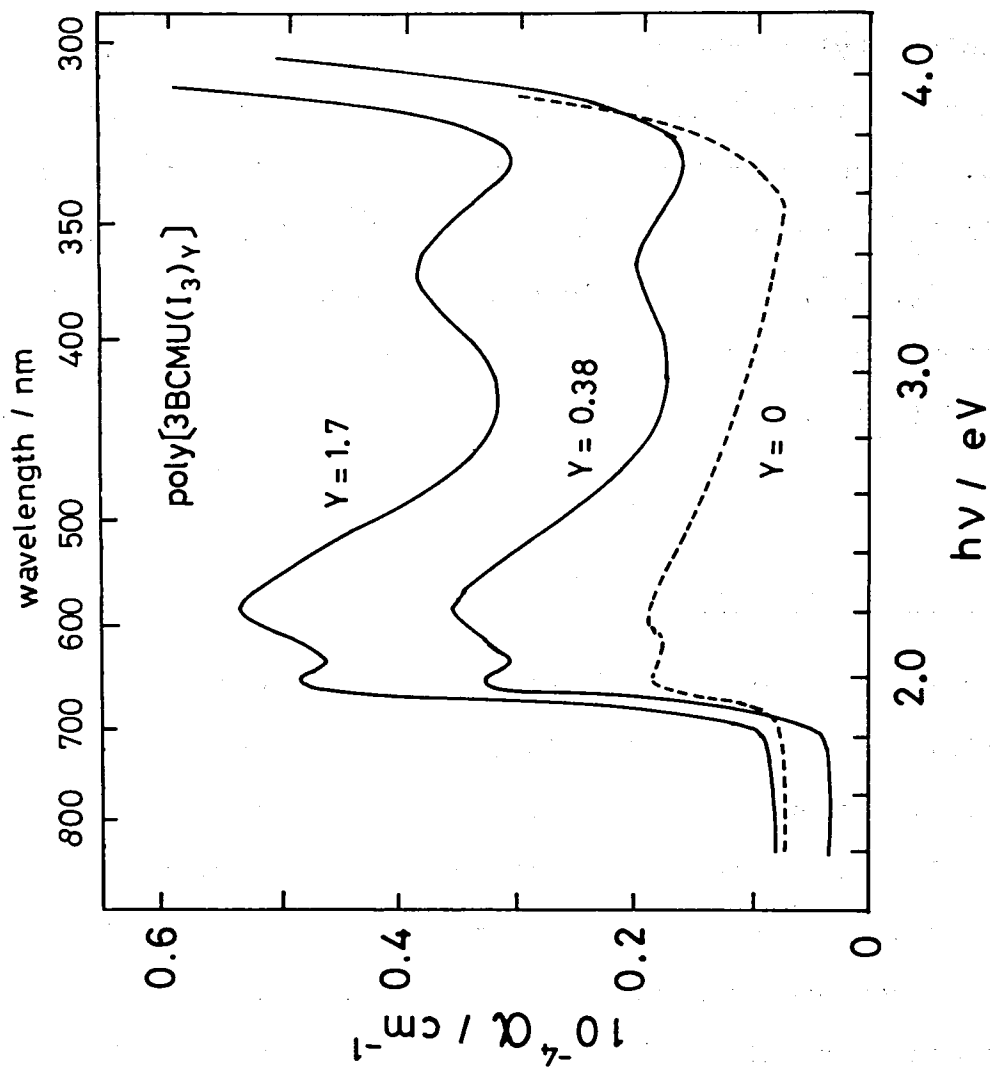suggests the increase in the transition probability of

Figure 4-4. Visible absorption spectra of pure and iodine doped poly(3BCMU) thin films.

electrons from the valence band to the conduction band. Thus, we expect an enhancement of the conductivity by doping. (2) The shape of the spectrum was essentially unchanged by doping. The result suggests that no transitions of the electronic state have occurred by doping, while doped polyacetylene shows the transition from an insulator to a metallic conductor.[D14] (3) The additional peak at about 3.4 eV suggests that the majority of iodine molecules exist in I_3^- form in doped poly(3BCMU).[D15] However, the ratio of I_2, I_3^-, and I_5^- could not be determined. This is the reason that we express a doped specimen as poly[nACMU(I_3)$_Y$].

4-3-3. DSC Measurements

DSC measurements were carried out for as-polymerized and purified monomer-free poly(3BCMU)/45 Mrad powder form samples. The as-polymerized sample was the one obtained immediately after the polymerization, and the purified sample was the one obtained by extracting the unreacted monomer by acetone from the as-polymerized one. The DSC measurements were also made for other poly(nACMU) samples.

DSC thermogram of as-polymerized poly(3BCMU) powder specimen showed two endothermic peaks: The first one at 332 K due to the melting of residual monomer, the second

one at 425 K due to the polymer melting. Two endorthermic

peaks due to interchain melting and to intrachain melting

seem to be overlapping at the second broad peak.

In the thermogram for the monomer-free powder specimen,

two endothermic peaks were observed at 418 K and 449 K.

However, in the thermograms of $CHCl_3$ cast films of

poly(3BCMU), poly(3ECMU) and poly(2ECMU) such as shown in

Figure 4-5-a, we observe only one peak [at 450 K for

poly(3BCMU)] tailing to the low temperature side.

For poly(4BCMU), we were able to make an additional

observation, because single crystalline specimens were

available. Figure 4-5 b shows typical thermograms of $CHCl_3$

cast and single crystalline specimens of poly(4BCMU).

These specimens usually exhibit two endothermic peaks at

about 380K and 410K, although the 380K peak for the

$CHCl_3$ cast films is rather samll. Its red color slightly

changes its tone at 380 K and further to yellow at 410 K,

while the black-purple single crystal turns to red at 380

K and then to yellow at 410 K.

From the areas under the endothermic peaks of all

these poly(nACMU) samples, we estimated the enthalpy of

fusion ΔH_f of these samples. The results are summarized

in Table 4-1.

For poly(3BCMU) samples, it was difficult to estimate

the degree of crystallinity X_c from these enthalpy data,

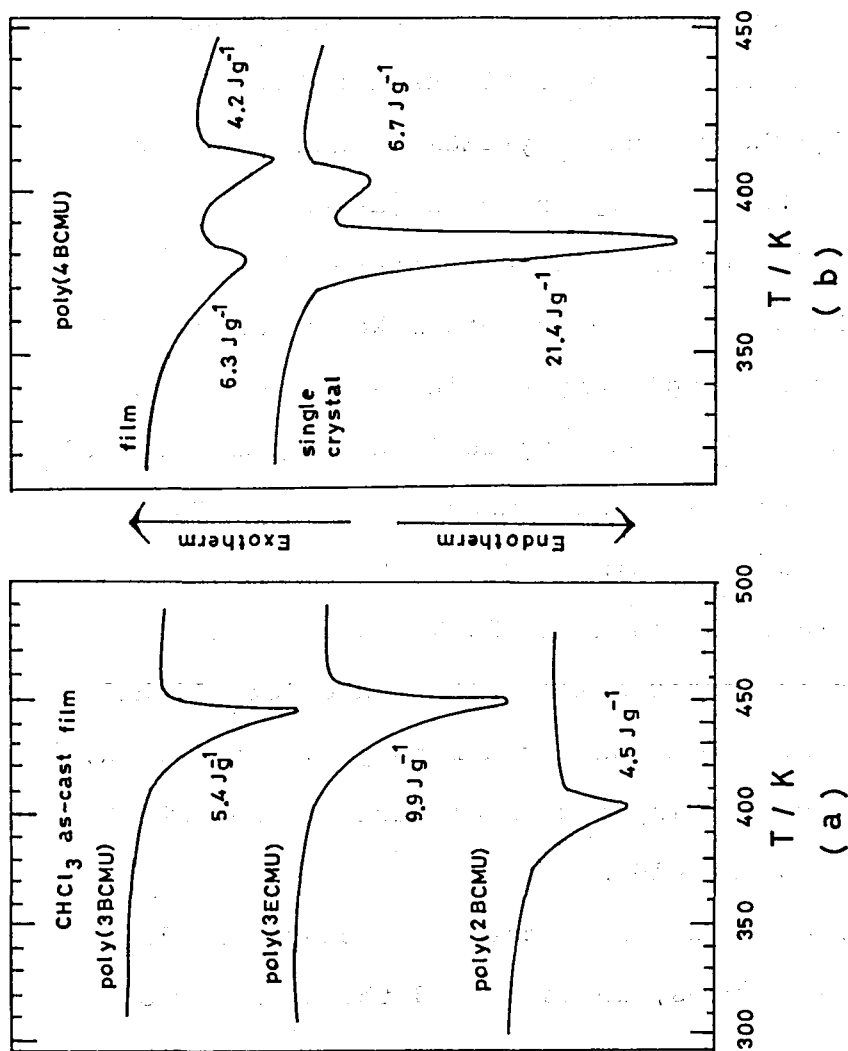because standared single crystalline samples were

Figure 4-5. Differential scanning calorimetric thermograms of poly(nACMU) samples: (a) CHCl$_3$ as-cast films of poly(3BCMU), poly(3ECMU) and poly(2BCMU); (b) powder-form like poly(4BCMU) immediately after polymerization and a single crystalline poly(4BCMU). The measurements were made with a heating rate of 10 K min^{-1}.

Table 4-1. The enthalpies ΔH_f of fusion for various poly(nACMU) samples.

Polymer	ΔH_f / J g^{-1}	
	low temperature	high temperature
Poly(3BCMU)/45Mrad/as-polymerized	24.1 (425K)	
Poly(3BCMU)/45Mrad/powder	8.8 (420K)	28.5 (450K)
Poly(3BCMU)/45Mrad/film		5.4 (450K)
Poly(3BCMU)/0.09Mrad/film		11.5 (450K)
Poly(3ECMU)/45Mrad/film		9.9 (450K)
Poly(2BCMU)/45Mrad/film		4.5 (400K)
Poly(4BCMU)/45Mrad/powder	18.5 (380K)	4.8 (410K)
Poly(4BCMU)/45Mrad/film	6.3 (380K)	4.2 (410K)
Poly(4BCMU)/45Mrad/single crystal	21.4 (380K)	6.7 (410K)

unavailable. However, assuming that the $\Delta H_f = 28.5$ J g^{-1}
for monomer-free powder-form sample represents that of
100 % crystalline sample, we estimated the X_c of $CHCl_3$
cast films of poly(3BCMU), poly(3ECMU), and poly(2BCMU) to
be about 20 %, 34 %, and 17 %, respectively.

On the other hand, for $CHCl_3$ cast poly(4BCMU) films
we estimated the X_c for the two peaks at 380 K and 410 K
are 29 % and 62 %, respectively, in comparison with those
of the single crystalline specimen.

From these results of ΔH_f or X_c values, we may
conclude that solvent-cast specimens are very poorly
crystalline, while powder form specimens as well as single
crystalline samples have rather high degree of crystallinity.
The results are consistent with those of X-ray diffraction
analysis which gives diffuse Debye-Scherrer rings for
these film-form samples as will be described in the next
section.

According to Patel and Miller, [D18] the polymer chains
of urethane-substituted soluble polydiacetylenes usually
asssume a planar flat-ribbon like conformation stabilized
by side-by-side hydrogen bondings between the C=O and -NH
groups of the adjacent substituents and these flat ribbons
are stacked regularly in the crystallites. The melting
peaks accompanying the color changes are due to transitions
from planar to nonplanar conformation leading to changes in
effective conjugation length of the polymer backbones. [D18]

These transitions are obviously induced by intermolecular
disordering, i. e., the destruction of ribbon stackings
[at 380 K for poly(4BCMU) and at 420 K for poly(3BCMU)] and
by intramolecular melting, i. e., the distruption of
hydrogen bondings [at 410 K for poly(4BCMU) and at 450 K
for poly(3BCMU)].

4-3-4. X-ray diffraction

    Figures 4-6-a and 4-6-b show the Debye-Scherrer
photographs of powder-form and $CHCl_3$ cast film specimens
of undoped poly(3BCMU)/45Mrad, respectively. Both
photographs show the characteristics of unoriented
semi-crystalline polymers. For the powder specimen, eight
diffraction rings are detected, while only five diffraction
rings for the film specimen. The latter photograph
suggests that the film specimen has very low degree of
crystallinity. This result is consistent with the DSC
result.

    An X-ray photograph of the doped poly$[3BCMU(I_3)_{0.42}]$/
45 Mrad film is shown in Figure 4-6-c. Only three
diffraction rings are detected for this doped film due to
the pronounced background scattering. The d-spacings
calculated from the X-ray diffraction patterns are listed
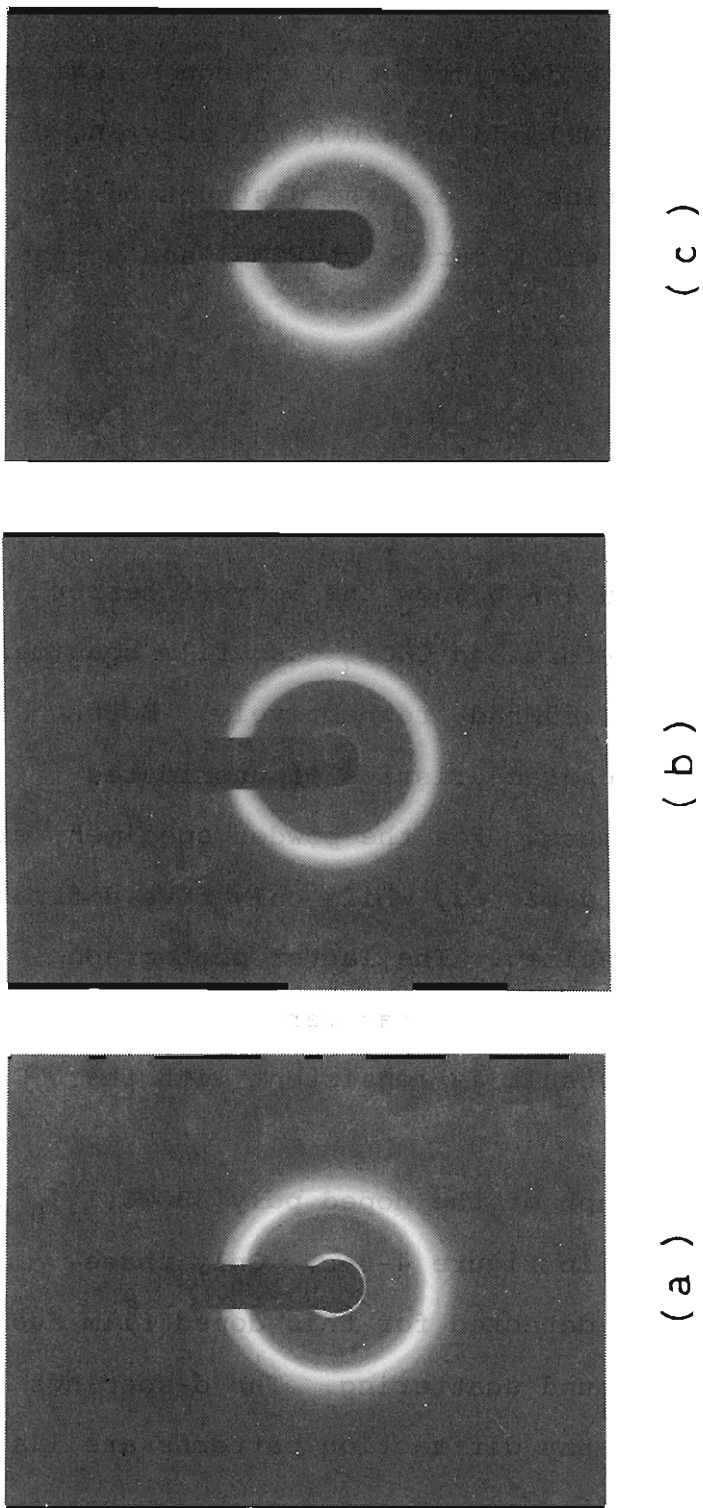in Table 4-2. The difference in the d-spacing between the

Figure 4-6. Debye-Scherrer photographs for (a) poly(3BCMU) powder specimen, (b) undoped poly(3BCMU)/45Mrad film, and (c) doped poly[3BCMU$(I_3)_{0.42}$]/45 Mrad film.

Table 4-2. The d-spacings* for the various
poly(3BCMU) specimens.

d-spacings* / nm		
Powder	Undoped film	Doped film
1.33 (s)	1.40 (s)	
0.90 (vw)		
0.53 (w)	0.45 (w)	0.45 (w)
0.43 (s)	0.42 (s)	0.42 (s)
0.38 (w)		
0.34 (vw)		
0.22 (vw)	0.23 (vw)	0.23 (vw)
0.20 (vw)	0.20 (vw)	

* The symbols in the parentheses indicate
the intensity of the X-ray diffractions :
s = strong; w = weak; v = very weak.

powder and film specimens suggests that their crystal

forms may be different. On the other hand, all the

d-spacings in the doped film are found to be the same as

those in the undoped film, and no differences in the

relative intensities of the corresponding diffractions

between the undoped and doped films are observed. These

results imply that the doping does not affect the crystal

form. Thus, we may conclude that the doping takes place

mostly in the amorphous regions.

4-3-5. Characteristics of Anisotropic Specimens

We prepared two different anisotropic specimens of

poly(nACMU)s: one was polymer single crystals of poly(4BCMU)

and the other partially oriented films of poly(3BCMU).

4-3-5-a. Poly(4BCMU) Single Crystals

To determine the relation between the unit cell and the

gross feature of the polymer single crystal of poly(4BCMU),

two rotational photographs were taken around the mutually

perpendicular axes along the length and width directions

lying in the plane of the platelet. From the repeating

distances determined from the diffraction angles of the

layer lines and from other results on microscopic

observations on the crystal, we decided that the fiber (c-)

axis is parallel in the width direction and the b axis

(the side groups) in the thickness direction, and thus,

the poly(4BCMU) chains are stacked along the length

direction of the crystal, as shown in Figure 4-7-b.

From the preliminary X-ray diffraction alalysis, D20

the fiber period (c-axis) of poly(4BCMU) single crystal

was found to be 0.488nm. The subcell dimensions

perpendicular to the c-axis were a' = 0.533 nm and b' =

5.436 nm with an assumption of γ' = 90°. The b'-axis is

almost parallel to the urethane group direction, and the

a'-axis perpendicular to both of the main chain and

urethane group directions.

Figure 4-7-a shows an X-ray rotation photograph of

poly(4BCMU) single crystal about the c-axis. We see

several discrete reflections on the equatorial line and

continuous scattering streaks on each layer line. These

features suggest that in the crystal the chain backbone

has as essentially regular periodic conformation, and the

packing of the chains in the a'- and b'-directions is also

periodic, but the mutual level of the chains in the c-axis

direction is irregular. A more detailed analysis of the

crystal structure is now in progress. D20

Poly(4BCMU)
Single Crystal

b-axis

$(CH_2)_4$ $(CH_2)_4$ $(CH_2)_4$ $(CH_2)_4$
$(CH_2)_4$ $(CH_2)_4$ $(CH_2)_4$ $(CH_2)_4$
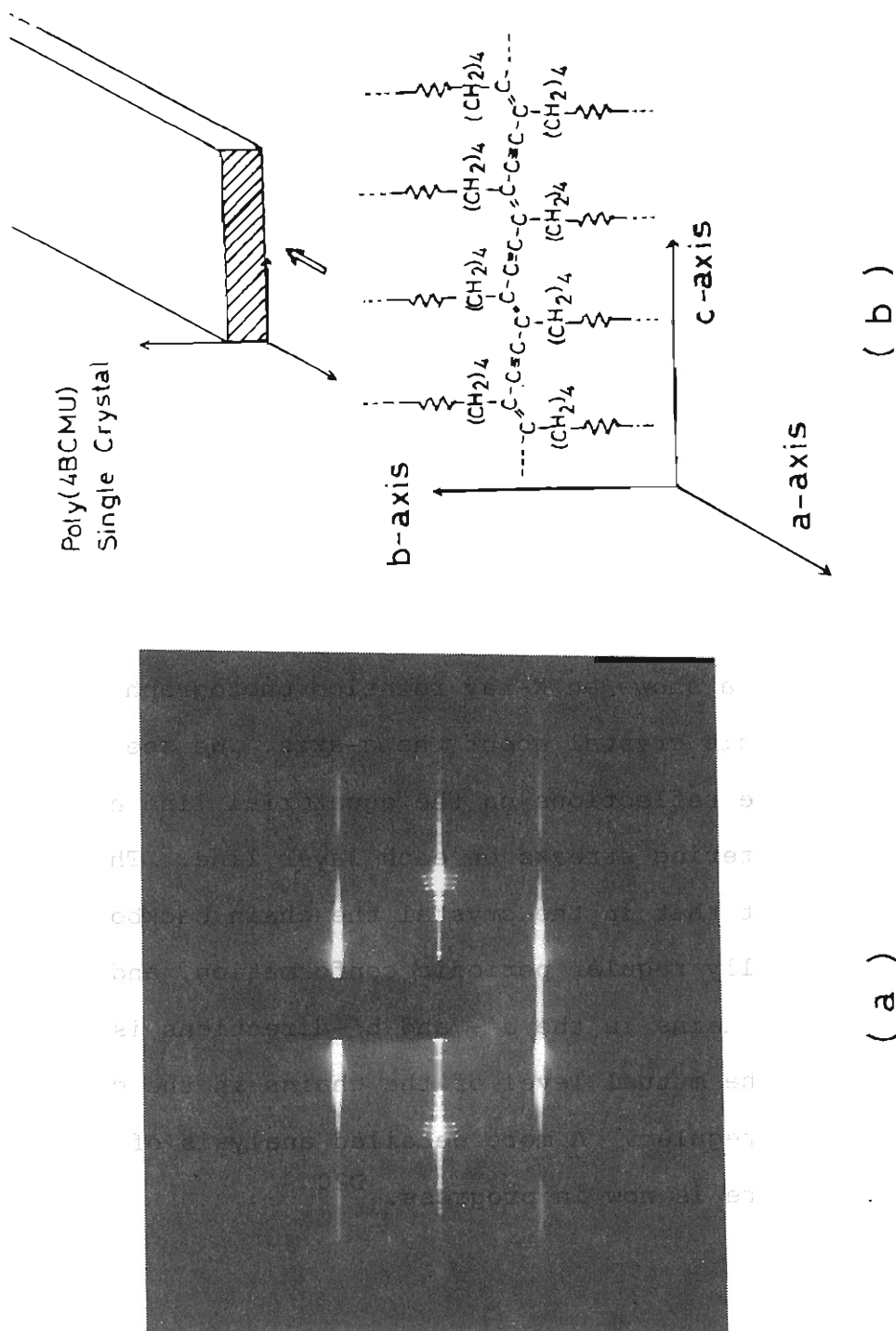
c-axis

a-axis

(b)

(a)

Figure 4-7. X-ray rotation photograph about (a) the c-axis and (b) schematic diagrams showing the molecular alignment in single crystalline poly(4BCMU).

4-3-5-b. Uniaxially Stretched Poly(3BCMU) Film

We prepared several uniaxially stretched films by
varying the elongation ratio, $\lambda = \ell/\ell_0$, where ℓ_0 was the
initial length of the sample, and ℓ the length after
stretching. Figure 4-8-a shows a typical example of
polarized infrared spectra for the film of $\lambda = 2.92$.

The infrared dichroic ratio is defined as $R = A_{11}/A\perp$,
where A_{11} and $A\perp$ are the absorbance of the same sample for
the polarized light parallel and perpendicular, respectively,
to the stretch direction. We choose the N-H stretching band
at 3330 cm^{-1} for the calculation of R. The absorption of
N-H stretching band for the polarized light paralle to
the elongation axis was always stronger than for the
perpendicular polarization. This means that poly(3BCMU)
molecules are oriented, at least, partially along the
stretch direction. The R values calculated from the
infrared spectra scattered between 1,5 and 2.1 from one
another, although λ was nearly the same for those specimens.
We defined the degree of orientation f of the molecules
in the polymer film by assuming that the transition
moment of N-H stretching is parallel to the polymer chain
direction. Then we have
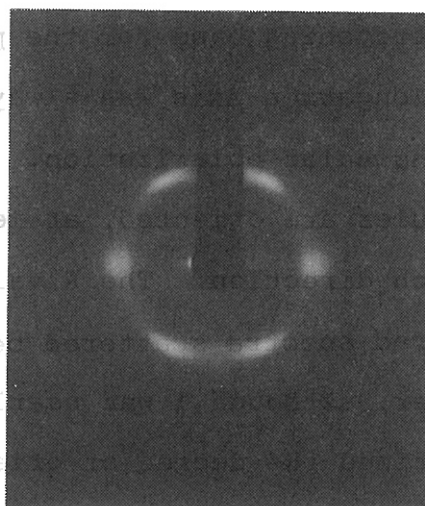
$$f = (R - 1) / (R + 2)$$

Presumably, this assumption may be rationalized from the
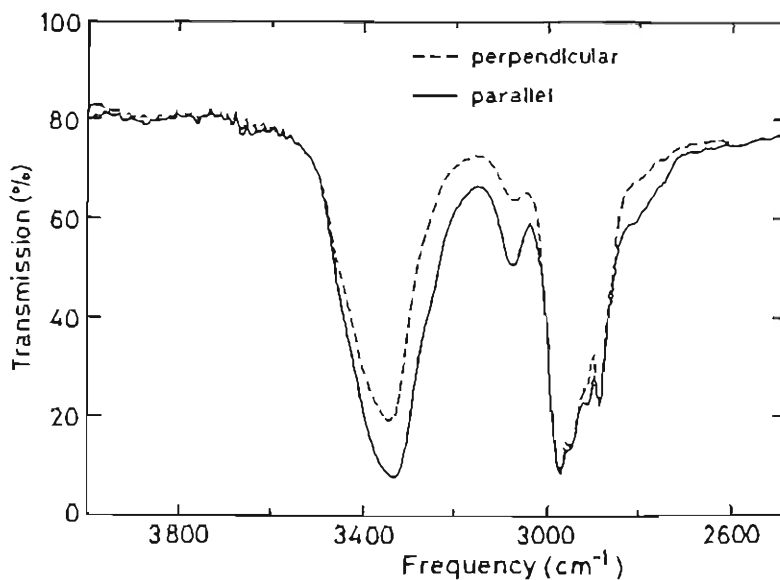
(a)
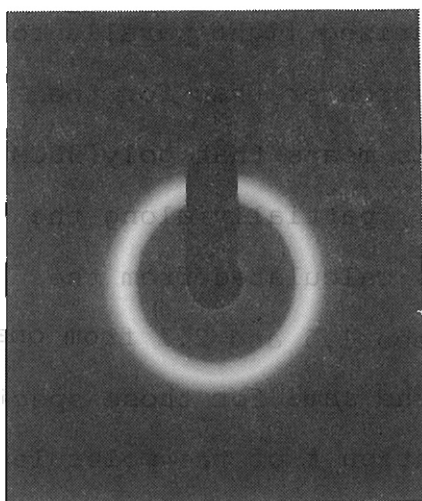
(b)

(c)

Figure 4-8. (a) Polarized infrared spectra parallel (——)
and perpendicular (---) to the stretch direction for a poly-
(3BCMU) film of $\lambda = 3.67$ and $R = 1.64$. X-ray diffraction
photographs (b) for an as-cast film and (c) for an oriented
film of poly(3BCMU)/0.09Mrad.

crystallcgraphic result of similar polydiacetylenes,
poly {1,2-bis [4-(phenylcarbamoyloxy)-n-butyn]-1-buten-3-
ynylene},[D21] although quantitative results of X-ray analysis
on poly(3BCMU) are not available now.

The X-ray diffraction patterns for an as-cast film
and for a stretched film with R = 1.78 and f = 0.21 are
compared in Fugure 4-8-b and 4-8-c. The diffuse
Debye-Scherrer rings observed for the as-cast film change
to diffuse spots for the stretched film. This X-ray
photograph implies that in the stretched film poly(3BCMU)
molecules are uniaxially oriented. The calculated fiber
period is 0.49 nm corresponding to the length of a repeat
unit of the polymer backbone. X-ray diffraction patterns
show that the samples are semicrystalline, but the degree
of crystallinity is very low.

4-3-6. Dynamical Mechanical Measurements

Figure 4-9 shows the temperature dependence of the
storage Young's moduli E', loss moduli E" and tan δ for
some poly(nACMU) samples. These films were sufficiently
tough to carry out the mechanical measurements. The E'
of all the films decrease gradually with increasing
temperature from 140 K to 240 K and then somewhat more
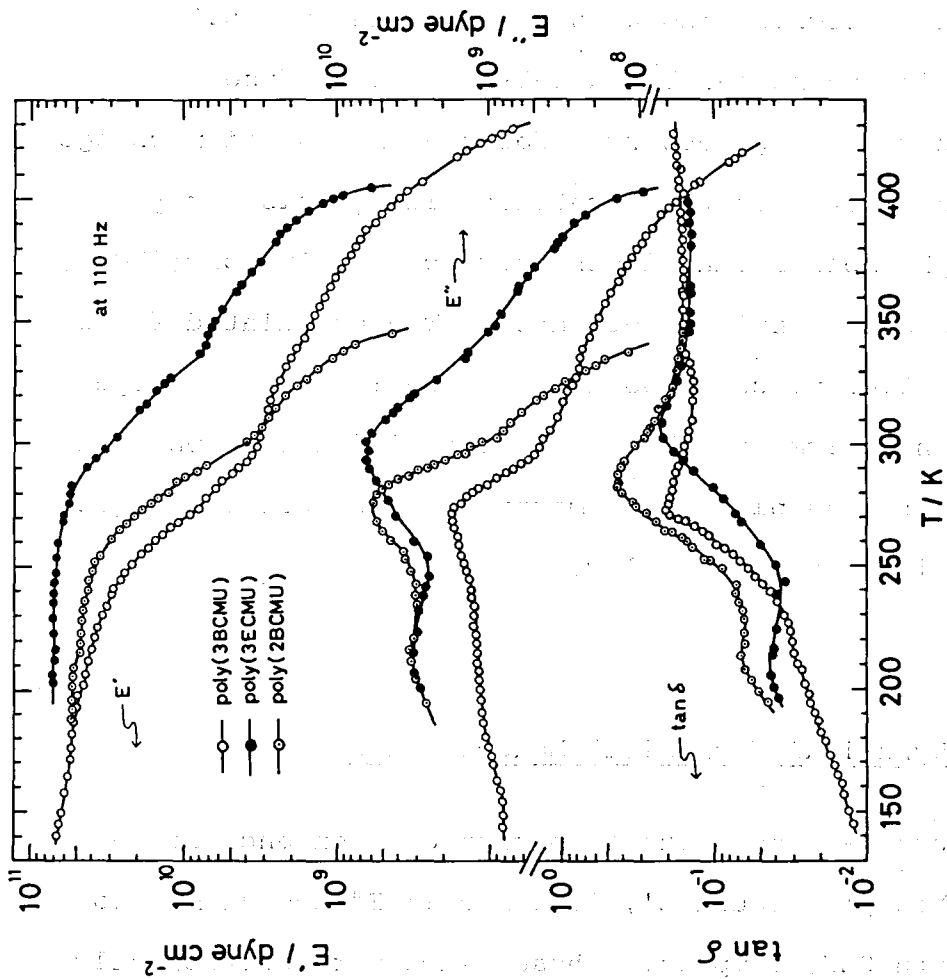rapidly from 240 K to 300 K. Poly(3BCMU) and poly(3ECMU)

Figure 4-9. Temperature dependence of the storage Young's moduli E', the loss moduli E" and tan δ at 110 Hz for poly(nACMU) films.

begin to flow at around 420 K, and poly(2BCMU) at around

360 K.   These results coincide with those of DSC:

Poly(3BCMU) and poly(3ECMU) exhibited the melting point

T_m at about 440 K, and poly(2BCMU) at about 390 K.   The

dynamic mechanical properties of the poly(nACMU)s are

similar in nature to those of common semicrystalline

polymers.   The E" and tan δ curves exhibit a broad

transition at about room temperature which presumably

corresponds to the glass transition temperature T_g.   The

T_g of poly(3BCMU), poly(3ECMU) and poly(2BCMU) were

estimated to be 273 K, 305 K and 283 K, respectively.

The T_g of these specimens are almost the same but are

slightly different from one another.

Figure 4-10 demonstrates the effect of iodine doping

on the mechanical properties of poly(3BCMU)/45Mrad sample.

The figure shows the temperature dependence of the storage

Young's moduli E', the loss moduli E", and tan δ for

poly(3BCMU), poly$[3BCMU(I_3)_{0.09}]$, and poly$[3BCMU(I_3)_{0.23}]$.

The E' of undoped poly(3BCMU) decreases rapidly with

increasing temperature from 240 K to 300 K.   The specimen

begins to flow at about 420 K.   Its E" and tan δ curves

exhibit a broad transition with the maximum temperature

T_{max} at 270 K, corresponding to the glass transition

temperature T_g.   The tempetature dependence of the complex

Young's Moduli were measured also on the doped specimens

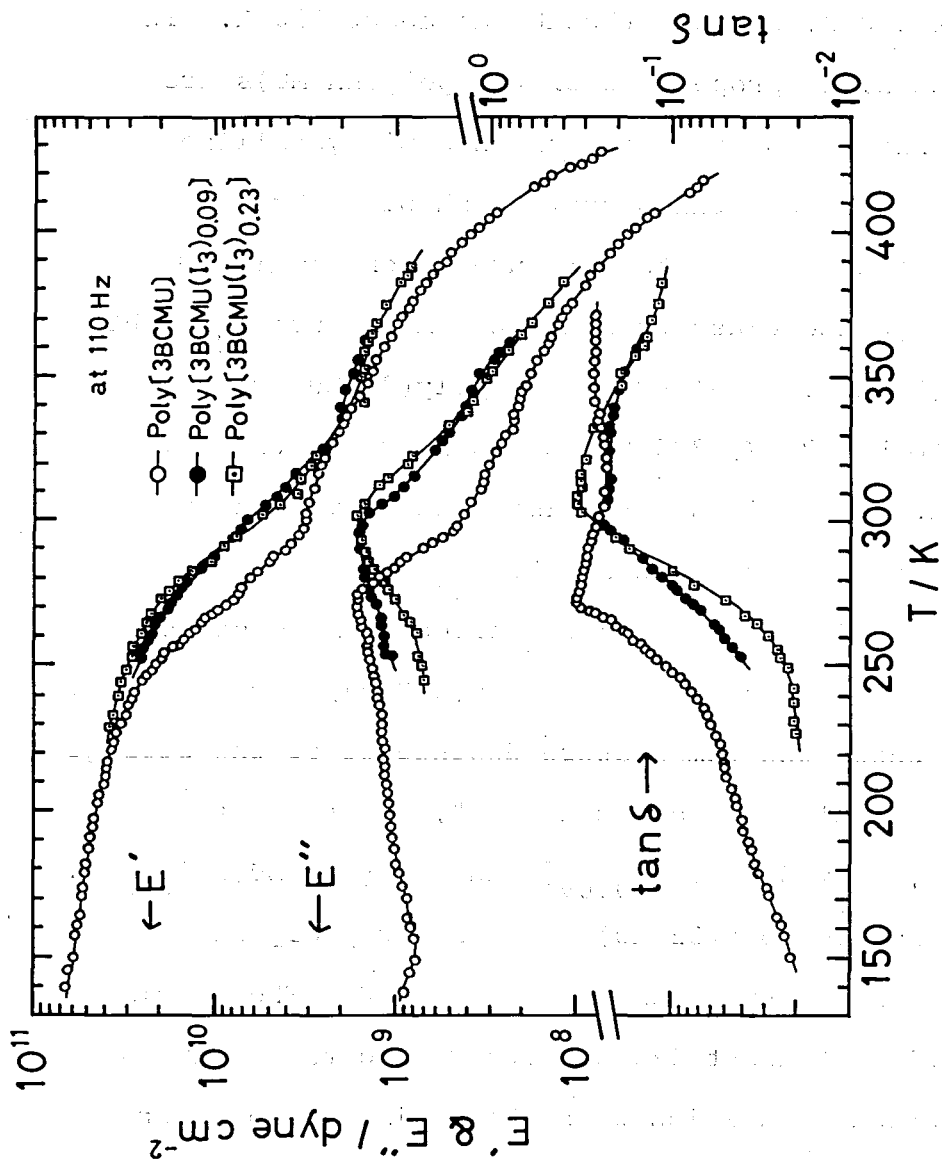of poly(3BCMU)/45Mrad.   The behavior of poly $[3BCMU(I_3)_{0.09}]$

Figure 4-10. Temperature dependence of the storage Young's moduli E', the loss moduli E" and tanδ at 110 Hz for pure and doped poly(3BCMU) specimens.
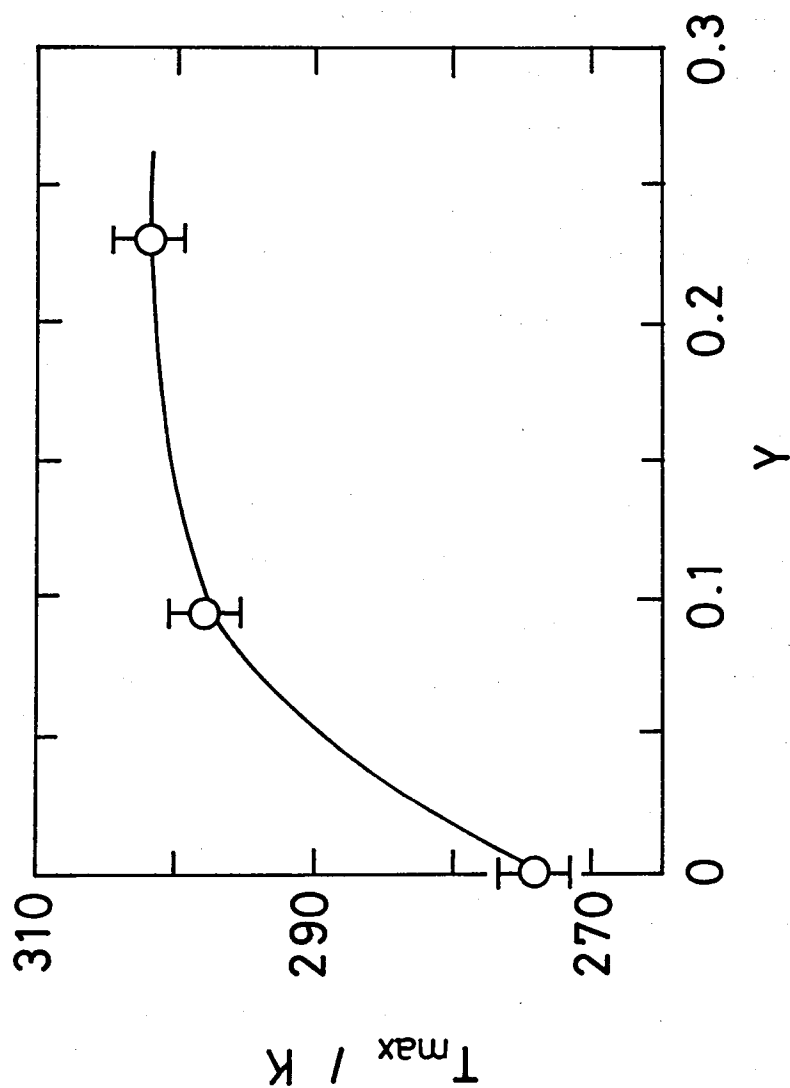
Figure 4-11. Plot of the loss maximum temperature T_{max} at 110 Hz versus dopant concentration Y (cf., Figure 4-10).

and poly $[3BCMU(I_3)_{0.23}]$ are similar to that of the undoped specimen, except that the T_{max} shifts to the higher temperature side. As shown in Figure 4-11 the T_{max} increases as Y increases upto Y = 0.09, and reaches a constant of approximately 300 K in the range of Y from 0.09 to 0.23. In the doped specimens, I_3^- ions might coordinate to several conjugated main chains or polar side chains and might form ionic clusters as those usually found in ionomers. [D9] This strong intermolecular interaction under the presence of I_3^- might cause the T_{max} to increase with increasing dopant concentration.

The T_g of poly(nACMU)s is usually below room temperature, and hence the doping with iodine at room temperature proceeds in the leathery and/or rubbery state of the poly(nACMU)s but not in the glassy specimens, where the diffusion of small molecules are often hindered. [D22]

4-3-7. Dielectric Measurements

Figure 4-12 shows the temperature dependence of the dielectric permittivity ε' and loss ε'' for undoped poly(3BCMU)/45Mrad and doped poly$[3BCMU(I_3)_{0.12}]$. The loss curve of the poly(3BCMU) has a small peak at 210 K (designated as β-peak), a peak at 280 K (α-peak), and
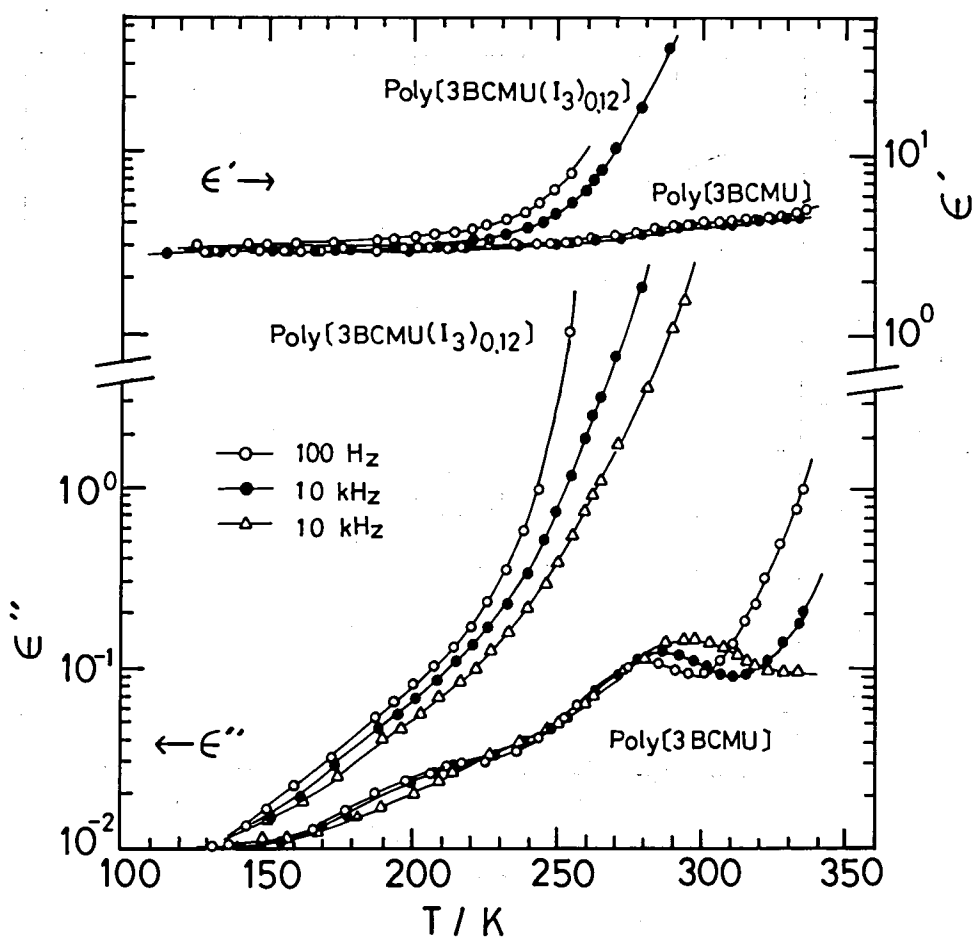
Figure 4-12. Temperature dependence of the dielectric
permittivity ε' and loss ε" for poly(3BCMU) and
poly[3BCMU(I$_3$)$_{0.12}$].
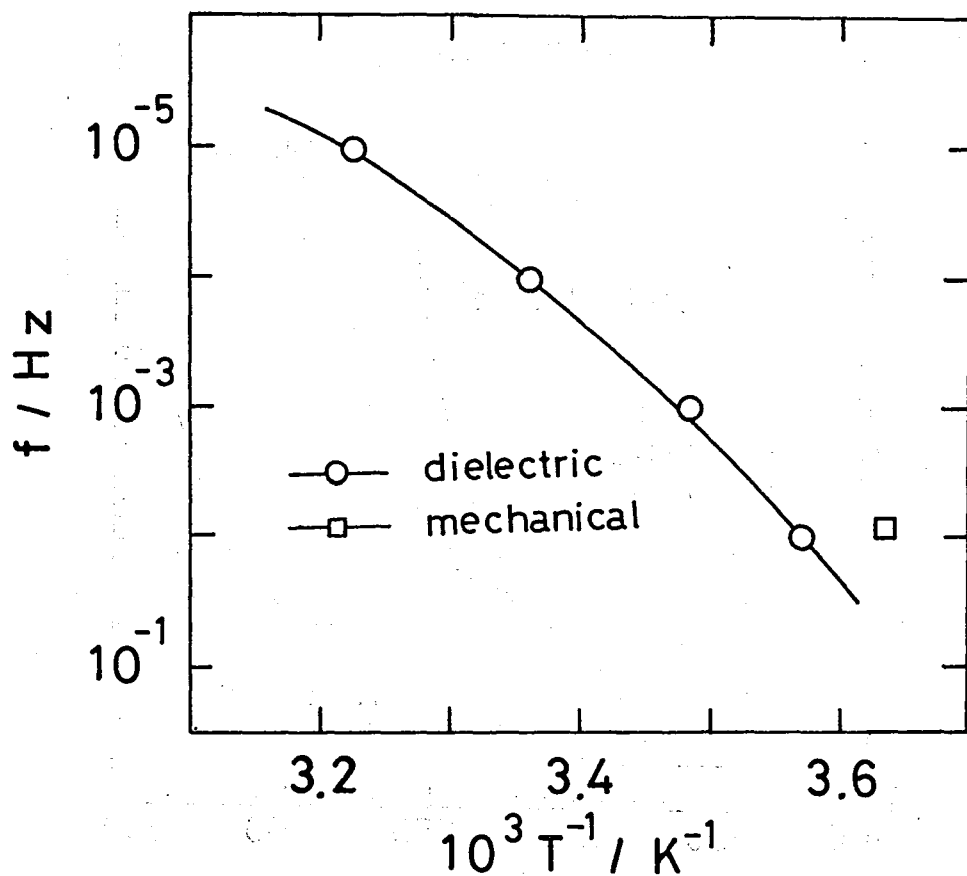
Figure 4-13. Plot of log f_{max} versus 1/T for the primary relaxation of pure poly(3BCMU)/45Mrad.

a steep rise in the high temperature side. The α-peak
temperature is roughly the same as the T_{max} of dynamic
mechanical transition, and may be attributed to the primary
relaxation due to the glass transition. The β-peak
temperature is also roughly the same as that of the dynamic
mechanical β-relaxation. The β-relaxation may be ascribed
to the motion of polar side groups.[D22] Figure 4-13 shows
that the frequency and temperature dependence of the α-peak
follows a Williams-Landel-Ferry (WLF) law. From the slope
of the plot at 1 kHz, the apparent activation energy was
estimated to be 163 kJ mol^{-1}. The ε' and ε" curves of the
doped poly[3BCMU(I_3)$_{0.12}$] exhibit steep rise in the high
temperature side, as the conductivity steeply increases
with increasing dopant concentration. The dielectric
α-relaxation peak was obscured because of this steep rise.
Therefore the dopant concentration dependence of the α-
and β-relaxations could not be elucidated.

4-3-8. Comlex Formation of Poly(nACMU)s With Iodine

Two evidence given in the previous sections showed
that the dopant iodine entered mostly into the amorphous
regions of the specimens. Namely, the d-spacings of the
X-ray diffraction patterns are essentially unaltered by
the doping, and the amount of iodine absorbed by single

crystalline poly(4BCMU) specimens is by a factor of 100

smaller than that of solvent-cast films. According to the

Raman spectra of undoped and doped specimens of poly(3BCMU),

iodine is likely to exist in the forms of I_2, I_3^-, and I_5^-.

Although the exact ratio is unknown, the I_3^- appears to be

dominant. The dopant increases the fluoresent background

which is probably due to the formation of charge transfer

complex between the conjugated main chains and dopant ions.

The glass transition temperature is shifted to the high

temperature side by the iodine doping. The strong

intermolecular interaction under the presence of I_3^- and/

or I_5^- ions tend the T_g to increase with increasing dopant

concentration. These results suggest that the I_3^- and I_5^-

ions might coordinate to several conjugated main chains or

polar side chains, and might form ionic clusters.

Polydiacetylene-iodine complexes may influence the

absorption coefficient of the spectra but not necessarily

the photo-excitation energy.

Polydiacetylene backbones are admixtures of poly(ene)

and poly(ene-yne) types. [D24, D25] In these structures,

some geometrical isomers such as trans- and cis- isomers

around double bonds, and also some rotational isomers

around single bonds are allowed. [D26-D28] Thus, poly(ene)

has three isomers of poly(ene)/trans-transoid, poly(ene)/

cis-transoid and poly(ene)/trans-cisoid, as shown in

Figure 4-14-a, -b and -c, respectively. The former symbol
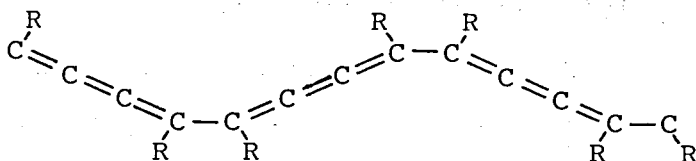
poly(ene) type

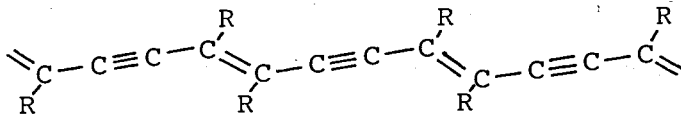(a) trans-transoid
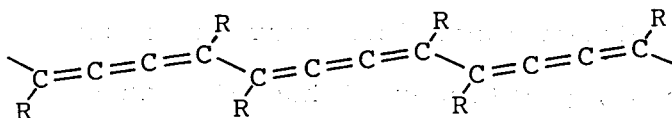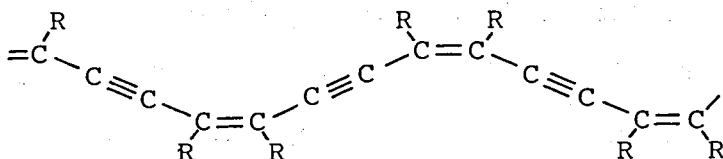
(b) cis-cisoid
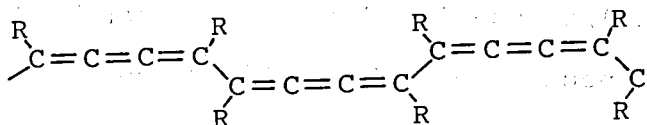
(c) trans-cisoid

poly(ene-yne) type

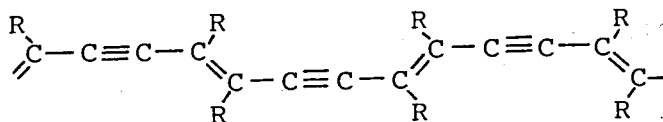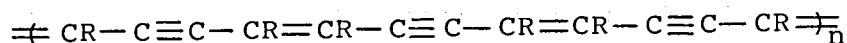(d) trans-transoid

(e) cis-transoid

(f) trans-cisoid

Figure 4-14. The geometrical and conformational isomers of polydiacetylenes.
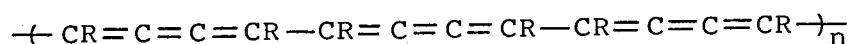
such as trans indicates a geometrical isomer around a double bond, and the latter symbol such as transoid a conformational isomer around a single bond. On the other hand, poly(ene-yne) has also three isomers of poly(ene-yne)/ trans-transoid, poly(ene-yne)/cis-transoid, and poly(ene-yne)/trans-cisoid such as shown in Figure 4-14-d, -e and -f, respectively. The combinations of -a and -d, -b and -f, and -c and -e are exchangable between poly(ene) and poly(ene-yne) structures.

Possible schemes for the backbone structures of polydiacetylenes are presented in Figure 4-15-c. Figure 4-15-d suggests a possible mechanism of a dopant iodine withdrawing an electron from the conjugated main chain given in Figure 4-15-c to become anions of I_3^- and/or I_5^-. Hence, an extra hole and radical can be produced in the chain. [D29, D30] This structural model also explains or, at least, is not contradictory to the observation that the T_g of poly(3BCMU) samples increases by doping. These extra holes in the conjugated main chains may play an important role in enhancing the conductivities of doped poly(3BCMU).
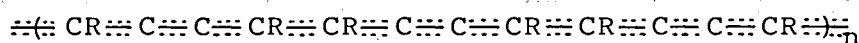
(a) Poly(ene-yne) Chain

$$\text{=}\!\!\!\!\big(\text{CR}-\text{C}\!\equiv\!\text{C}-\text{CR}\!=\!\text{CR}-\text{C}\!\equiv\!\text{C}-\text{CR}\!=\!\text{CR}-\text{C}\!\equiv\!\text{C}-\text{CR}\text{=}\!\!\!\!\big)_n$$

(b) Poly(ene) Chain

$$\text{+}\big(\text{CR}\!=\!\text{C}\!=\!\text{C}\!=\!\text{CR}-\text{CR}\!=\!\text{C}\!=\!\text{C}\!=\!\text{CR}-\text{CR}\!=\!\text{C}\!=\!\text{C}\!=\!\text{CR}\big)_n$$

(c) Conjugated Polydiacetylene Chain

$$\text{=}\!\!\big(\text{CR}\!\equiv\!\text{C}\!\equiv\!\text{C}\!\equiv\!\text{CR}\!\equiv\!\text{CR}\!\equiv\!\text{C}\!\equiv\!\text{C}\!\equiv\!\text{CR}\!\equiv\!\text{CR}\!\equiv\!\text{C}\!\equiv\!\text{C}\!\equiv\!\text{CR}\big)_n$$

(d) Polydiacetylene-Iodine Complex

hole $\searrow$ $\oplus$ $\cdot\!\swarrow$ radical

$$\text{=}\!\!\big(\text{CR}\!\equiv\!\text{C}\!\equiv\!\text{C}\!\equiv\!\text{CR}-\text{CR}\!\equiv\!\text{C}\!\equiv\!\text{C}\!\equiv\!\text{CR}\!\equiv\!\text{CR}\!\equiv\!\text{C}\!\equiv\!\text{C}\!\equiv\!\text{CR}\big)_n$$
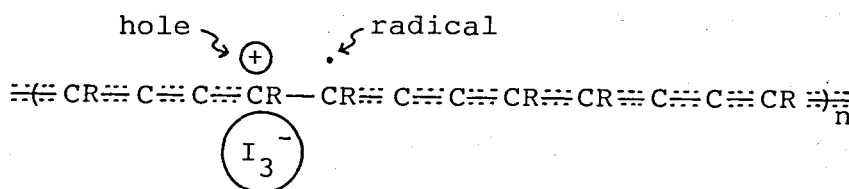
$\left(I_3^{-}\right)$

Figure 4-15. Possible schemes for conjugated polydi-
acetylene chains and complexes with iodine.

4-4. Conclusion

The DSC, X-ray diffraction and mechanical studies indicated that poly(nACMU) films were semicrystalline , although the degrees of crystallinity are usually low. Their melting points and degrees of crystallinity were in the rang of 400 K to 450 K, and in the range of 17 % to 62 %, respectively. The glass transition temperatures of poly(nACMU)s were found to be approximately 273 K by the mechanical and dielectric spectroscopies.

Poly(nACMU) films were easily doped with iodine by exposing them to iodine vapor at room temperature. An X-ray diffraction study suggested that the doping mostly occurs in the amorphous region. The doping increased the glass transition temperature as much as 27 K. Raman and visible absorption spectra indicated the presence of iodines in the form of I_3^- and I_5^- in poly(nACMU)s. Possible model of poly(nACMU) film-iodine complexes were presented. Dopant iodines withdraw electrons from the conjugated main chains of poly(nACMU)s to become anions. Hence, extra holes and radicals can be produced in the chains. These extra holes existing in the amorphous regions of doped poly(nACMU) specimens should play a key role in the electric conductivity.

We succeeded in preparing polymer single crystals of poly(4BCMU). The fiber (c-) axis is lying parallel to

the width direction of the crystal. On the other hand,

in uniaxially stretched films of poly(3BCMU) the degrees

of orientation of the polymer chains were found to be

roughly 0.20, regardless of the stretch ratios of the

films.

References

D1. Shirakawa, H.; Louis, E. J.; MacDiarmid, A. G.;
    Chiang, C. K.; Heeger, A. J. J. Chem. Soc., Comm.,
    1977, 578.

D2. Chance, R. R.; Schacklette, L. W.; Miller, G. G.;
    Ivory, D. M.; Dowa, J. M.; Ehsenbaumer, R. L.;
    Baughman, R. H.; J. Chem. Soc., Chem. Comm., 1980, 348.

D3. Ivory, D. M.; Miller, G. G.; Dowa, J. M.; Schaklette,
    L. W.; Chance, R. R.; Baughman, R. H. J. Chem. Phys.,
    1979, 71, 1506.

D4. Kuwane, Y.; Masuda, T.; Higashimura, T. Polymer J.,
    1980, 12,387.

D5. Park, Y. W.; Oruy, M. A.; Chiang, C. K.; MacDiarmid,
    A. G.; Heeger, A. J.; Shirakawa, H.; Ikeda, S.
    J. Polym. Scil, Polym. Lett. Ed., 1979, 17, 203.

D6. Delhaes, P.; Coulon, D.; Amiell. J.; Flandrois, S.
    Mol. Cryst. Liq. Cryst., 1979, 50, 43.

D7. Ivin, K. J., "Structural studies of Maxromolecules by
    Spectroscopic Method", John Wiley and Sons, Ltd.,
    New York, 1976. Chapter 8.

D8. Baughman, R. H.; Witt, J. D.; Yee, K. C. J. Chem.
    Phys., 1974, 60, 4755.

D9. Eisenberg, A.; King, M., "Ion-Containing Polymers",
    Academic Press, New York, 1977.

D10. Nakatani, K.; Sakata, T.; Tsubomura, H. Bull. Chem.
    Soc., Japan, 1975, 48, 657.

D11. Shirakawa, H.; Ito, T.; Ikeda, S. Polymer J., <u>1973</u>, 4, 460.

D12. Leagraut, S.; Lichtmann, L. S.; Temkin, H.; Fitchen, D. B.; Mitter, D. C.; Whitwell, G. E.; Birlitch, J. M. Solid State Comm., <u>1979</u>, 29, 191.

D13. For example, Seanor, D. A., Ed, "Electrical Properties of polymers", Academic Press., New York, <u>1982</u>.

D14. Fincher, C. R.; Ozaki, M.; Tanaka, M.; Peebles, D.; Lauchlan, L.; Heeger, A. J.; MacDiarmid, A. G. Phys. Rev., <u>1979</u>, B20, 1589.

D15. Sumita, O.; Fukuda, A.; Kuze, E. Appl. Polym. Sci., <u>1979</u>, 23, 2279.

D16. Patel, G. N. Polym. Prep., Am. Chem. Soc., <u>1979</u>, 20, 452.

D17. Khana, Y. P.; Patel, G. N. Polym. Prep., Am. Chem. Soc., <u>1979</u>, 20. 457.

D18. Patel, G. N.; Miller, G. G. J. Macromol. Phys., <u>1981</u>, B20, 111

D19. Se, K.; Ohnuma, H.; Kotaka, T. Macromolecules, to be submitted.

D20. Ohnuma, H.; Inoue, K.; Se, K.; Kotaka, T. Macromolecules, in press.

D21. Enkelmann, V.; Lando, J. B. Acta. Cryst., <u>1978</u>, B34, 2352.

D22. Mazid, M. A.; Enayetullah, M. A.; Walker, S.

J. Chem. Soc., Faraday Trans. 2, 1981, 77, 1143.

D23.   For example, McCrum, N. G.; Read, B. E.; Williams, G.
        "Anealstic and Dielectric Effects in Polymer Solid",
        John Wily and Sons. Ltd., New York, 1967.

D24.   Wegner, G. Macromol. Chem., 1972, 154, 35.

D25.   Baughman, R. H.; Chance, R. R. J. Chem. Phys.,
        1980, 73, 4113.

D26.   Shirakawa, H.; Ito, T.; Ikeda, S. Macromol. chem.
        1978, 179, 1565.

D27.   Chien, J. C. W.; Karasz, F. E.; Wnek, G. E.   Nature
        1980, 390.

D28.   Su, W. P.; Schrieffer, J. R.; Heeger, A. J. Phys.
        Rev. Lett., 1979, 42, 1698.

D29.   Day, D.; Lando, J. B. J. Appl. Polym. Sci., 1981,
        26, 1605.

D30.   Bernasioni, J.; Schneider, T., Ed., "Physics in one
        Dimention", Proceeding of an International Conference.
        Fribourg, Switzerland, August 25-29, 1980. (Springer-
        Verlag, Berlin)

Chapter 5

ELECTRICAL PROPERTIES OF POLY(nACMU)S

5-1. Introduction

Although common polymeric materials are generally
insulators of electricity, some conductive polymers have
been attracting attention in recent years. [E1] These
conductive polymers have two intriguing characteristics
beside their rather high conductivity. One is the
anisotropy of the conductivity. Therefore, these materials
may be called linear-chain conductors or one-dimensional
conductors. [E2] The other is the possibility of easy
processability. They may be molded into thin films which
might be utilized as solar cell materials and/or recharge-
able organic batteries.

Polydiacetylenes as well as polyacetylene are
insulators of electricity, unless they are doped adequately
with some electron acceptors (or donors) such as halogens
or arsenic pentafluoride (AsF_5). The conductivity rapidly
increases with increasing dopant concentration. [E3-E5]
A key problem is undoubtedly the mechanism of enhancing
the conductivity by doping. In order to solve this

difficult problem we carried out studies on the conductivities of four different poly(nACMU)s: Poly(3BCMU), poly(3ECMU), poly(2BCMU) and poly(4BCMU). First, we investigated whether the mechanism of the conduction of doped poly(nACMU)s is ionic or electronic. Secondly, we examined the dependence of electrical conductivity of poly(nACMU)s on the dopant concentration and temperature. We also examined dependence of the conductivity on the types of molecular species and on the molecular weight. Furthermore we attempted to develop a new technique of doping in order to prepare specimens with much higher conductivity.

In order to study the anisotropy of the conductivity, we prepared single crystals of poly(4BCMU) and compared the properties with those of $CHCl_3$ cast films. We also prepared partially oriented films of poly(3BCMU) by stretching them near the crystalline melting temperature, and examined the anisotropy in the doped state.

We also attempted to formulate the dependence of the conductivity on the varieties of molecular characteristics as well as the empirical parameters with simple terms as much as possible. Taking these empirical relations between the molecular structure and the conductivity into account, we attempted to clarify the mechanism of electric conduction of poly(nACMU)s as well as that of enhancing the conductivity by doping in molecular terms.

5-2. Experimental Procedures

5-2-1. Materials

poly(nACMU) Sample: The characteristics of poly(3BCMU),
poly(3ECMU), poly(2BCMU) and powder-form and single
crystalline poly(4BCMU) samples prepared were described in
Chapter2.

Knowledges on molecular weight dependence of the
conductivity of Polymer semiconductors should be important
for elucidating the mechanism of the electric conduction.
However, there are few works reported so far on this
problem, because of the difficulties in carrying out the
molecular characterization experiments on polymeric
semiconductors. The soluble polydiacetylenes such as
poly(3BCMU) [E6-E8] are an excellent model system to solve
this problem by the following two reasons: One is that
poly(nACMU) samples with different molecular weights can
be easily obtained by adjusting the total dose of ^{60}Co
γ-rays in the solid state polymerization. [E8] Particularly,
in the early stage of polymerization high molecular weight
and narrow distribution samples may be obtained. [E8] In
the later stage, however, low molecular weight and broad
distribution samples were produced. The other reason is
that poly(nACMU)s are soluble and the molecular
characterization can be easily carried out.

We carried out an extensive study on the conductivity,

employing several poly(3BCMU) samples with different

molecular weight. Typical GPC chromatograms of poly(3BCMU)

samples are shown in Figure 5-1. The molecular character-

istics determined is summarized in Table 5-1. It should

be noted that the molecular weight values listed in Table

5-1 are smaller than those in Table 2-1. The former values

were determined on the samples recovered from solvent cast

films, while the latter values on powder form fresh samples

obtained immediately after the polymerization. By casting

from $CHCl_3$ solution, poly(3BCMU) chains might have been

degraded by some oxidants existing in $CHCl_3$.

Poly(3KAU) Samples: KOH hydrolyzed poly(3BCMU), poly(3KAU),

is soluble in water, and hence, as-cast films of poly(3KAU)

were obtained from poly(3KAU)/water solution by evaporating

water. The films were dried under 10^{-4} torr for 60 hours

and subjected to conductivity experiments.

5-2-2. Methods

5-2-2-a. Measurements of Conductivity

   The direct-current conductivity σ_{dc} is defined by the

current I, potential drop ΔV, area A, and separation ΔX as

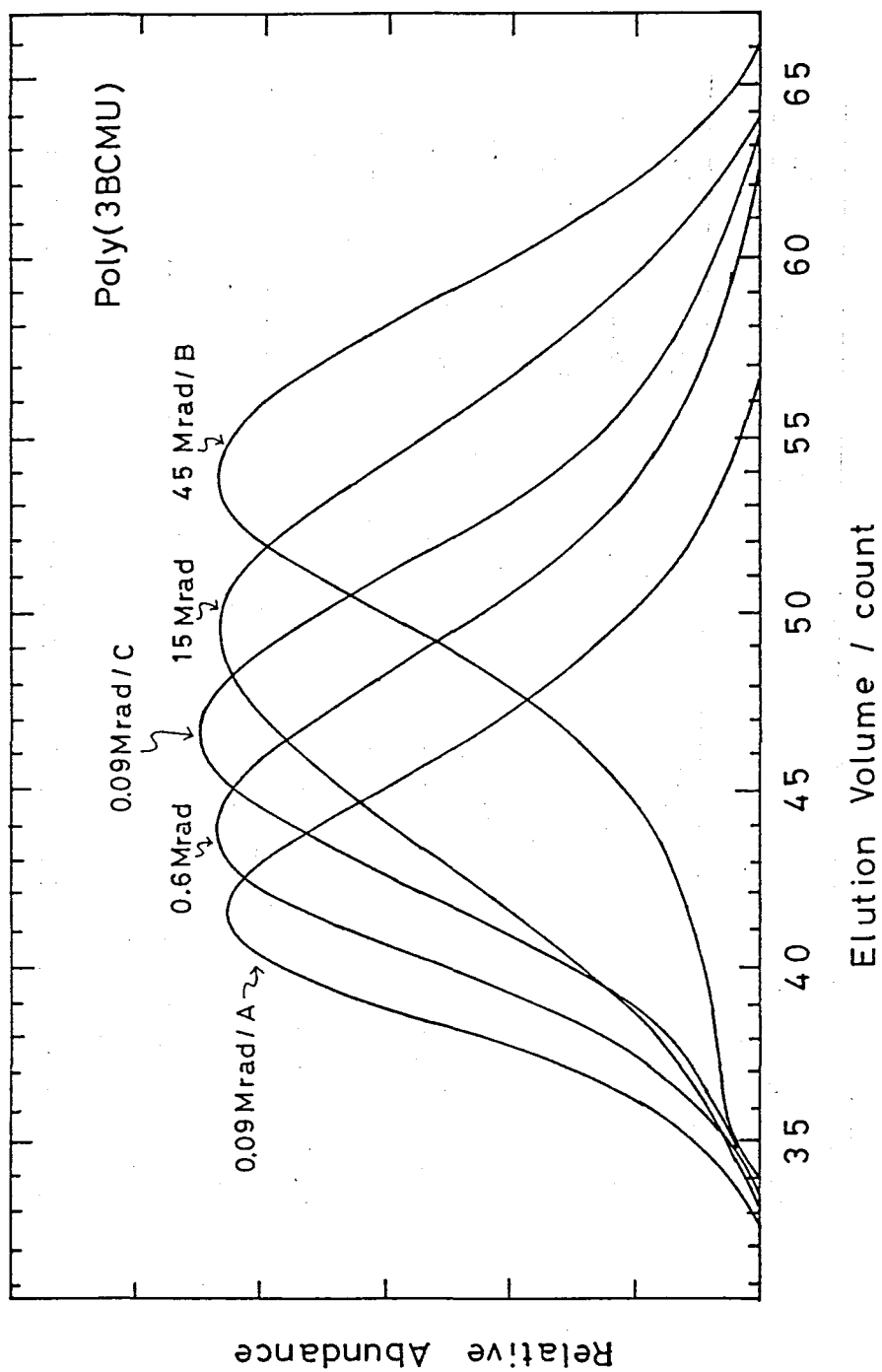$$j = I \,/\, A, \quad E = \Delta V \,/\, \Delta x \qquad (5\text{-}1a)$$

Figure 5-1. Typical GPC chromatograms of redissolved CHCl$_3$ cast films of poly-(3BCMU) used in this study. For the numerical values and symbols see Table 5-1.

Table 5-1. Molecular characteristics[a] and the enthalpies ΔH_f of fusion[b] of poly(3BCMU) films having different molecular weight.

Poly(3BCMU)[c]	$10^{-6}M_n$	$10^{-6}M_w$	M_w/M_n	$\dfrac{\Delta H_f}{J \cdot g^{-1}}$
45 Mrad/B	0.0203	0.419	20.5	1.29
45 Mrad/A	0.0394	2.31	58.6	2.60
15 Mrad	0.0446	0.737	16.5	2.64
0.09Mrad/C	0.0716	0.634	8.86	2.60
0.09Mrad/B	0.154	0.870	5.67	—
0.6 Mrad	0.102	0.583	5.68	2.05
0.09Mrad/A	0.236	1.38	5.86	2.75

a) PS reduced molecular weights estimated from GPC.

b) Enthalpies of fusion at about 450K estimated from DSC thermograms.

c) The codes, A, B, and C refer the samples recovered from different batches and/or films.

$$\sigma_{dc} = \frac{E}{j} \qquad\qquad (5\text{-}1b)$$

where j and E are the current density and electric field strength, respectively. To carry out accurate measurements of the conductivity, one must be careful on the following three points, which otherwise cause a large error. (i) The electrical resistance of the specimen must be much smaller than the input resistance of the voltmeter. [E10] Otherwise, the current flows between the input terminals of the voltmeter via routes other than the intended one through the specimen. Recently, electrometers having high input impedance are available, and hence, this difficulty may be readily avoided by use of such high-performance electrometers. (ii) When a voltmeter and an ammeter are used simultaneously in the same circuit, mutual interference between them often gives anomalous apparent current in the circuit. Electrical noises through the earth terminals also cause a trouble. In order to avoid this trouble from the mutual interference, the power source of the ammeter must be changed from the 100 V alternating-current source to a battery. (iii) The last problem is concerned with electrodes used. The electrodes must form an ohmic contact with specimen. It may be convenient to apply conductive paint such as silver dispersions or Aquadag (dispersion of colloidal graphite) directly to the surface of the specimen. However, paints often contain

toluene as the solvent, and such solvents often cause some trouble in carrying out the measurements. On the other hand, use of gold electrodes evaporated on the sample surface is reliable but is often inadequate for doped specimens, because the dopant is lost in the high vacuum chamber during evaporating gold.

In order to avoid the troubles mentioned above, we used a Keithley 640 Electrometer as an ammeter and Keithley 610 Electrometer as a potentiometer which has a high input impedance. A battery was employed as the source for the ammeter to avoid the mutual interference with the voltmeter. A toluene dispersion of colloidal graphite, Dotite XC-12,(Fujikura Kasei Co.) was used to attain ohmic electrical contacts.

Alternating-current (ac) conductivity σ_{ac} was measured with a transformer bridge (General Radio Model 1615A) in the range of 0.1 kHz–100 kHz.

## 5-2-2-b. Electrical Circuits in Measuring conductivity

In this study we employed following four different methods of measuring conductivity. Each method has its own advantages and disadvantages.

4-terminal Method: A better way to measure the conductivity

is a 4-terminal method, as illustrated in Figure 5-2-a.

The electrodes were formed by painting Dotite XC-12 on the

specimen and platinum wires were attached. A known current

I is injected into electrode 1 to the electrode 4, while

the potential difference ΔV between the electrodes 2 and

3 was measured. The cross section of electrode and

separation of electrodes were also measured. Then, the

conductivity was calculated by Eq. 5-1. The potential

difference ΔV was not affected by the contact resistance

and polarization effect between specimen and electrode.

These facts are the advantage in using a 4-terminal method.

4-Point Probe Method: A 4-point probe shown in Figure

5-2-b was employed for measuring the dopant concentration

dependence of σ_{dc}. Tungusten point probes were used as

electrodes. We can observe the net potential difference

ΔV between the electrodes 2 and 3 under a given current I

between the electrodes 1 and 4. If the specimen is a

semi-infinite block, the conductivity σ_{dc} is given by

$$\Delta V = \frac{1}{2\pi} \frac{1}{\sigma_{dc}} \left(\frac{1}{d_1} - \frac{1}{d_2+d_3} - \frac{1}{d_1+d_2} + \frac{1}{d_3} \right) \quad (5-2)$$
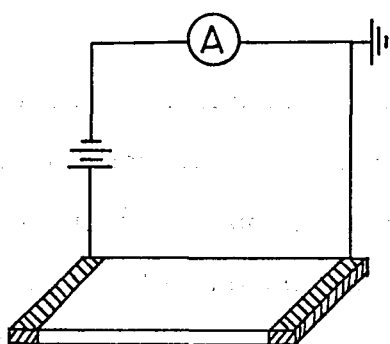
If the separations between the electrodes are the same
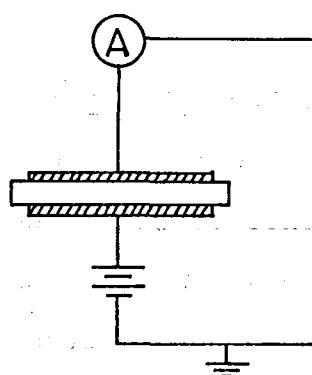
and equal to d, Eq. 5-2 reduced to
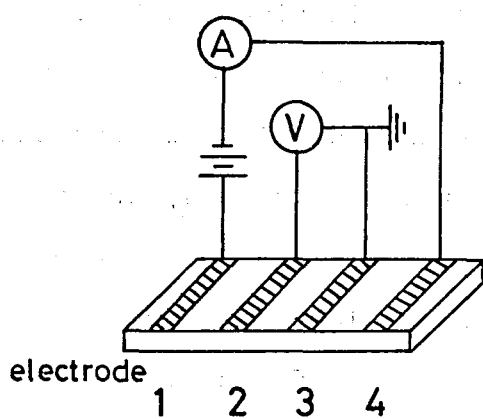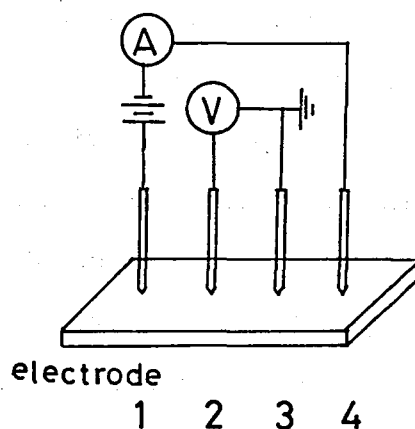
Figure 5-2. Schematic circuit diagrams for conductivity measurements: (a) 4-terminal method; (b) 4-point method; (c) 2-terminal method parallel to film; (d) 2-terminal method perpendicular to film. (A) and (V) are an ammeter and a potentiometer, respectively.

$$\sigma_{dc} = \frac{1}{2\pi d} \frac{I}{\Delta v} \qquad (5-3)$$

Since we usually use a specimen of finite size, especially, thin film, the corrections are necessary on using Eq. 5-3. Such a correction of conductivity in the direction perpendicular to the film is dominant rather than that in parallel to the film. The true value σ_{dc} may be about 6 times larger than the apparent value. However, we did not make any corrections for the finite size of the specimens. The 4-point probe method is a simple but convenient technique for anisotropic specimens as well as usual films, because no extra care such as Dotite pastings is necessary.

2-terminal Methods: The dimensions of poly(4BCMU) single crystals were usually small, and the conductivity of even doped specimens was very low at low temperature so that the 4-terminal and 4-probe methods could not be used. For these cases we had to use a 2-terminal method. There are two different types of 2-terminal method.

Electrode configuration used for single crystalline poly(4BCMU) is shown in Figure 5-2-c. To prepare a specimen, we first selected platelet like crystals with good quality by examining them with a polarizing microscope. Gold was evaporated onto both ends of each specimen to

form electrodes such as shown in Figure 5-2-c, while masking the rest of the specimen. We attached electrodes along the direction normal to the c-axis and also to the a-axis so that we could measure the conductivities $\sigma_{//}$ and $\sigma_{\perp}$ in the directions parallel to the c- and a-axes of the crystal, as shown in Figure 5-2-a, respectively. The area and the distance between the electrodes were measured with a Peacock dial thickness gauge (0.01 mm) and Ocular micrometer attached to a polarizing microscope.

Another 2-terminal electrode configuration is shown in Figure 5-2-d. The electrodes were formed by Dotite. Occasionally we used a dielectric cell with guard electrode. Some troubles such as the contact resistance and the polarization effect between the electrodes and the specimen may arise in these devices. It is noted that the apparent conductivity measured is lower than the true one in these two terminal methods.

3-Terminal Method: In order to measure the volume and surface conductivities separately, three terminal methods were used. The two variations of these three terminal configuration are shown in Figure 5-3-a and -b.

The 3-terminal-specimen-holder consisted of a high-voltage electrode, a guarded electrode and a guard electrode. In order to estimate the volume current I_v, a certain voltage was applied between the guarded and
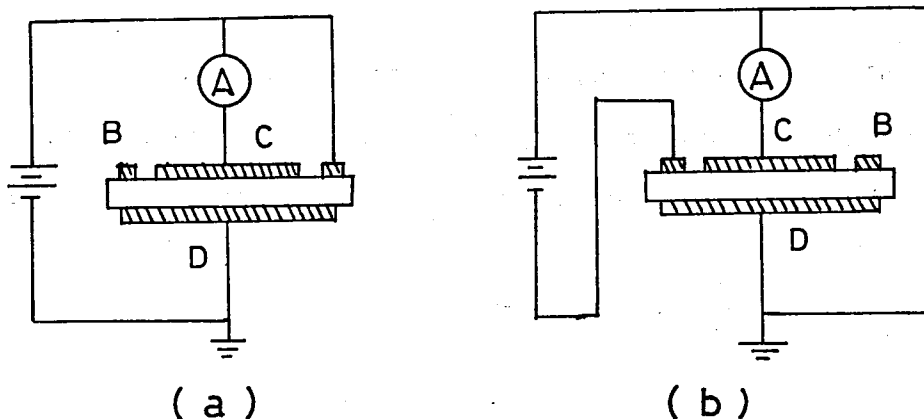
Figure 5-3. 3-terminal specimen holder: (a) circuits for volume conductivity measurement and for (b) surface conductivity measurement. B, C, and D denote guard electrode, guarded electrode and high-voltage electrode, respectively. (A) is an ammeter.
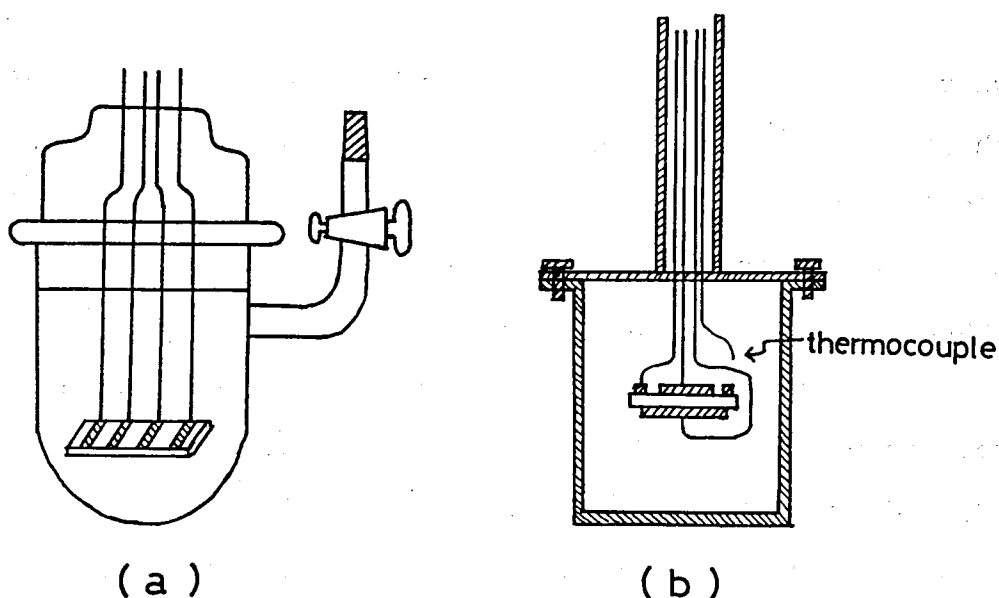

Figure 5-4. Home-made electrode cells: (a) a home made glass cell for 4-terminal method and (b) a home-made brass cell for 3-terminal method.

high-voltage electrodes, and the guard electrode to the battery through an ammeter, as shown in Figure 5-3-a. Then, the volume conductivity σ_v was determined as follows,

$$\sigma_v = \frac{d}{A} \frac{I_v}{V} \qquad [\ \Omega^{-1}\ cm^{-1}] \qquad (5-4)$$

where A is the area of the guarded electrode and d is the thickness of the specimen held between the guarded and high-voltage elctrodes.

For a rectangular specimen the surface conductivity σ_s is defined by

$$\sigma_s = \frac{q}{p} \frac{I_s}{V} \qquad [\ \Omega^{-1}] \qquad (5-5)$$

where p and q is the length and width, respectively, of the specimen between the electrodes, and I_s is the current flowing on the surface of the specimen. A more convenient method of determing σ_s is to use a 3-terminal electrode shown in Figure 5-3-b.

For measuring the surface current I_s, a certain voltage was applied through an ammeter between the guarded (B) and guard (c) electrodes, and the high-voltage electrode (D) was connected to the earth terminal, as shown in Figure 5-3-b. Concentric ring electrodes are convenient for measuring of the surface current. With this

type of electrodes, the σ_s is given by, E10

$$\sigma_s = \frac{1}{2\pi} \ln(\frac{r_2}{r_1}) \frac{I}{V} \qquad (5-6)$$

Where r_1 and r_2 are the outer radius of the guarded electrode and the inner radius of the guard electrode, respectively. The results will be discribed later.

5-2-2-c. Special Purpose Cells

Occasionally, measurements of the conductivity were carried out during doping with iodine using a specially designed home-made glass cell, which is shown in Figure 5-4-a. Four platinum wires were sealed on the top of the glass cell, and the four terminals were connected to the measuring circuits. A glass tube from the side of the cell was connected to a vacuum line connected to a special vessel of iodine vapor through a vacuum cock. The glass cell was evacuated to 10^{-3} torr by a rotary pump. Then, iodine vapor was introduced, and the measurement of conductivity was started simultaneously. By using this glass apparatus, the effect of aging on the conductivity was also studied.

In making measurements of temperature dependence of σ_{dc}, a specimen was inserted in an air-tight brass container, shown in Figure 5-4-b, filled with heliem and

the container was cooled or heated. The temperature was
monitored by a copper-constantan thermocouple mounted close
to the specimen.

5-3. Results

5-3-1. Volume and Surface conductivities

Usually the current in a specimen flows through
both the surface and the bulk of the specimen, i. e.,
$I_t = I_v + I_s$ in which I_t, I_v and I_s are total current,
volume current and surface current, respectively. The
ratio of the I_v and I_s is affected by the ratio of volume
and surface of samples. We attempted to estimate the
ratio of I_v and I_s of the 4-terminal devices which were
usually used in conductivity measurements. For example,
the volume conductivity σ_v and surface conductivity σ_s
of poly[2BCMU(I_3)$_{0.70}$] measured by the 3-terminal method
were 1.5 x 10^{-6} $\Omega^{-1}cm^{-1}$ and 2.6 x 10^{-9} Ω^{-1}, respectively.
Using these values, we estimated I_v and I_s as 120 x 10^{-10} A
and 9.3 x 10^{-10} A, respectively, for a typical case of
conductivity measurement on poly[2BCMU(I_3)$_{0.70}$] specimen
with a 4-terminal device. Thus, we may concluded that
the ratio of I_v/I_t was 93 %. The apparent conductivity σ_{dc}
measured by the 4-terminal method is almost equal to the
volume conductivity.

5-3-2. Dopant Concentration Dependence

The direct-current (volume) conductivities σ_{dc} of undoped poly(3BCMU)/45Mrad and poly(3BCMU)/0.09Mrad films are of the order of 10^{-11} $\Omega^{-1}cm^{-1}$, although they have the metallic appearance of golden color. The σ_{dc} of an undopted specimen by the 4-terminal method after about 4 hours evacuation at 10^{-3} torr in the home-made glass cell decreased from 2.3 x 10^{-11} $\Omega^{-1}cm^{-1}$ to 0.8 x 10^{-11} $\Omega^{-1}cm^{-1}$. The σ_{dc} became constant after 70 hours evacuation as shown in Figure 5-5. After the constant was reached, a small amount of air was introduced into the cell and then the σ_{dc} increased to the initial value of 2.3 x 10^{-11} $\Omega^{-1}cm^{-1}$ after about 4 hours. This behavior was reversible. This increase in σ_{dc} may be a result of oxygen acting as a dopant.[E14] However, such an increase in σ_{dc} was usually far less than that due to iodine doping. Hence, the σ_{dc} of iodine doped specimens were measured under usual atmosphere.

The change in σ_{dc} during doping poly(3BCMU) was also measured. Figure 5-6 shows the results. The curve I is the change in σ_{dc} for poly(3BCMU) placed directly in a sealed glass cell at room temperature. The increase in the conductivity is very rapid. After doping the specimen for 3 hours, the cell was evacuated under 10^{-3} torr. The σ_{dc} began to decrease with time with an almost constant
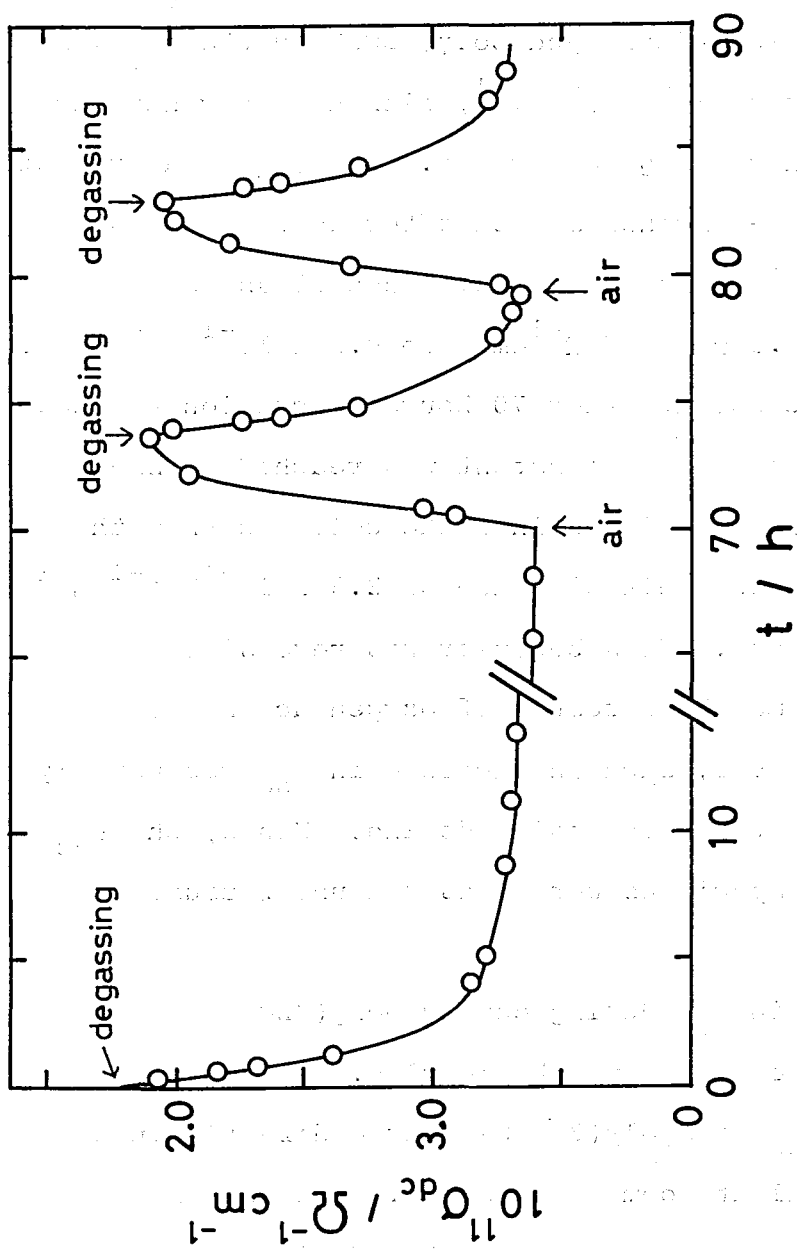
Figure 5-5. Change in the conductivity of pure poly(3BCMU) specimen degassing and introducing air into the cell.
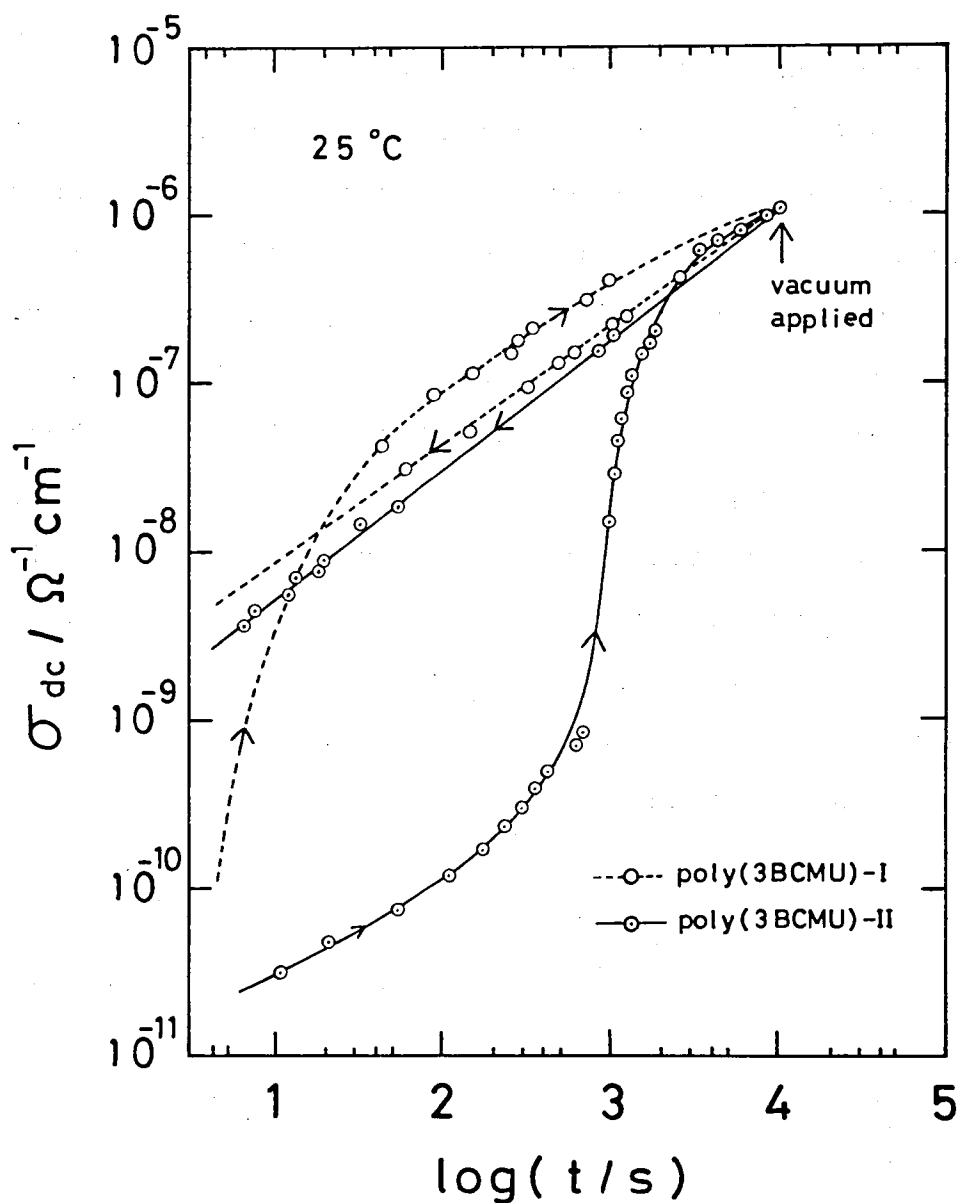
Figure 5-6. Change in the conductivity at room temperature by doping of poly(3BCMU) with iodine and sublimating iodine. The conductivity was about 10^{-11} Ω^{-1} cm^{-1} at $t = 0$ and about 10^{-6} Ω^{-1} cm^{-1} at $t = 3$ hours. Different methods of doping were employed for specimen-I and -II (see text).

rate, as shown in the figure. On the other hand, the curve II represents the similar data for poly(3BCMU) doped with iodine contained in a separated ampule connected to the cell through glass tubes and stopcocks. The σ_{dc} increased slowly with time in the early stage of doping. The specimen may be doped with iodine at a slow rate. After doping the specimen under this condition for about 1 hour, the σ_{dc} began to increase rapidly in a manner similar to that of the initial stage of the curve I, and finally reached the same level as of the curve I. And then by evacuation of the cell, the σ_{dc} decreased in a manner similar to that of the curve I. The difference in the doping behavior of the curve I and II obviously reflects the difference in the dopant pressure in the early stage of doping. The conductivity σ_{dc} of solvent-cast poly(3BCMU) films increases with the dopant concentration, and after about 3 hours of doping the σ_{dc} become enhanced by a factor of as much as almost 10^5. The processes were completely reversible.

Figure 5-7 shows the dependence of σ_{dc} on the dopant concentration Y for a few poly(nACMU)s and polybutadiene at 25°C. The σ_{dc} increases with increasing Y and finally reaches to the semiconductivity region of about 10^{-5} $\Omega^{-1} cm^{-1}$ at Y of about 0.7. These results may be the first demonstration[E15, E16] that the σ_{dc} of poly(nACMU)s among varieties of other polydiacetylene derivatives,[E17-E19]
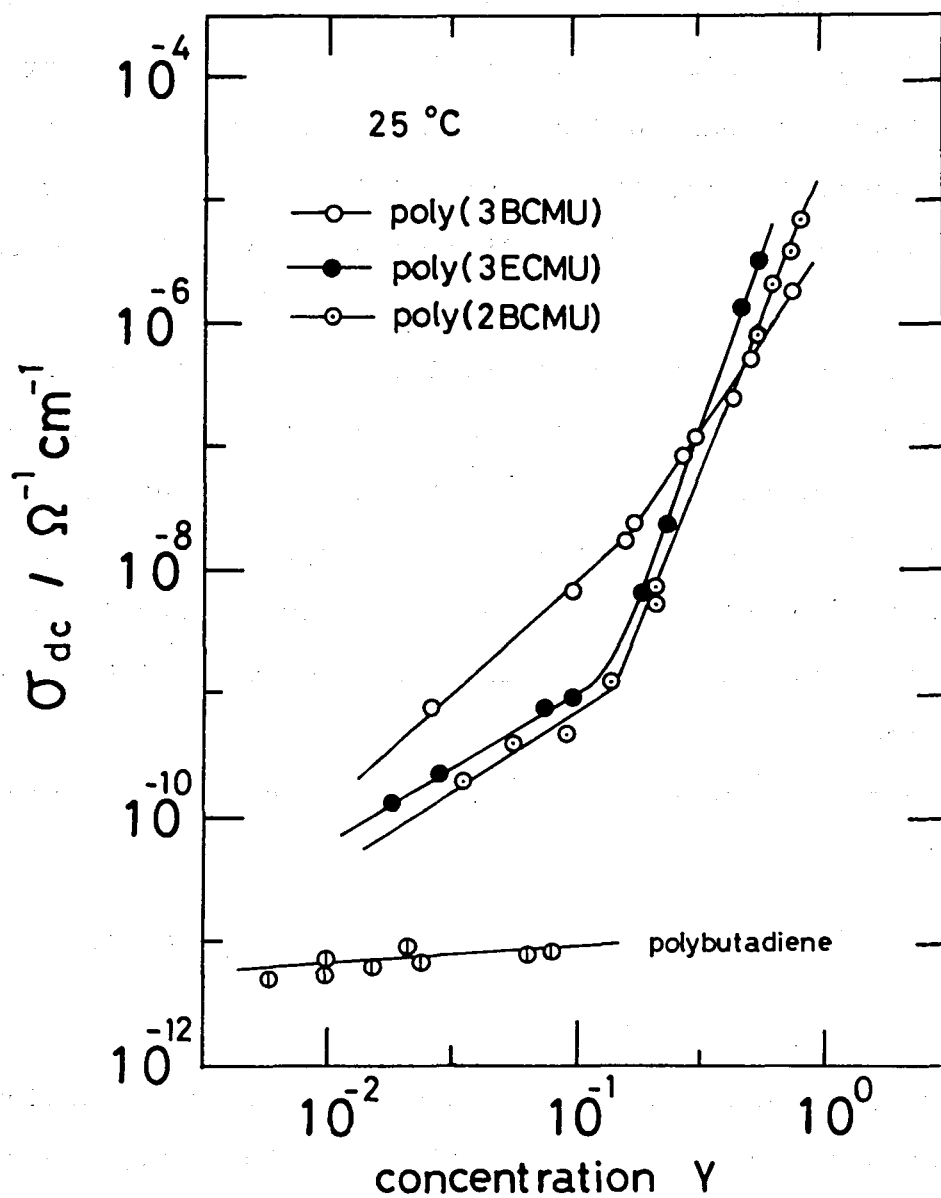
Figure 5-7. Dc conductivity of three poly(nACMU)s and polybutadiene at 25°C as a function of dopant concentration Y.

reaches as high as semiconductive level by adequate doping

with iodine. This high level of conductivities was stable

for about two years under the atmosphere and sunlight. [E17]

The drop of 90 % of the conductivities after two years

may be attributed to the iodine desorption during the two

years.

For comparison, we examined the σ_{dc} of polybutadiene

doped with iodine. The σ_{dc} of doped polybutadiene remained

almost constant at about 10^{-11} level in the range of Y

about 10^{-2} to 10^{-1}. These results suggest that iodine is

not acting merely as an ionic charge carrier but interacts

with the conjugated main chains of doped poly(nACMU)s to

increase the σ_{dc}.

According to Drude, [E10] the σ_{dc} is generally given by

$$\sigma_{dc} = q \; n \; \mu \qquad\qquad (5-7)$$

where q, n and μ are the amount of charges per a carrier,

the number density, and the mobility of the charge carrier,

respectively.

On the other hand, the σ_{dc} of doped poly(nACMU) may

be represented as a function of Y by

$$\sigma_{dc} \; (\; Y \;) = A \; Y^{\,\alpha} \qquad\qquad (5-8)$$

where A and α are the parameters independent of Y. If
the dopant iodine is acting merely as an ionic carrier, the
q and μ should be virtually constant and n would be directly
proportional to the carrier concentration Y. However, the
σ_{dc} for poly(3BCMU)/45Mrad first increases in proportion
to $Y^{2.0}$ and later to $Y^{3.0}$. The parameters of poly(3ECMU)
and poly(2BCMU) in the low Y side of the curves are 1.3
and 1.2, respectively, and those in the high Y side are
4.8 and 5.7, respectively.

The large values of α above the break points of the
σ_{dc} versus Y curves suggest that iodines are acting as
electron acceptors which withdraw electrons from the main
chains thus producing charge carriers, in this case, holes.
The iodines may also act as bridges for hopping of holes
from one chain to another. On the other hand, the small
values of α below the break points might imply that the
conduction is ionic rather than electronic.

Precisely speaking, the values of α below the break
points are still large than one. Hence the dopant iodines
may be interacting to some extent with the conjugated main
chains of poly(nACMU)s.

For the break points on the σ_{dc} versus Y curve, we
notice that the Y* is about 0.14 and almost constant for
three different poly(nACMU)s, while the σ_{dc} of poly(2BCMU)
and poly(3ECMU) are about $10^{-9}\Omega^{-1}cm^{-1}$ and that of
poly(3BCMU) is about $10^{-8}\Omega^{-1}cm^{-1}$.

5-3-3. Temperature Dependence

Figure 5-8 shows the temperature dependence of σ_{dc} for some doped poly(nACMU)s. The σ_{dc} decreases with decreasing temperature and then becomes almost constant below a certain temperature T*. In the high temperature region, the plots of log σ_{dc} vs. 1/T give approximately straight-lines with the thermal activation enthalpy E_a of 1.07 eV mol^{-1} for poly(3BCMU), 0.98 eV mol^{-1} for poly(3ECMU) and 0.99 eV mol^{-1} for poly(2BCMU). For undoped specimens, only the result of poly(3BCMU) is shown in Figure 5-8. However, other poly(nACMU)s show similar behavior. The values of E_a for undoped specimens are the same as those of the doped specimens, although the conductivities of the former are far smaller than those of the latter. That is to say, the dopant affects the conductivity but not the E_a. On the other hand, in the low temperature region the E_a of doped poly(nACMU)s become very small. The σ_{dc} of undoped poly(3BCMU) specimen was too low to be measured accurately, and is not shown in Figure 5-8.

The temperature dependence of σ_{dc} suggests that there are at least two independent mechanisms of conduction: One is the thermal activation process in which the rise in temperature increases both the current-carrier concentration and the carrier mobility. The other is an electronic process such as tunneling mechanism, by which
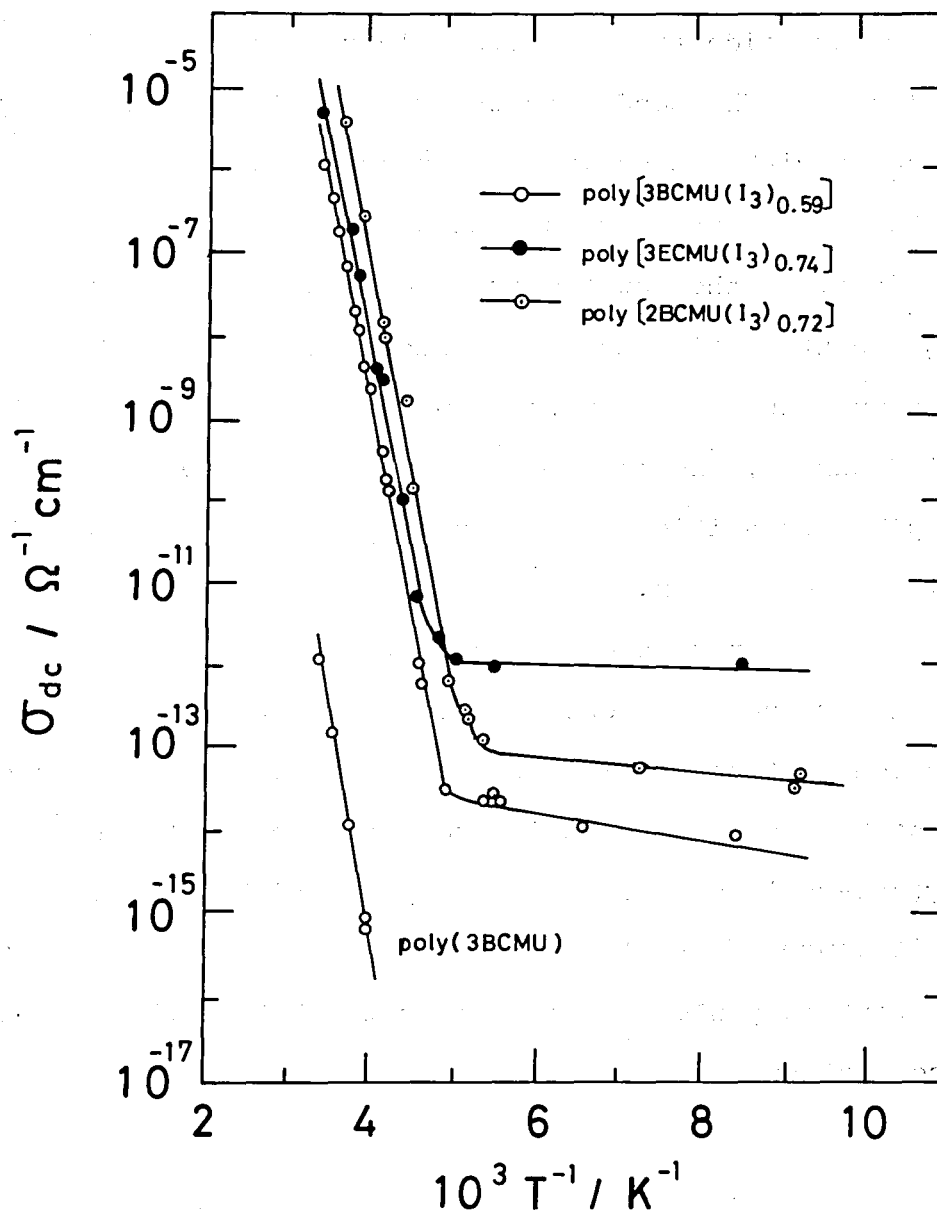
Figure 5-8. Temperature dependence of dc conductivity for pure and doped poly(nACMU)s prepared by the irradiation of 45 Mrad dosage.

the conductivity does not depend on temperature. At high

temperature side the former has larger contribution than

the latter. The conductivity by thermal activation rapidly

decreases with decreasing temperature, while the conductivity

due to the latter process remains almost constant.

Therefore, at the low temperature side, the latter has a

larger contribution to the conductivity than the former.

The temperature T^* is merely an intersect of the two σ_{dc}

vs $1/T$ curves, and is not a material parameter such as

the glass transition temperature T_g but an apparent

empirical parameter.

The temperature dependence of the conductivity does

not differ much from one species to another. The

electronic structure is affected very little by the side

chains but appears to be inherent and common to the

poly(ene-yne) type backbones of poly(nACMU)s. The

indifference of the temperature dependence of σ_{dc} among the

different poly(nACMU)s is similar to that of the dopant

concentration dependence.

5-3-4. Alternating-Current Conductivity

Measurements of the conductivity σ_{ac} for alternating

current often provide an important informaion on the

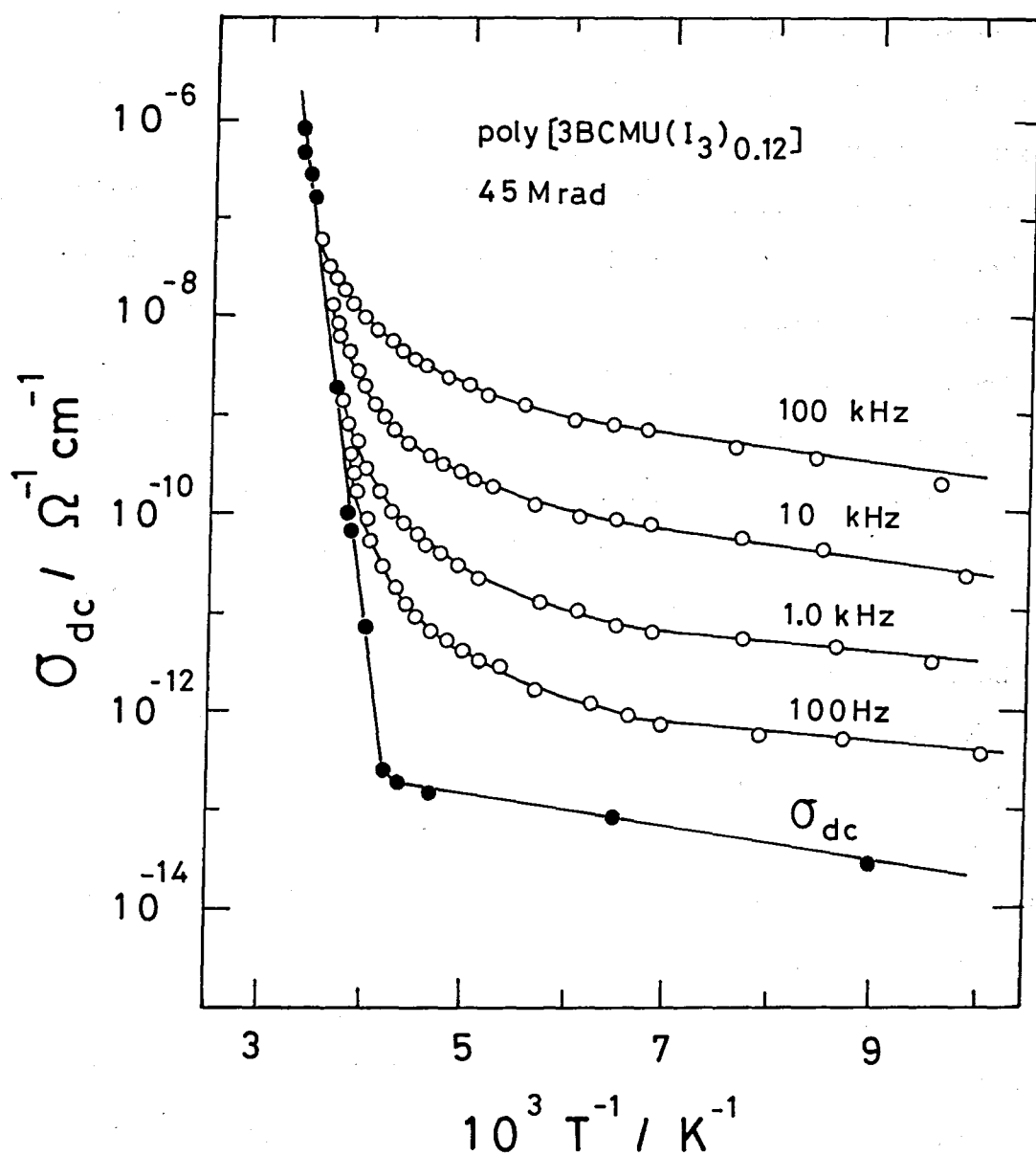mechanism of electrical conductivity of materials. Figure

Figure 5-9. Temperature dependence of ac conductivity at
0.1 kHz, 1 kHz, 10 kHz and 100 kHz (open circles) and
dc conductivity (solid circles) for poly[3BCMU(I_3)$_{0.12}$].

5-9 shows the temperature dependence of ac conductivity σ_{ac} of poly[3BCMU(I_3)$_{0.12}$]/45Mrad specimen. The σ_{ac} is much larger than the σ_{dc} and the difference becomes progressively greater as temperature is lowered. Similar temperature dependence of σ_{ac} was found in some inorganic semiconductor [E21, E22] such as single crystalline silicon.

The electrical properties of single crystalline silicon have been interpreted on the basis of the band theory. [E23] There may be band and hopping conduction in single crystalline silicon. The σ_{dc} is attributed essentially to the band conduction with less significant hopping carriers. On the other hand, the σ_{ac} is attributed to both band and hopping between the localized states in the forbidden region and the carrier mobility is extremely smaller than that by the band conduction. The band conduction is a dominant factor at the high temperature side where the number of thermally activated carriers in the band region becomes larger. On the other hand, the hopping conduction is a dominant factor at the low temperature side where there is few carriers in the band region. Hence, in the low temperature side ac conductivity σ_{ac} due to the hopping conduction may be dominant rather than dc conductivity σ_{dc} due to the band conduction.

Figure 5-10 shows the frequency dependence of σ_{ac} at various temperatures for poly[3BCMU(I_3)$_{0.12}$]/45Mrad. The data may be cast into the form; [E21]
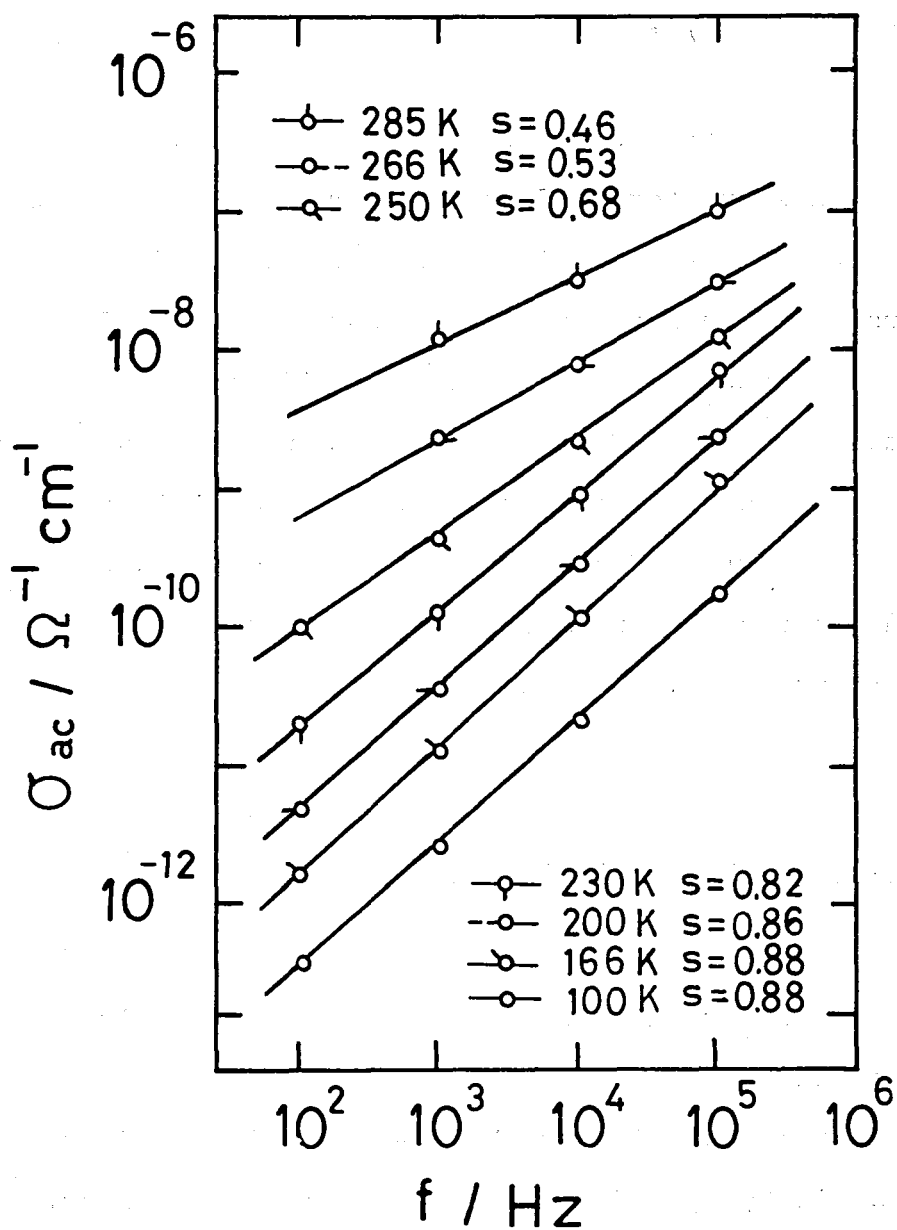
Figure 5-10. Frequency dependence of ac conductivity for poly[3BCMU(I_3)$_{0.12}$]. The values of s indicated are the slopes of the curves at the corresponding temperature.

$$\sigma_{dc}(f) = A f^s \qquad\qquad (5-9)$$

where A and s are constant and f is the frequency. The σ_{ac} of an insulator is directly proportional to f (s = 1), while the σ_{ac} of a metal does not depend on f (s = 0) in the usual frequency region. As seen in Figure 5-10, the value of s decreases from 0.88 to 0.46 as the temperature is raised from 100 K to 285 K. This result suggests that the transition from an insulator to a metal is taking place in doped poly(3BCMU)s as the temperature is increased, besides the steep increment of conductivity at high temperature side.

5-3-5. Molecular Weight Dependence

It has been known that some physical properties such as dielectric relaxation of semicrystalline polymer are influenced not only by the molecular weight and its distribution but also by the variation in the degree of crystallinity X_c and in the crystalline morphology.[E13, E24] Sometimes, the X_c itself depends on the molecular weight and its distribution. However, several poly(3BCMU) samples having different molecular weights invariably yield poorly crystalline specimens, when cast from $CHCl_3$. As judged from the enthalpy of fusion the X_c of those $CHCl_3$ cast

films are very small and nearly the same from one sample

to another, as shown in Table 5-1. Therefore, in this

chapter, we interpret the results of the electric

conductivities of the solvent-cast films of these samples

as reflecting the molecular weight dependence but not

necessarily the X_c dependence of the conductivities.

Figure 5-11 shows the dependence of σ_{dc} on Y at 18°C

for different samples. The σ_{dc} increases with increasing

Y. Obviously the values of σ_{dc} compared at given Y depend

on the samples used. This finding may be the first evidence

that demonstrates the molecular weight dependence of σ_{dc}

for polymer semiconductors. E16, E25, E26 There was no

correlation between the σ_{dc} at a given Y and M_w, but a

good correlation was found between the σ_{dc} and M_n. The

values of σ_{dc} read at three different values of Y are

plotted against M_n in Figure 5-12. We see that the σ_{dc}

at any Y is increasing linearly with M_n. The σ_{dc}

extrapolates to zero at M_n = 0. This result suggests that

3BCMU monomer doped with iodine may be an insulator.

The slope of the straight line for Y = 0.4 is larger

than those for Y = 0.3 and Y = 0.2. Namely, the molecular

weight dependence of σ_{dc} for poly(3BCMU) with large Y is

larger than that for those with small Y. Presumably, the

migration of electrons and/or holes in the conjugated

backbones may be delayed at the chain ends. Therefore,
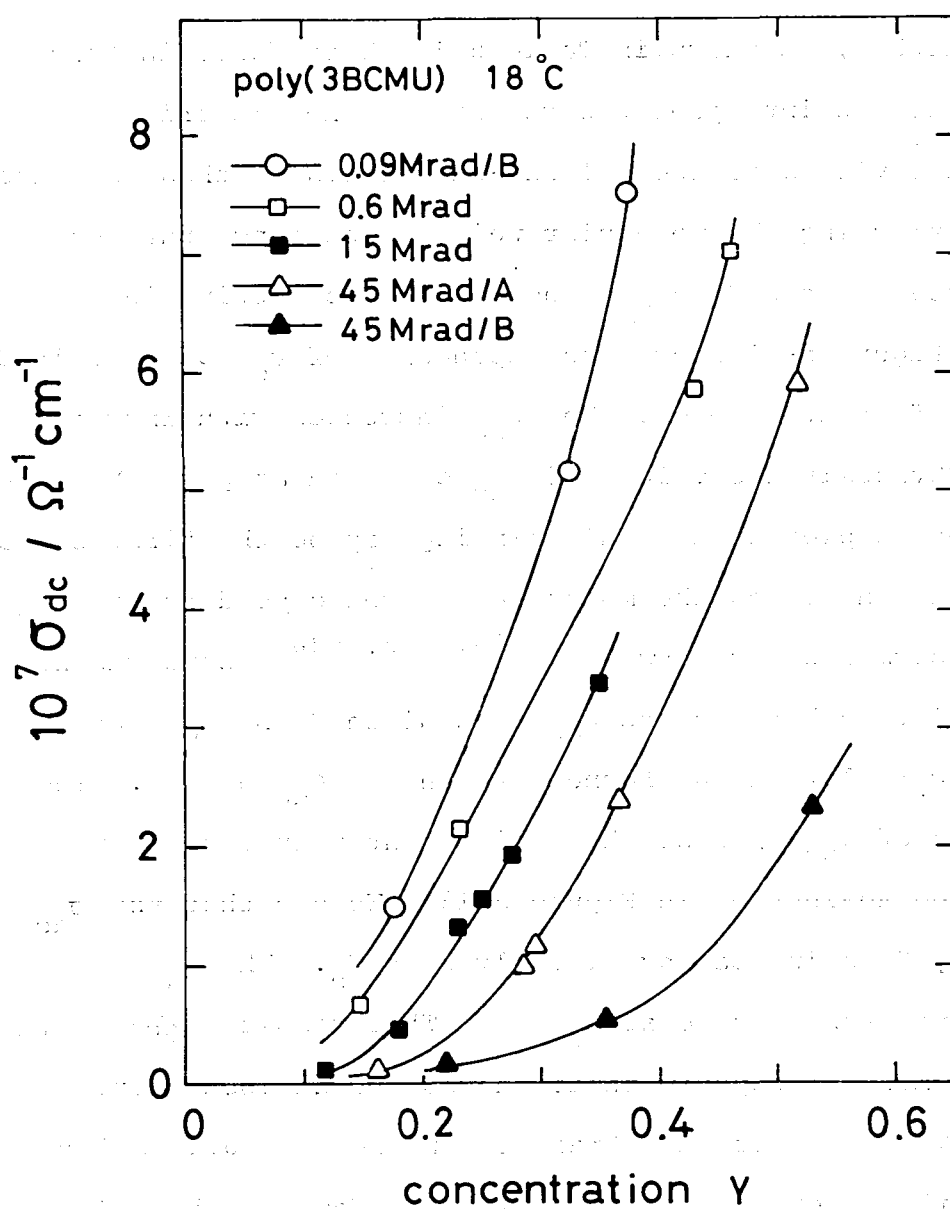
the resistivity is proportional to the number of chain

Figure 5-11. Dependence of dc conductivity at 18°C on dopant concentration for five poly(3BCMU) samples having different molecular weights and their distributions.
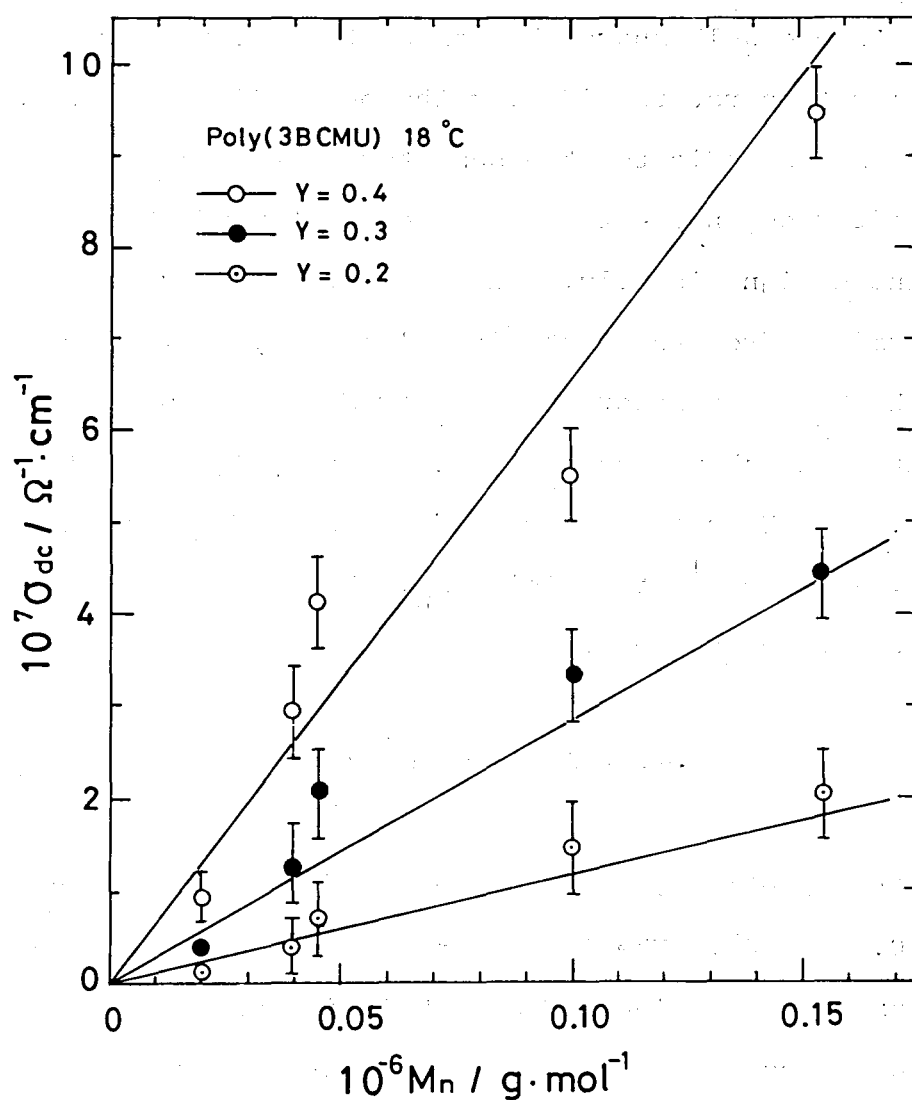
Figure 5-12. Dependence of dc conductivity on number-average molecular weight M_n for poly(3BCMU) specimens with three different dopant levels Y of 0.2, 0.3 and 0.4. The plots were determined from the data in Figure 5-10.

ends, i. e., the σ_{dc} is directly proportional to M_n.

Figure 5-13 shows the temperature dependence of σ_{dc} at high temperature side for the poly(3BCMU) samples. All the samples indicated the same temperature dependence before and after doping, although the conductivity itself is enhanced significantly. The activation energies E_a determined from the Arrhenius plot of σ_{dc} vs. 1/T depend on the M_n but neither on Y, M_w or M_w/M_n ratio of the samples. Figure 5-14 shows the activation energy E_a plotted against M_n^{-1}. The E_a decreases with decreasing M_n^{-1} and extrapolates to 0.44 eV mol^{-1} at infinite M_n. Hence the E_a may be given by the following equation

$$E_a = 0.44 + 0.023 \times 10^6 / M_n \qquad (5\text{-}10)$$

for the samples with M_n in the range between 0.02×10^6 and 0.23×10^6. The first term corresponds to the energy for exciting an electron or a hole in the conjugated backbone and for transporting the charge carrier along the backbone chain with infinite length. The second term of Eq. 5-10 represents the molecular weight dependence of E_a and is inversely proportional to M_n. This result is reasonable, because the resonance energy and the effective conjugation length of the backbone increase with increasing molecular weight.
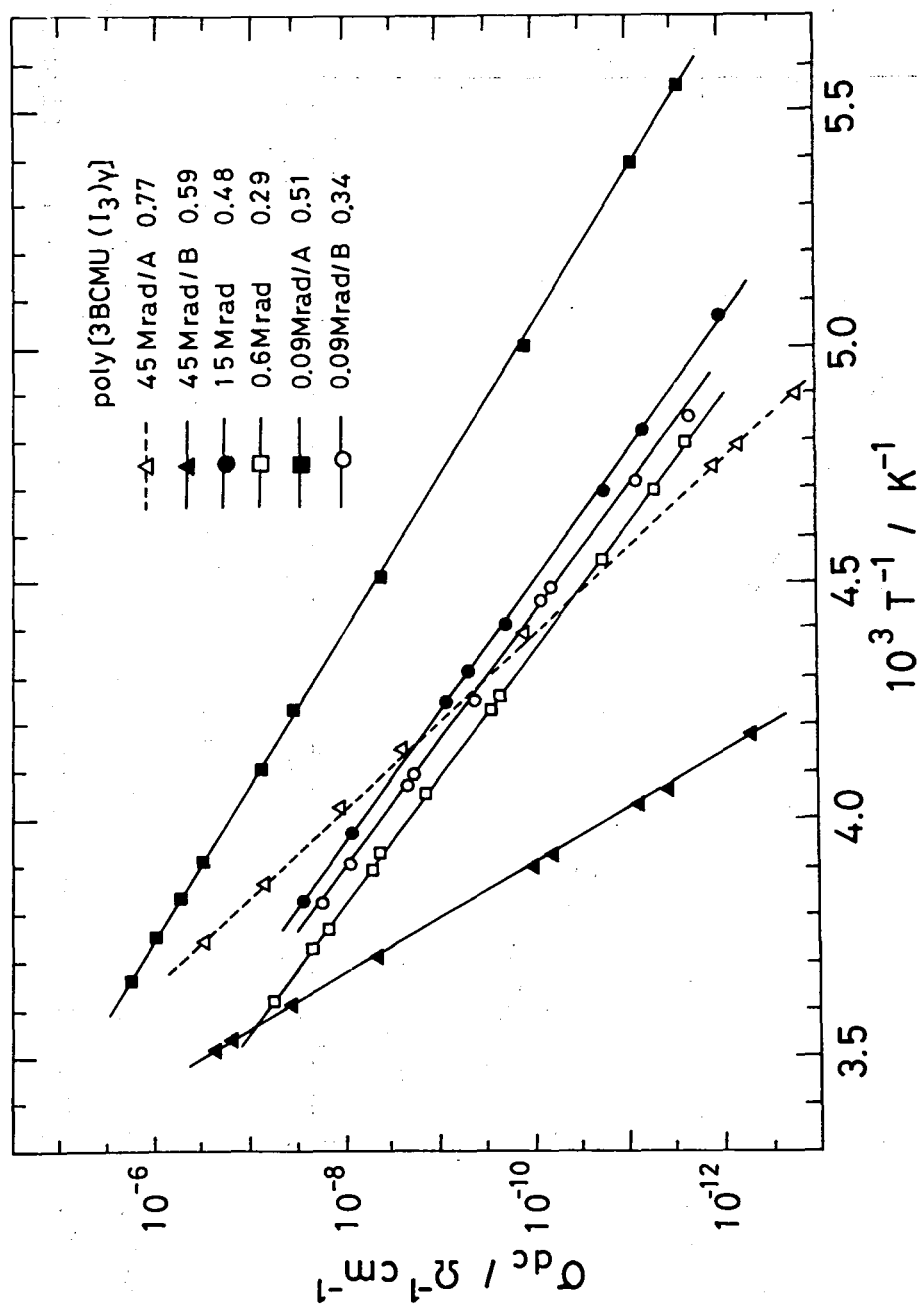
Figure 5-13. Temperature dependence of dc conductivity for doped poly(3BCMU) specimens having different molecular weights and their distributions.
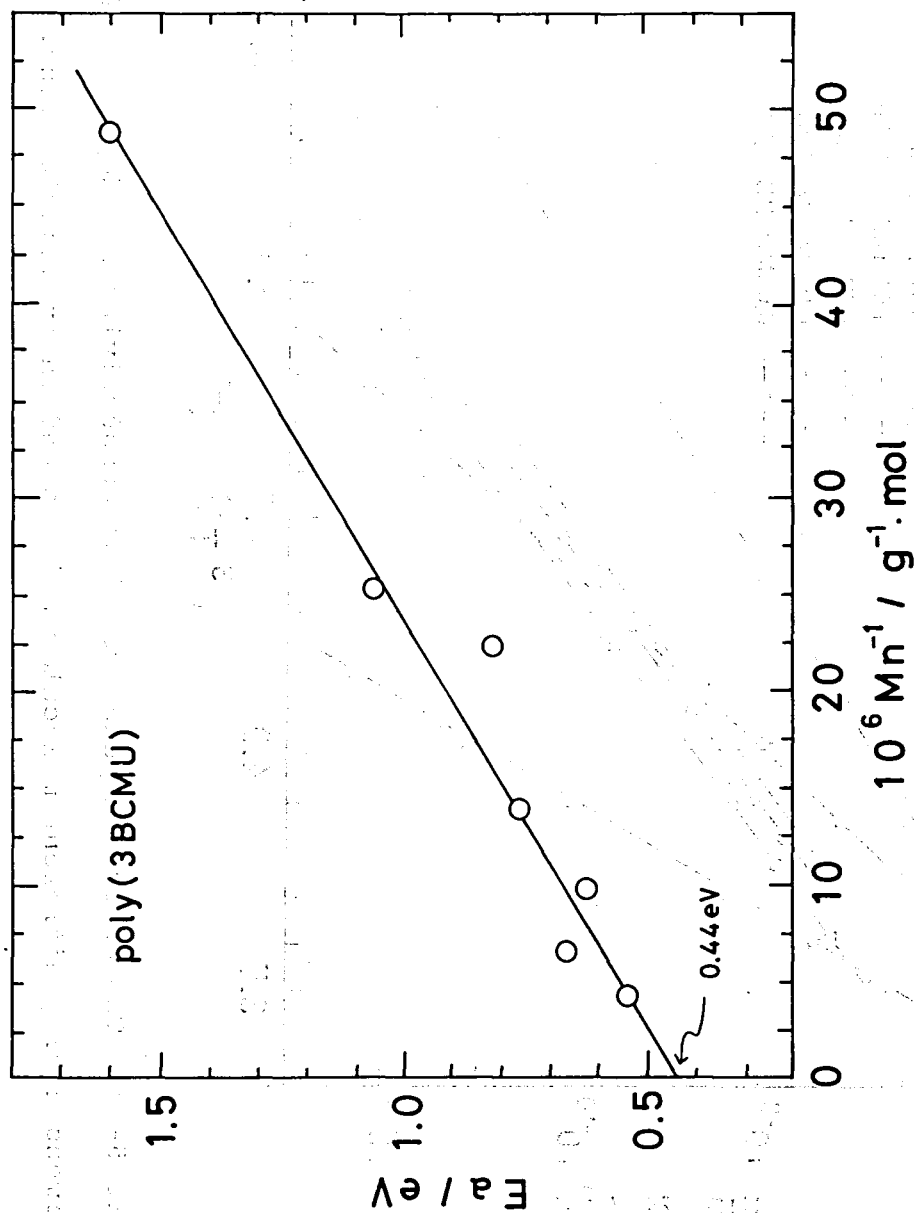
Figure 5-14. Plot of apparent-activation-energy E_a versus M_n^{-1} for poly(3BCMU) samples. The E_a were determined from the slope of the curves shown in Figure 5-13

5-3-6. Anisotropic Conductivity

5-3-6-a. Single Crystalline poly(4BCMU)

Figure 5-15 shows temperature dependence of electrical (direct current) conductivity σ_{dc} for undoped and iodine-doped films of poly(4BCMU). Two data points for the conductivities along the c'-axis $\sigma_{//}$ and along the a'-axis $\sigma_{\perp}$ of single crystalline poly(4BCMU) are also shown in the figure. For single crystals, the $\sigma_{//}$, and $\sigma_{\perp}$ at 20°C were measured at various dopant concentrations. These values and the apparent activation energy E_a are compared in Table 5-2. For the doped single crystals of Y = 0.005-0.010, the E_a values for $\sigma_{//}$ and $\sigma_{\perp}$ were estimated to be 0.92 and 1.09 eV, respectively. For all the samples, the E_a value appears to decrease slightly by doping. The E_a value for $\sigma_{//}$ appears to be slightly smaller than that for $\sigma_{\perp}$.

Figure 5-16 compares the conductivities as functions of Y for single crystals with that for $CHCl_3$ cast films at 20°C. For single crystals, the conductivities rapidly level off at a level of Y by a factor of 100 times lower than that for $CHCl_3$ cast films. The maximum attainable values of $\sigma_{//}$ and $\sigma_{\perp}$ are also lower than that for the solvent cast films. This result is presumably due to the difficulty in doping the highly crystalline specimens effectively. For example, a cast film could be doped to Y = 0.13 after
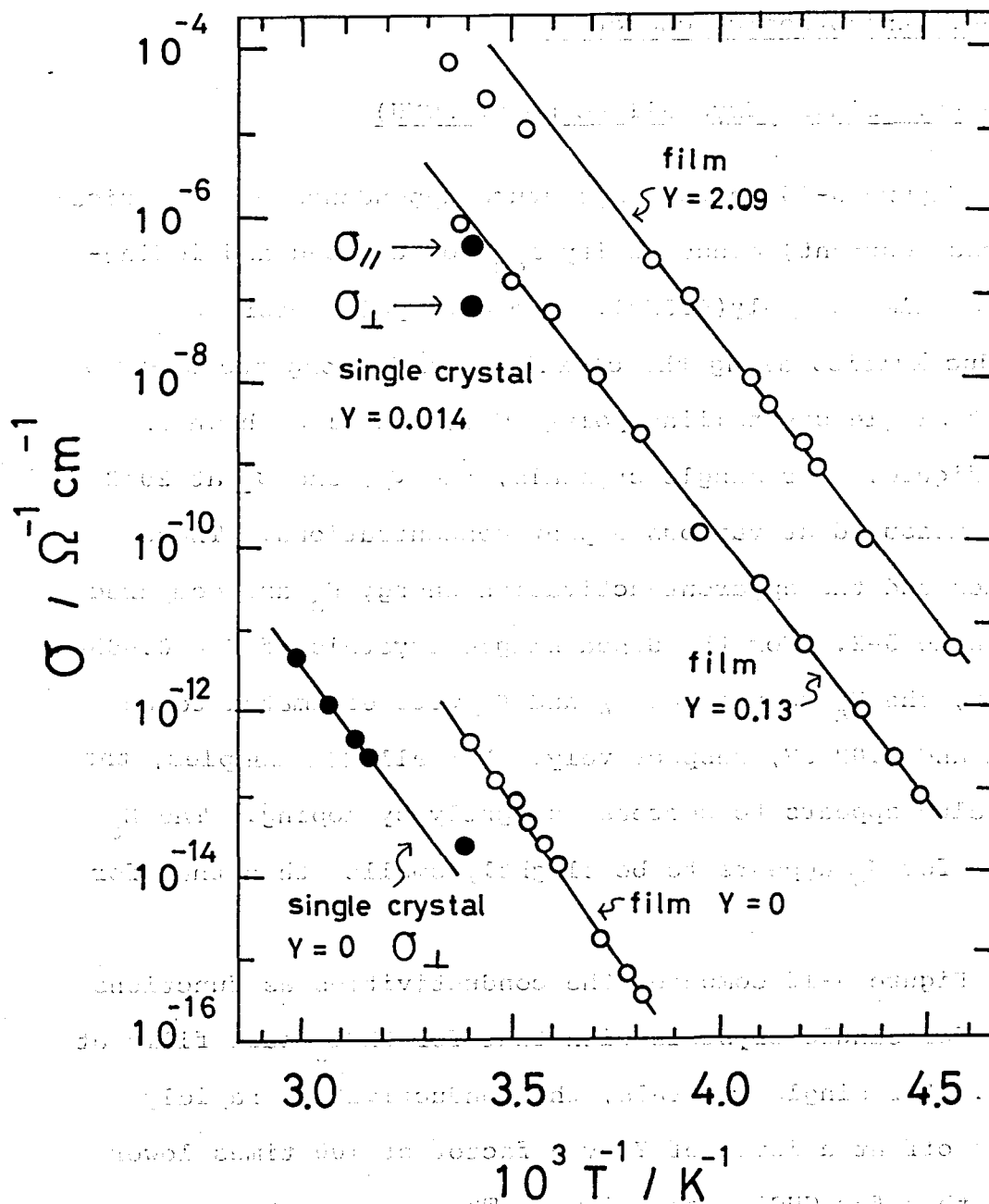
Figure 5-15. Temperature dependence of dc conductivity σ_{dc} for $CHCl_3$ cast and single crystalline poly(4BCMU).

Table 5-2. the electrical conductivities and their apparent activation energy E_a at 20°C for $CHCl_3$ cast films and single crystalline specimens with various dopant concentrations.

Samples	Y	σ / Ω^{-1} cm^{-1}		E_a/eV
$CHCl_3$cast film	0	3.1 x 10^{-13}		1.48
	0.13	3.6 x 10^{-7}		1.32
	2.09	4.0 x 10^{-5}		1.30
Single crystal	0	2.8 x 10^{-14}	($\sigma_\perp$)	1.32[a]
	0.014	4.1 x 10^{-7}	($\sigma_{//}$)	(0.92)[b]
		6.5 x 10^{-8}	($\sigma_\perp$)	(1.09)[b]

[a] Estimated at 50°C.

[b] these values are estimated for single crystals with slightly different values of Y.
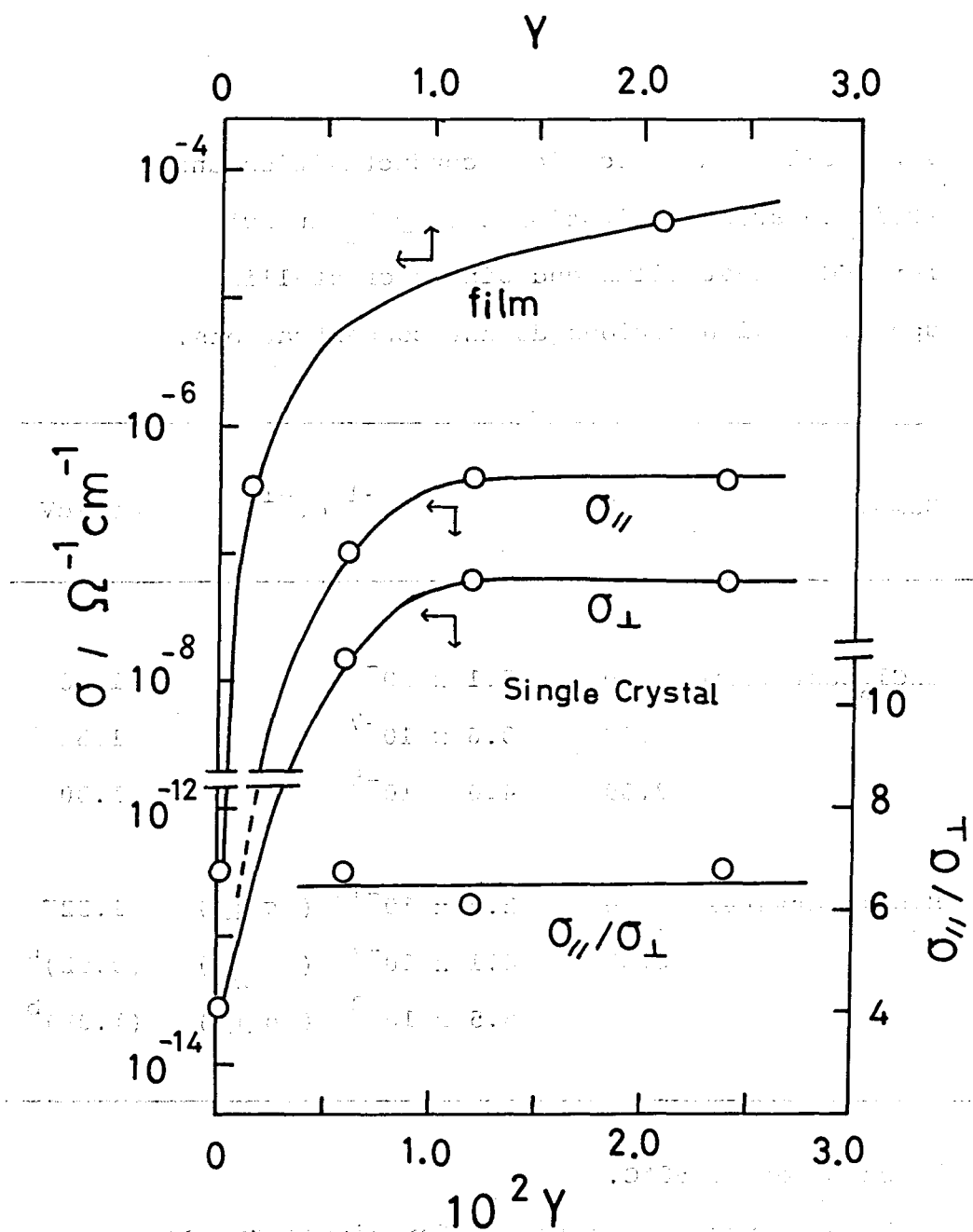
Figure 5-16. Dependence of conductivities and the ratio $\sigma_{//} / \sigma_{\perp}$ on dopant concentration Y for $CHCl_3$ cast and single crystalline poly(4BCMU)s at 20°C.

5 h exposure to iodine, while a single crystalline specimen gave Y = 0.026 even after as long as 50 h exposure. Figure 5-16 also shows that the anisotropy in the conductivities $\sigma_{//}/\sigma_{\perp}$ of the single crystal is 6.5 ± 0.4, and is nearly independent of Y. This value of anisotropy is comparable to that reported by Schermann and Wegner[E17, E27] on dark conductivities of a single crystalline poly(diacetylene p-toluence sulfonic acid) derivative (PDA-TS).

Recently, Siddiqui and Wilson[E27] reported that the anisotropy for PDA-TS is $\sigma_{//}/\sigma_{\perp} = 10^3$, which is in sharp contrast with the results obtained by Schermann and Wegner. They pointed out that Schermann and Wegner had used undesirable arrangement of electrodes on the same face (surface electrodes). When examining currents along the chains with this arrangement, the current must also flow in the directions perpendicular to the chains. However, this is not the reason for the low anisotropy of our poly(4BCMU) single crystals, since we adopted evaporated gold electrodes covering the edges of the specimen completely as shown in figure. Then, the difference in the anisotropy between poly(4BCMU) and PDA-TS single crystals might have been resulted from the difference in their crystal forms. The single crystal of PDA-TS is known to be the most perfect among various polydiacetylenes, but poly(4BCMU) single crystal contains the disorder in the mutual level of the chains in the c-axis direction as

above-mentioned. In addition, the nearest neighbor

distance of the chains for poly(4BCMU) is 0.533 nm in the

direction of a'-axis ($\sigma_\perp$ direction), which is much shorter

than that of 0.75 nm for PDA-TS.[E27-E29] These evidences

seem to give the reasons for the low anisotropy of

poly(4BCMU) single crystals.

From the results given above, we may conclude as

follows. (i) The conduction along the polymer chain is

prevailing. (ii) The doping takes place mainly in the

amorphous regions of the specimens. (iii) The dopant

iodine is interacting with and providing charge carriers

along the conjugated backbones of poly(4BCMU). (iv)

presumably the dopant may be acting also as bridges for

hopping of charge carriers from one chain to another.

5-3-6-b. Partially Oriented Poly(3BCMU)

The relationship between current I and voltage V of

an oriented film of poly(3BCMU) was examined for the

electric fields applied parallel and perpendicular to the

stretch direction. Figure 5-17 shows the result for a

film with R = 1.75, f = 0.27 and the dopant concentration

Y = 0.409. The I-V plots are linear, and obey the ohmic

law in the range examined. From these plots, the
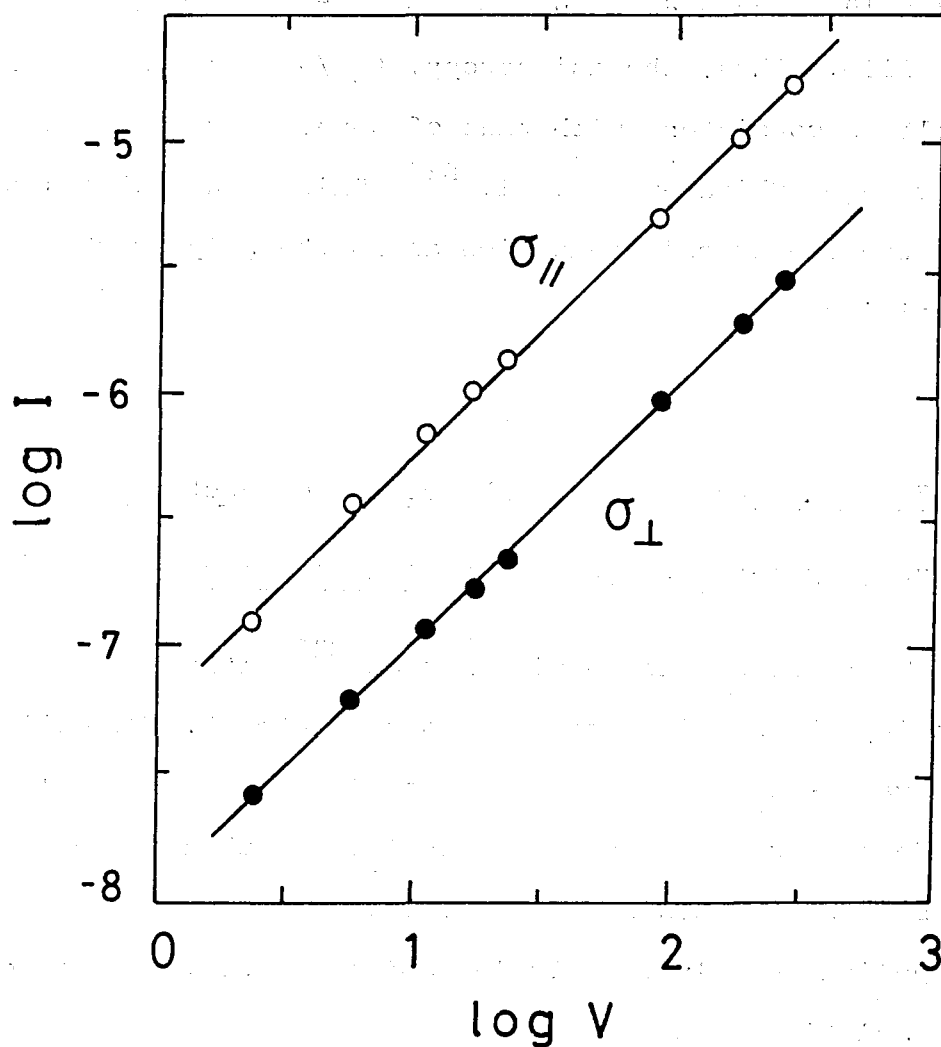
electrical conductivities parallel and perpendicular to

Figure 5-17. The I-V characteristics in the direction parallel (O) and perpendicular (●) to the stretched direction for an oriented poly[3BCMU(I_3)$_{0.409}$] film (R =1.75, f = 0.27).

the stretch direction, $\sigma_{//}$ and $\sigma_{\perp}$ were estimated to be 2.47 x 10^{-7} and 5.85 x 10^{-8} $\Omega^{-1}cm^{-1}$, respectively, for this film. Thus, the anisotropy, $\sigma_{//}/\sigma_{\perp}$ is 4.26. Our result is consistent with that of doped polyacetylene reported by Shirakawa et. al.[E28] This result also suggests that the electrical conduction along the polymer chain is prevailing.

5-3-7. Other Attempts to Enhance the Conductivity

5-3-7-a. Solution-Method of Doping With Iodine

There is another doping method[E29] different from exposing the specimen to the vapor of dopant. We called it a vapor-method. Another method is to dissolve polymers and dopants simultaneously in $CHCl_3$, and then evaporate the solvent to obtain a doped film. This doping technique is applicable only to soluble semiconductors. We may call it a solution-method.

First we attempted to dope poly(3BCMU) with iodine by the solution-method. Three films were cast from $CHCl_3$ solution of poly(3BCMU) and iodine and dried for 2 days. About 90 % of iodine initially dissolved in $CHCl_3$ solution was sublimed at room temperature and the amount of residual iodine in doped poly(3BCMU) was only 10 % of initial amount of iodine. The dopant concentration Y was estimated from

this residual amount of iodine. The conductivities σ_{dc} of three specimens were measured by the 4-terminal method. The result is listed in Table 5-3. The σ_{dc} of poly[3BCMU$(I_3)_{0.032}$] by the solution methods is larger than that by the vapor-method by a factor of 10^3 times. The increment in σ_{dc} by the solution method was saturated at heavy dopant concentration and then became ultimately the same as that by the vapor method.

These poly(3BCMU) specimens doped with iodine by the different methods to the same dopant concentration possessed the different conductivities. This result suggests that only a part of dopant iodine is active as the effective dopant with the concentration Y_{eff}: The dopant concentration Y might represent the total amount of dopant such as I_2, I_3^- and I_5^- forms, while the effective dopant concentration Y_{eff} the amount of iodine ions such as I_3^- and I_5^- forms conjugating effectively with poly(nACMU) backbones. The ratio of Y_{eff} and Y could not be estimated quantitatively.

5-3-7-b. Charge Transfer Complexes as Dopants

The solution-method for doping soluble poly(nACMU)s is particularly convenient for dopants having low vapor pressure. Examples of such dopants are 7,7,8,8-tetra-cyanoquinodimethane TCNQ [E30] which is a very strong

Table 5-3. Dc conductivities σ_{dc} of the samples by the solution-method and reduced conductivity increments by a vapor-method of iodine.

Polymer[a]	$\sigma_{dc}^{s}/\Omega^{-1}cm^{-1}$	$\sigma_{dc}^{s}/\sigma_{dc}^{v}$ [b]
Poly[3BCMU(I_3)$_{0.032}$]	5.2×10^{-7}	1×10^{3}
Poly[3BCMU(I_3)$_{0.23}$]	2.9×10^{-6}	2×10
Poly[3BCMU(I_3)$_{0.81}$]	2.6×10^{-6}	2×10^{-1}
Poly[3BCMU(TCNQ)$_{0.43}$]	3.4×10^{-9}	
Poly[3BCMU(TTF)$_{0.68}$]	1.2×10^{-7}	
Poly[3BCMU(TTF/TCNQ)$_{0.068}$]	3.7×10^{-5}	
Poly(3KAU)	5.3×10^{-4}	

a) Poly(3BCMU)/0.09Mrad

b) σ_{dc}^{s} and σ_{dc}^{v} indicate the conductivities by the solution-method and those by the vapor-method.

electron accepter, tetrathiafulvalene TFF [E31] a strong

electron donor, and TFF/TCNQ complex [E32] which itself has

a very high conductivity. The σ_{dc} values of poly(3BCMU)s

doped with these dopants are listed in Table 5-3. TCNQ or

TTF alone were not effective dopants for poly(3BCMU). On

the other hand, TTF/TCNQ complex was an effective dopant

for poly(3BCMU). Only 0.068 moles of the complex enhanced

the conductivity to $3.7 \times 10^{-5} \Omega^{-1}cm^{-1}$. If poly(3BCMU)

is doped with the same amount of I_3, the conductivity

reaches to the level as low as $10^{-10} \Omega^{-1}cm^{-1}$. In this

sense, the complex is as much as 10^5 times more effective

than iodine. Such a large enhancement may not be due to

the conduction through the TTF/TCNQ complex itself but to

poly(3BCMU) activated by TTF/TCNQ complex, because the

dopant concentration was so low that TTF/TCNQ complex were

not forming continuous phase in the doped poly(3BCMU) film.

It should be noted that such a film was as tough as

polyethylene.

5-3-7-c. Poly(3KAU)

The σ_{dc} of poly(3KAU) measured under atmosphere was
$5 \times 10^{-4} \Omega^{-1}cm^{-1}$, as listed in Table 5-3. Assuming that
all potassium ions introduced became the dopant like
iodine, we estimated the dopant concentration to be about 2.

The σ_{dc} of poly(3KAU) is almost identical with that of poly(3BCMU) doped with iodine. However, a significant difference in the conductivity between them was that for poly(3KAU) specimen under the applied voltage of 23 V cm^{-1} the current rapidly decreased with time and then after 100 hours under the atmosphere it leveled off to the value by a factor of 1000 smaller than the original current.

On the other hand, when poly(3KAU) specimen was dried at 10^{-3} torr the σ_{dc} decreased more rapidly and become 1000 times smaller than that measured under the atmosphere. Under the 23 V cm^{-1} and at 10^{-3} torr for 100 hours, the σ_{dc} of poly(3KAU) decreased by a factor of 10^{6} times smaller than the original current.

These results suggest that potassium ions K^{+} mainly contributed to the σ_{dc} of poly(3KAU) as the ionic carriers. E10, E33. The ionic conduction may be activated by a trace of moisture in the atmosphere.

5-4. Discussion

5-4-1. Basic Mechanisms of Electric Conduction

Phenomenologically the electric conduction of doped poly(nACMU)s may involve two mechanisms; one is ionic conduction due to the migration of iodine ions, while the other is due to hole conduction through the bands created

in the main chains. A most conclusive evidence for the
ionic conduction is detection of electrolysis products
formed on discharge of the ions as they arrive at the
electrodes. However, the technique is not very practical,
because the amount of electrolysis products under such a
conduction is usually too small to be analyzed.

In order to estimate the relative conduction of these
two mechanisms, the electric current was measured as a
function of time under a constant voltage. If the ionic
conduction is dominant, the current would decrease with
time, as the ionic carriers are eventually purged from the
system, It is also known that for ionic conductions the
Ohm's law does not hold but the sine-hyperbolic law becomes
valid. E10

The behavior due to ionic conduction is seen for
potassium salt of KOH hydrolyzed poly(3BCMU), coded as
poly(3KAU). E9   For poly(3KAU) specimen under the applied
voltage of 1.5 V the current rapidly decreases, as is seen
in Figure 5-16. The voltage versus current relation was
not ohmic for the poly(3KAU) specimen. On the other hand,
for iodine doped poly(3BCMU), as is seen in Figure 5-18,
the current under the applied voltage of 1.5 V and that
under 132 V are almost constant up to about 230 h. The
slight drop of the current after a prolonged application
of the voltage to the doped poly(3BCMU) may be attributed
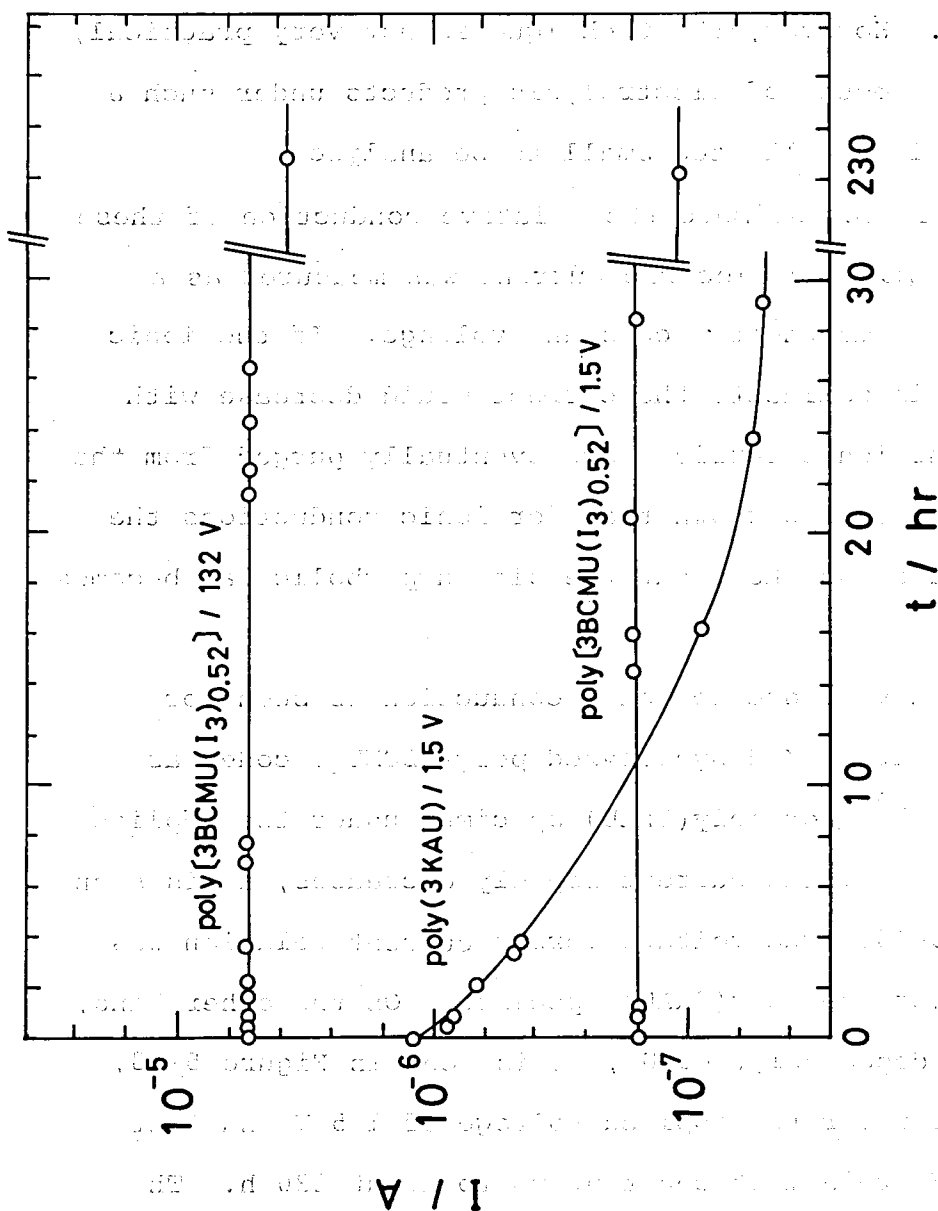to the iodine desorption during the period as judged from

Figure 5-18. Electric current versus applied time for doped poly(3BCMU) specimens under constant applied voltages. For comparison, the figure shows data for poly-(3KAU), which is KOH hydrolyzed poly(3BCMU)/45Mrad specimen.

the absorption and desorption features of iodine by poly(3BCMU) iodine system mentioned previously. We also found that the current was proportional to the applied voltage. That is, the conduction is approximately ohmic. These results strongly suggest that the electronic conduction is the main process in the doped poly(3BCMU).

Under the applied voltage of 132 v, the constant current was about 5.0×10^{-6} A. The transported charges during 230 h, then, amount to 4.0 coulombs. The dimension of this specimen was $3.15 \times 1.70 \times 0.13$ mm^3 and the dopant concentration Y was 0.52. If we assume that the polymer density is one and the dopant exists only in the form of I_3^- ion, all the ionic charges in this specimen is as small as 4.2×10^{-2} coulombs. The observed value is larger than that of the estimated ionic charges by a factor of 100. This observation also suggests that the electronic conduction may be the dominant factor in this specimen.

The conductivity σ_{dc} of doped poly(nACMU)s increases and the activation energy E_a decreases with increasing number-average-molecular weight M_n. Anisotropic conductivities $\sigma_{//}$ and $\sigma_\perp$ were measured for poly(4BCMU) single crystals and also for partially oriented films of poly(3BCMU). The values of $\sigma_{//}/\sigma_\perp$ were roughly 6.5 for the former and 4.2 for the latter. The direction of the

maximum electronic conduction corresponds to that of the conjugated main chains.

The fact that doped poly(nACMU)s possess the nature of electronic conductor is an encouraging factor when we seek for applications of the polymer as semiconductor devices such as rectifying behavior and photo-conduction.

5-4-2. Characteristics of Electric Conductivity of poly(nACMU)

The characteristic features of the conductivity of the present systems are summerized as follows: (i) the conductivity increases with increasing dopant concentration, while (ii) the activation energy of the conductivity is independent of the dopant concentration. (iii) Highly crystalline specimens such as single crystalline poly(4BCMU) could not be doped to high extent, and hence, the highest conductivity attained was low as compared to doped films. (iv) Anisotropy in the conductivities $\sigma_{//} / \sigma_{\perp}$ of the single crystalline poly(4BCMU) and partially oriented poly(3BCMU) are 6.5 and 4.2, respectively. (v) The conductivity is dependent on the number-average molecular weight M_n and (vi) the activation energy is also dependent on M_n. (vii) With decreasing temperature the activation energy

changes abruptly at a certain temperature T* from a substantially large value to nearly zero.

Comparing the results on poly(nACMU)s with those of iodine-doped polyacetylene (PA) [E34, E35] we see three characteristics in their behavior: (1) An undoped and doped PA have a semiconductive σ_{dc} of 10^{-6} $\Omega^{-1}cm^{-1}$ and a metallic value of 10^1 $\Omega^{-1}cm^{-1}$, respectively, while undoped and doped poly(nACMU)s have an insulative σ_{dc} of 10^{-12} $\Omega^{-1}cm^{-1}$ and a semiconductive value of 10^{-5} $\Omega^{-1}cm^{-1}$, respectively. (2) The σ_{dc} of PA is saturated at the Y of about 0.1, while that of poly(nACMU) at the Y of about 0.9. Finally, (3) the doping of PA and poly(nACMU)s results in an increase in σ_{dc} by the same factor of about 10^7. These characteristics may be attributed to the difference in the molecular and/or crystal structure between PA and poly(nACMU) films. In the latter only 10 % of the total molecular volume are the conjugated main chains and the rest 90 % are insulative side chains. Furthermore, the former has a fibrillar structure with high degree of crystallinity [E36, E37], while the latter, especially a cast-film is nearly amorphous with very low degree of crystallinity. [E16]

Two different type of behavior were found in the conduction of poly(nACMU)s; the one is semiconductivity observed in high temperature region and the other is insulative property in low temperature region. The former

is a thermally activated process, i. e., the σ_{dc} increases with temperature, while the latter σ_{dc} is almost independent of temperature. We will examine the detailed mechanisms involved in the electric conduction in high and low temperature regions.

5-4-3. Empirical Formula of Conductivity

The conductivity σ_{dc} of iodine doped poly(nACMU)s was independent of time and electric field strength, but found to dependent on dopant concentration Y, number-average molecular weight M_n and temperature T,

$$\sigma_{dc} \equiv \sigma_{dc} (Y, M_n, T) \tag{5-11}$$

The experimental results given so far suggest that the effects of Y, M_n and T on the σ_{dc} may be independent of one another under the experimental conditions employed in our study.

From the results, we may cast the σ_{dc} into

$$\sigma_{dc}(Y, M_n, T) = 1.1 \times 10^{-10} Y^3 M_n \exp[(\frac{1}{T_1} - \frac{1}{T}) \frac{1}{R}$$

$$(0.44 + 0.023 \times 10^6/M_n)] \tag{5-12}$$

for T_1 = 291 K > T > T*, which is the break point of the σ_{dc} versus 1/T plot and for M_n between 0.02 x 10^6 and 0.23 x 10^6. The empirical formula of σ_{dc} describes reasonably well the experimental data within an error of about 5 times.

In order to clarify the mechanisms of the electric conduction in more detail, it is desirable to estimate the charge carrier density and the mobility of the charge carrier separately. We attempted to carry out the measurements of Hall effect [E38] of iodine doped poly(3BCMU) specimens. However, it is in general very difficult to apply such a measurement on low-dimensional, anisotropic semiconductors such as the present systems. Unfortunately, we could not obtain satisfactory results on the Hall effect. Another possibility might be the measurements of photoconductivity by the time-of-flight method. [E39]

5-4-4. Conduction in Low Temperature Region

In the high temperature region the current I versus voltage V relation was ohmic in the voltage range of 1 V to 150 V. On the other hand, in the low temperature region the I-V relation was not ohmic, as shown in Figure 5-19. However, the differece in the I-V plots would give a further significant information on the conduction mechanism.
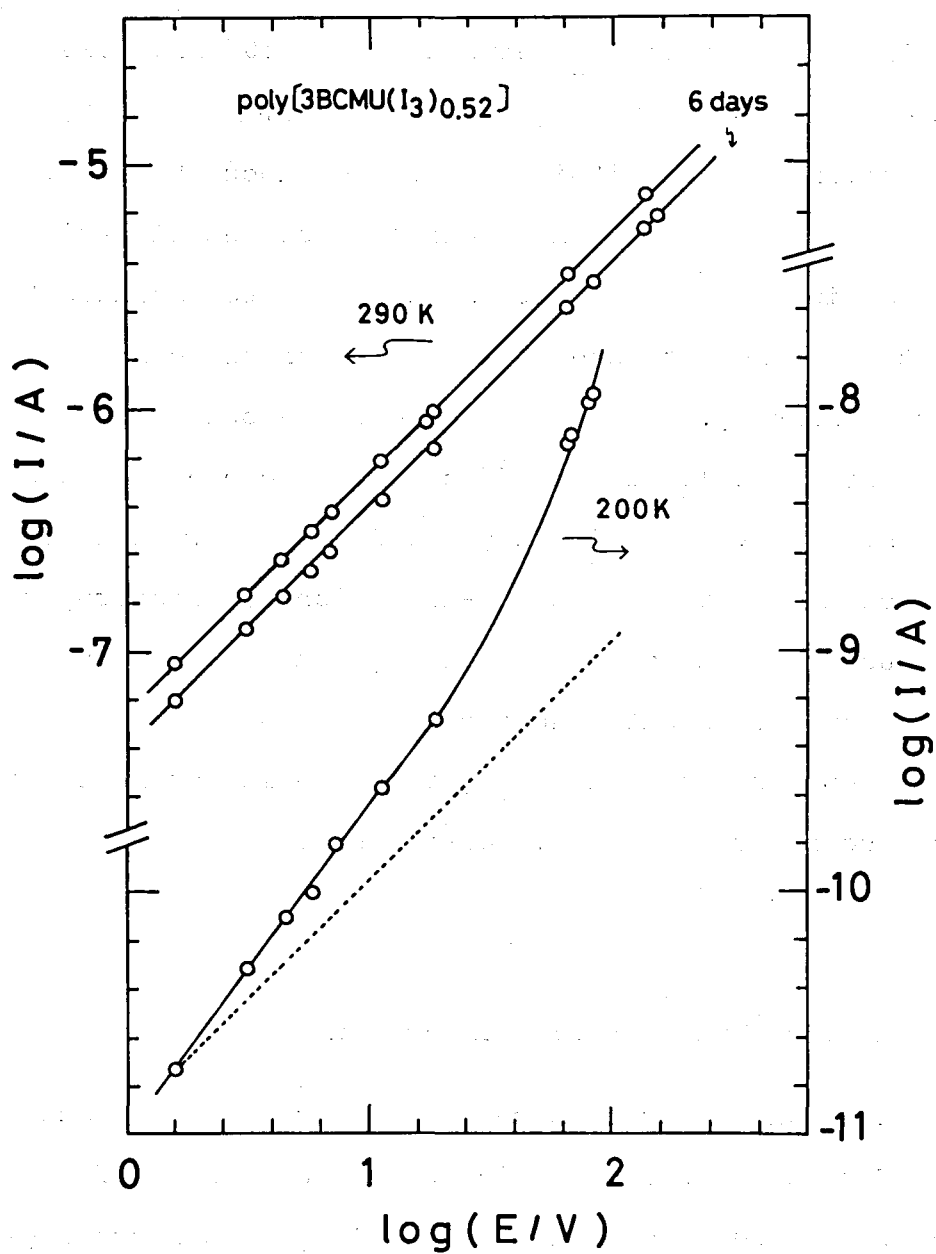
The characteristics of varieties of conduction

Figure 5-19. The I-V characteristics of poly[3BCMU(I$_3$)$_{0.52}$] at 290 K and at 200 K. The dashed line indicates an ohmic characteristics having a slope of one.

Table 5-4. Basic conduction processes in insulators.

Process	Voltage Dependence	Voltage and Temperature Dependence
Schottky Emission	$\log I \sim V^{1/2}$	$\log(I/T^2) \sim 1/T$
Frankel-Poole Emission	$\log(I/V) \sim V^{1/2}$	$\log I \sim 1/T$
Tunnel or Field Emission	$\log(I/V^2) \sim 1/V$	$I \sim \text{const.}$
Space-Charge Limited	$I \sim V^2$	$I \sim \mu(T)$
Ohmic	$I \sim V$	$\log I \sim 1/T$
Ionic Conduction	$I \sim V$	$\log(T I) \sim 1/T$

processes involved in insulators may be summarized as shown in Table 5-4. [E22] The Schottky emission process is thermionic emission across the metal-insulator interface or the insulator-semiconductor interface. The Frenkel-Poole emission is due to field-enhanced thermal excitation of trapped electrons into the conduction band. Since this process involves electrons in the trapped states with coulomb potentials, the process is virtually identical to that of the Schottky emission. The tunnel emission is due to field ionization of trapped electrons into the conduction band or due to electron tunneling from the Fermi level of the metal into the insulator conduction band. The tunnel emission process has the strongest dependence on the applied voltage but is essentially independent of temperature. The space-charge-limited current results from carriers injected into an insulator which has no compensating charges. At low voltage and high temperature, current is carried by thermally excited electrons hopping from one isolated state to the next. This mechanism yields an ohmic I-V relation which exhibits characteristic exponential dependence on temperature. The ionic conduction is similar to a diffusion process. The dc ionic conductivity decreases with time during the electric field is applied.

For a given insulator, each of these conduction processes may dominate in the particular ranges of

temperature and voltage. Also the process is not exactly
independent of one another. For example, the large space-
charge effect and the tunneling phenomenon were found to
be very similar to the Schottky type emission.

The current I of poly(nACMU)s in the low temperature
region is almost independent of temperature or shows
Arrhenius type dependence with a small activation energy.
Figure 5-20 shows I versus V plots for iodine doped
poly(3BCMU) based on the different mechanisms of conduction.
The experimental data do not satisfy the relation based
on the tunneling mechanism and field emission mechanism,
while they satisfy those based on the Schottky or Frenkel-
Poole emission mechanisms.

5-4-5. Molecular Schemes of Mechanism of Conduction

On the basis of the experimental evidences on the
conduction described so far together with the knowlegdes
on the structure-property relationships of iodine-poly-
(nACMU)s systems, we discuss in detail how the extra holes
may be produced in poly(nACMU) chains to exhibit electronic
conduction.

The fact that the T_g of poly(nACMU)s is increased by
iodine doping suggests that iodine molecules, at least
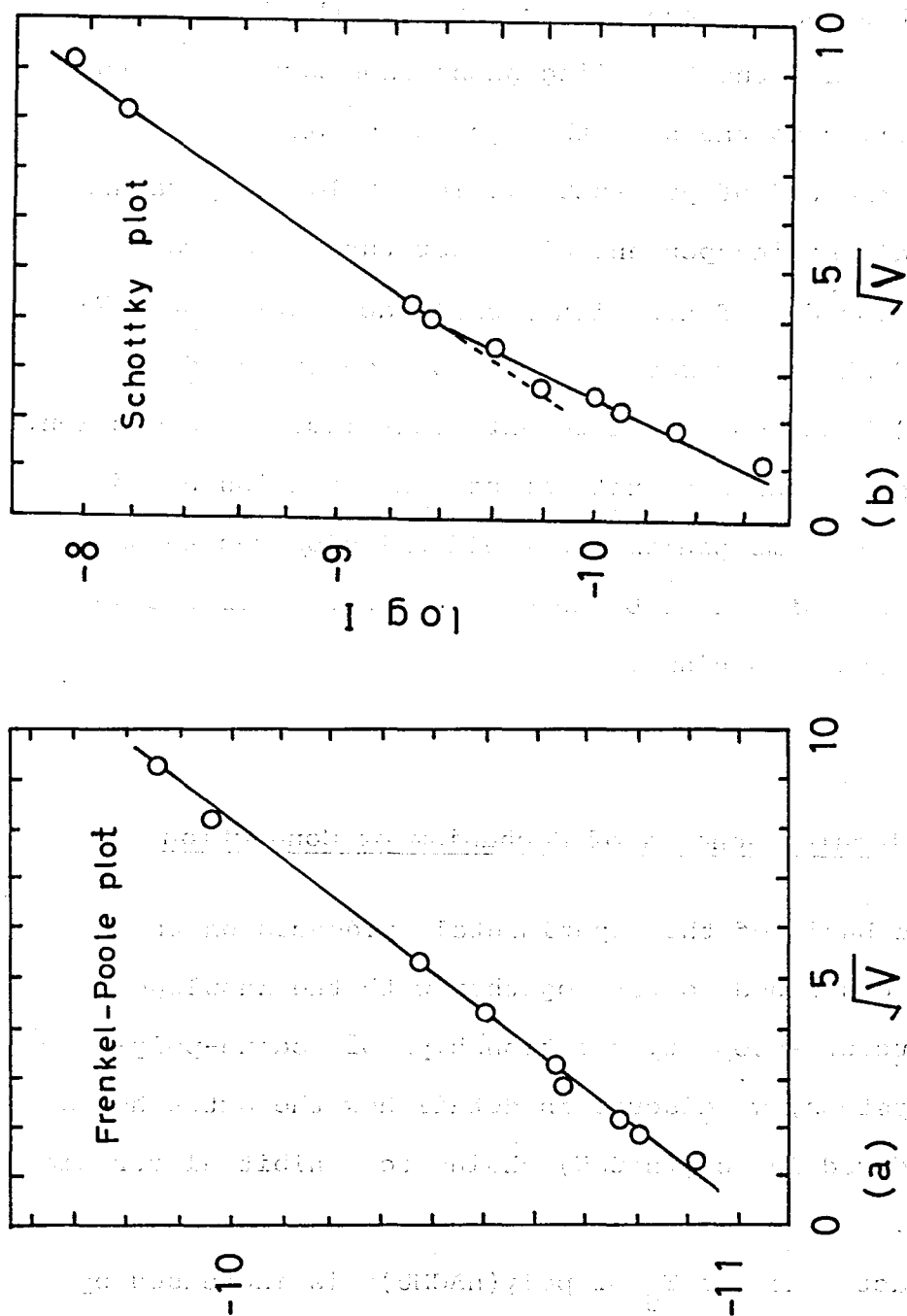some of them, coordinate with the conjugated chain back-

Figure 5-20. The I-V characteristics of poly[3BCMU(I_3)$_{0.52}$] in the voltage
range of 1 V to 150 V at 200K: (a) Frenkel-Poole Emission plot;
(b) Schottky Emission plot.

bones and withdraw electrons to become I_3^- and/or I_5^- ions. First way of production of the extra holes is that unpaired spins appear on isomerization from poly(ene) type to poly-(ene-yne) type or vice versa as the result of mobile bond-alternation domain wall, as shown in Figure 5-21-a. Such a localized unpaired electron called neutral soliton[E41-E43] may be a topological kink in the electron lattice system. Theoretical calculations also indicate that [E41, E44, E45] the electron state of the neutral soliton is located at the center of band gap. That is to say, since the unpaired electrons exist in the antibonding orbital which is located at the center of the band gap of the magnitude 2Δ, the ionization potential is the Δ smaller than the potential of high-occupied-molecular-orbital in the valence band and the potentials of their electron affinities are the Δ larger than the potential band, as shown in Figure 5-21-b. Therefore the iodine as dopant is thought to preferentially attack the neutral solitons located at higher electronic energy state. As shown in Figure 5-21-c, a localized hole is produced by the attack of iodine to an unpaired elec-tron, and the hole is called a charged soliton. [E43, E44]

The second way producing an extra hole is that the dopant accepts the electron from the regular bond-alternation structure as poly(ene) and/or poly(ene-yne) and the radical cation is produced on the conjugated chain, as shown in Figure 5-21-d. Since the phase of
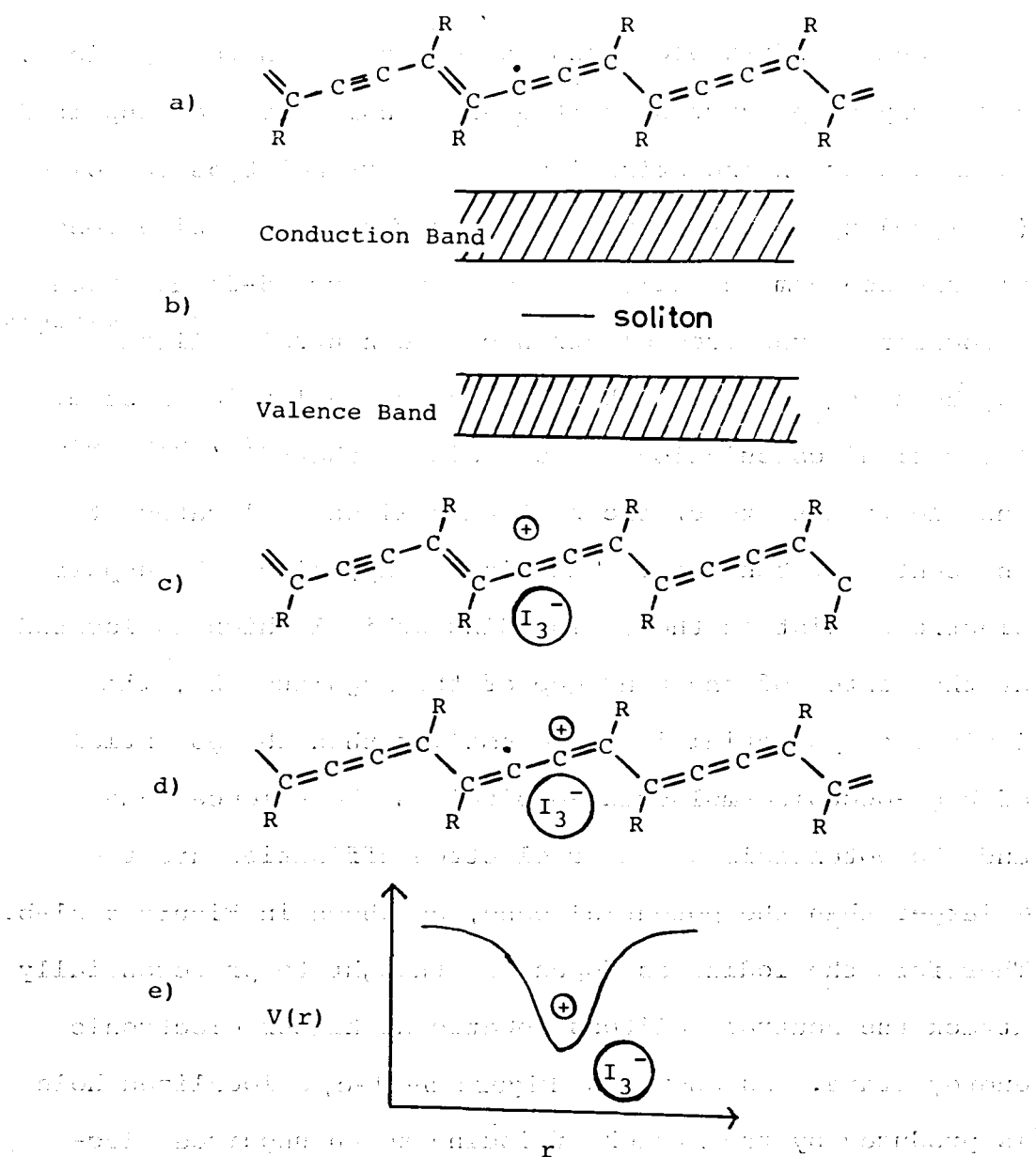
Figure 5-21. Schematic diagrams of I_3^- ion near a poly-diacetylene chain; (a) Neutral soliton defect in undoped polydiacetylenes; (b) Schematic energy diagram of a neutral soliton state; (c) a charged soliton kink and (d) a polaron after iodine-doping; (e) hole is bound by Coulomb potential $V(r)$ to the region of a chain near the iodine ion.

bond-alternation to both sides of such a radical cation

is identical to each other, it can not be regarded as

soliton. Such a radical cation may be considered as the

metastable excited-state produced on the conjugated chain.

This radical cation is called as polaron. [E45, E46] A

polaron as well as a charged soliton has a charge.

Although a charged soliton may be produced with a

lower energy than a polaron, the number of soliton may be

smaller than that of polaron. Therefore we can not con-

clude which ones of charged solitons or polarons are

dominant charge carriers in doped poly(nACMU) systems.

A dopant iodine molecule accepts an electron from

the poly(nACMU) chain and the extra hole produced on the

chain will be an empty space in valence band. A weak

Coulomb binding between the hole and charged acceptor

ion is produced. Such a bound state is the localized hole

on the polymer chain in the vicinity of the charged

acceptor ion. The binding energy may be dependent on tem-

perature and hence this scheme is qualitative agreement

with the experimental results.

Extra holes play the main role of conduction phenomena.

The most dominant process in the semiconductivity of doped

poly(nACMU)s appears to be the activation of charge car-

riers, i. e., the production of free holes from conjugated

backbones by dopant iodine and the transfer of the carriers

from one chain to another, presumably by hopping at high

temperature in the crystalline (ordered) regions and/or
in the amorphous regions through dopant iodine ions.

5-5. Conclusion

The direct-current conductivities σ_{dc} of undoped
poly(nACMU)s are of the order of 10^{-11} Ω^{-1} cm^{-1}, while the
doping with iodine enhanced the σ_{dc} by about 10^7 fold.
This result is the first demonstration of semiconductive
poly(nACMU)s. The ratio of the surface to volume conduc-
tivities for doped poly(nACMU)s is less than about 10 %,
and hence the enhanced conductivity is almost due to the
volume conduction. The activation energy E_a is virtually
unchanged by doping. The E_a in the high temperature region
is in the range of 1.07-0.98 eV mol^{-1} and the E_a in the low tem-
perature region is in the range of 0.033-0.008 eV mol^{-1}. The
alternating-current conductivity σ_{ac} varies with the fre-
quency as f^s with the value of s decreasing from 0.88 to
0.46 as the temperature is raised from 100 K to 285 K.
The σ_{dc} of iodine doped poly(3BCMU) increases with increas-
ing number-average molecular weight M_n, while the E_a
decreases with increasing M_n. We suggested an empirical
formula of the σ_{dc} as a function of Y, M_n and T. The
anisotropy in the conductivities $\sigma_{11}/\sigma_{\perp}$ of poly(4BCMU)

single crystals and that of oriented poly(3BCMU) films are about 6.4 and 4.2, respectively. At low dopant concentration, the σ_{dc} of poly(3BCMU) specimens doped by the solution method is 10^3 times larger than that by the vapor vapor method. TCNQ or TTF alone were not effective dopants for poly(nACMU)s. The σ_{dc} of poly[3BCMU(TTF/TCNQ)$_{0.068}$] at 18°C is 5.3 x 10^{-4} Ω^{-1} cm^{-1}. The conduction of poly(3KAU), whose conductivity is almost 5 x 10^{-4} Ω^{-1} cm^{-1}, is of ionic mechanism.

All evidences suggested that the conduction is mainly electronic. The main processes are the activation of charge carriers from dopant iodine to the conjugated backbones of poly(nACMU)s and the transfer of carriers from one chain to another. Dopant iodine withdraws electrons from the conjugated main chains to become ions, and hence extra holes such as charged solitons and polarons can be produced in the conjugated main chains. Such extra holes may play the essential role in the enhanced electronic conduction.

References

E1.   Street, G. G.; Clarke, T. C.   Synthetic Metals, 1980,
      1, 99-347.

E2.   Charles, B. D.; Schein, L. B.   Physics Today, 1980,
      February, 42.

E3.   Shirakawa, H.; Louis, E. J.; MacDiarmid, A. G.;
      Chiang, C. K.; Heeger, A. J.   J. Chem. Soc., Chem.
      Comm., 1977, 578.

E4.   Chiang, C. K.; Druy, M. A.; Fau, S. C.; Heeger, A.
      J.; Louis, E. J.; MacDiarmid, A. G.; Park, Y, W.;
      Shirakawa, H.   J. Am. Chem. Soc., 1978, 100, 1013.

E5.   Chiang, C. K.; Heeger, A. J.; MacDiarmid, A. G.;
      Ber. Bunsenges. Phys. Chem., 1979, 83, 407.

E6.   Patel, G. N.; Walsh, E. K.   J. Polym. Sci., Polym.
      Lett. Ed., 1979, 17,203.

E7.   Patel, G. N.; Chance, R. R.; Witt, J. D.   J. Chem.
      Phys., 1979, 70. 4387.

E8.   Se, K.; Ohnuma, H.; Kotaka, T.   Polymer J., 1982,
      14, 895.

E9.   Bhattacharjee, H. R.; Preziosi, A. F.; Patel, G. N.
      J. Chem. Phy., 1980, 73, 1478.

E10. Blythe, A. R., "Electrical Properties of Polymers",
      Cambridge Univ. Press., England, 1979.

E11. Uhlir, A. Jr.   Bell Systems Tech. J., 1955, 105.

E12. Valdes, L. B.,   Proc. Inst. Radio. Engrs, 1954, 42,
      420.

E13. Se, K.; Adachi, K.; Kotaka, T. Polymer J., <u>1981</u>, 13, 1009.

E14. Pochan, J. M.; Gibson, H. W.; Bailey, F. C. J. Polym. Sci., Polym. Lett. Ed., <u>1980</u>, 18, 447.

E15. Se, K.; Ohnuma, H.; Kotaka, T. Rept. Prog. Polym. Phys. Jpn., <u>1981</u>, 24, 209.

E16. Se, K.; Ohnuma, H.; Kotaka, T. Macromolecules, <u>1983</u>, 16, in press.

E17. Schermann, W.; Wegner, G. Macromol. Chem., <u>1974</u>, 175, 667.

E18. Chance, R. R.; Baughman, R. H. J. Chem. Phys., <u>1976</u>, 64, 3889.

E19. Lochner, K.; Reimer, B.; Bassler, H. Chem. Phys. Lett., <u>1976</u>, 41, 388.

E20. Day, D. R.; Lando, J. B. J. Appl. Polym. Sci., <u>1981</u>, 26, 1605.

E21. Diaconu, I.;Dumitrascu,; Simionescu, Cr. European Polym. J., <u>1980</u>, 16, 511.

E22. Sze, S. M., "Physics of Semiconductor Devices", John Willey and Sons, New York, <u>1969</u>.

E23. Inuishi, Y.; Hamakawa, Y.; Shirafuji, J.. "Handotai Bussei (Physical Properties of Semiconductors)", Asakura, Japan., <u>1977</u>.

E24. Se, K.; Adachi, H.; Kotaka, T. Rept. Prog. Polym. Phys., Jpn., <u>1982</u>, 22, 393.

E25. Se, K.; Ohnuma, H.; Kotaka, T. Rept. Prog. Polym.

Phys. Jpn., 1982, 25, 429.

E26.   Shirakawa, H.; Sato, M.; Hamano, A.; Kawakami, S.;
        Soga, K.; Ikeda, S. Macromolecules, 1980, 13, 457.

E27.   Lochner, K.; Reiwer, B.; Bassler, H. Chem. Phys.
        Lett., 1976, 41, 388.

E28.   Part, Y. W.; Druy. M. A.; Chiang, C. K.; MacDiarmid,
        A. G.; Heeger, A. J.; Shirakawa, H.; Ikeda, S.
        J. Polym. Sci., Polym. Lett. Ed., 1979, 17, 203.

E29.   Nakanishi, H.; Hashumi, K.; Mizutani, F.; Ichimura,
        K.; Fujishige, s.; Kato, M. Jpn. Chem. Soc. Prep.,
        1981, 44, II, 671.

E30.   Acker, D. S.; Harder, R. J.; Hertler, W. R.; Mahler,
        W.; Melby, L. R.; Benson, R. E.; Mochel, W. E.;
        J. Am. Chem. Soc., 1960, 82, 6408.

E31.   Wudl, f.; Smith, G. M.; Hufuager, E. J. J. Chem.
        Soc., Chem. Commun., 1970, 1453.

E32.   Engler, E. M., Chem. Tech., 1976, 6, 274.

E33.   Seanor, D., Ed., "Electrical Properties of Polymers",
        Academic Press, New York, 1982.

E34.   Kwak, J. F.; Clarke, T. C.; Green, R. L.; Street, G.
        B. Solid State Comm., 1979, 31, 355.

E35.   Park, Y. W.; Heeger, A. J.; Druy, M. A. J. Chem.
        Phys., 1980, 73, 949.

E36.   Shirakawa, H.; Ikeda, S. Synthetic Metals, 1980,
        1, 175.

E37.   Akaishi, T.; Miyasaka, K.; Ishikawa, K.; Shirakawa,

H., Ikeda, S. J. Polym. Sci., Polym. Phys., Ed.,
1980, 18, 745.

E38. Seeger, K.; Gill, W. D.; Clarke, T. C.; Street, G. B.
Solid State Commun., 1978, 28, 873.

E39. Gill, W. D. J. Apply. Phys., 1972, 43, 5033.

E40, Day, D.; Lando, J. B. J. Appl. Polym. Sci., 1981,
26, 1605.

E41. Su, W. P.; Schrieffer, J. R.; Heeger, A. J.; Phys.
Rev. Lett., 1979, 42, 1698.

E42. Chien, J. C. W.; Karasz, F. E.; Wnek, G. E. Nature,
1980, 390.

E43. Bernasioni, J.; Schneider, T., Ed., "Physics in One
Dimention", Proceeding of an International Conference.
Fribourg, Switzerland, August 25-29, 1980.
(Springer-Verlag, Berlin)

E44. Fincher, C. R. Jr.; Ozaki, M.; Heeger, A. J.,
MacDiarmid, A. G., Phys, Rev., 1979, 19,4140.

E45. Yamabe, T.; Akagi, K.; Ohzeki, K.; Fujii, K.;
Shirakawa, H. J. Phys. Chem. Solid, 1982, 43, 577.

E46. Kittle, C., "Introduction to Solid State Physics",
John Wiley and Sons, Ltd., New York, 1976.

E47. Ozaki, M.; A Doctoral thesis on, "Semiconductor and
Metallic Properties of Pure and Doped Polyacetylene",
Osaka Univ., Jpn. 1981.

Chapter 6

SEMICONDUCTOR PROPERTIES OF POLY(nACMU)S

6-1. Introduction

The emergence of conductive polymers [F1] as a new class
of semiconducting materials is of considerable interest
from the points of view of developing potentially low-cost
and easily processible materials for solar energy
conversion and other applications such as new types of
sensors and rechargeable organic batteries. [F2, F3]

We have demonstrated that doped poly(nACMU)s acquire
a substantial increase in conductivity due not to ionic
but to electronic mechanism. In particular, semiconductive
poly(nACMU)s are promising for the applicability for solar
cell materials and other devices because of the following
characteristics [F5]: (1) their light weights and easy
processibility due to solubility in organic solvent; (2)
their absorption spectrum close to the spectrum of sunlight,
as indicated in chapter 4; (3) their absorption coefficient
(10^4 - 10^5 cm^{-1}) larger than that of single crystalline
silicon; (4) the band gap, the twice of the apparent
activation energy of conductivity, of around 1.5 eV which

coincides with the wavelength of the maximum of the solar spectrum. (5) The band gap is unchanged by iodine-doping, while the conductivity is enhanced by 10^6 fold.

Solar cell devices of polyacetylene have been reported by Shirakawa et al., [F6, F7] Ozaki et al., [F8, F9] Tsukamoto et al., [F5, F10] and MacDiarmid et al. [F11, F12] In order to make use of polydiacetylenes as solar cell devices, we must investigate the photoconductivity of doped poly(nACMU)s and the possibility of forming Schottky barriers.

Furthermore we attempted to apply poly(nACMU)s to new type of physical sensors.

6-2. Theoretical Aspects of Semiconductor Devices

Before discussing polymeric semiconductor devices, we shall explain briefly a Schottky barrier device [F13] and some primitive concepts of solar cells [F14, F15] of inorganic compounds. When a semiconductor is in contact with a metal, the electron diffusion process depends on the work functions for the metals ϕ_m and the semiconductor ϕ_{ns} (n-type) or ϕ_{ps} (p-type).

When $\phi_m > \phi_{ns}$, electrons diffuse into the metal, lowing the Fermi level of the semiconductor and creating a depletion region near the interface. If electrons from

the semiconductor are to diffuse further into the metal,

they must overcome the diffusion potential, determined by

$\phi_m - \phi_{ns} > 0$. The result is a rectifying or blocking

contact. When $\phi_m < \phi_{ns}$, electrons of the metal diffuse

into the semiconductor, raising the Fermi levels. There

appears an Ohmic contact.

By similar analysis of p-type Schottky devices,

when $\phi_m < \phi_{ps}$, an Schottky barrier results. Thus, we have

the following rules.

$$\phi_{ps} > \phi_m \quad \overset{or}{} \quad \phi_{ns} < \phi_m \quad = \text{Schottky barriers}$$

$$\phi_{ps} < \phi_m \quad \overset{or}{} \quad \phi_{ns} > \phi_m \quad = \text{Ohmic barriers} \tag{6-1}$$

The dark current I_d from a Schottky device is given

by Eq. 6-2, F13

$$I_d = I_0 \left[\exp(eV/nkT) - 1\right] \tag{6-2}$$

where I_0 and V are the constant current and the applied

voltage, respectively, e is the electron charge, n is the

quality factor of the diode, and kT has the usual meaning.

This equation explains the rectifying behavior observed

in a Schottky diode. If one applied an appreciable reverse

bias (v < o) to the cell, the term exp(eV/nkT) becomes

negligible compared to 1 and the current I_d approaches to

the value $-I_0$. If an appreciable forward bias($v > 0$) is applied, then I_d becomes to $I_0 \exp(eV/nkT) \gg 1$. Figure 6-1 shows a typical dark current I_d vs. applied voltage V curve for an ideal Schottky diode.

Exposure of a semiconductor to light may produce a temporary increase in the number of free charge carriers, and the resulting extra current under the influence of applied potential is called photoconduction current. The photovoltaic cell generates photocurrent and this photo-current is offset by a Schottky diode forward dark current, as shown in Figure 6-1.

As shown in Figure 6-1, the Maximum output power p_{max} of a solar cell device is simply the product of the short-circuit current I_{sc} and the open-circuit voltage V_{oc}: $P_{max} = I_{sc} V_{oc}$. The output power V is the shaded area in the lower right quadrant of the photo-I-V curve in Figure 6-1. The fill factor FF is defined as

$$FF = IV / I_{sc} V_{oc} \qquad\qquad (6\text{-}3)$$

For an ideal generator FF = 1, whereas for typical photo-volatic devices the FF ranges from 0.2 to 0.95.

For most of organic materials, high-bulk large trap densities, recombination, etc., result in field-dependent and space-charge-limited effects that cause the photo-voltage and photocurrent output to be load-dependent.
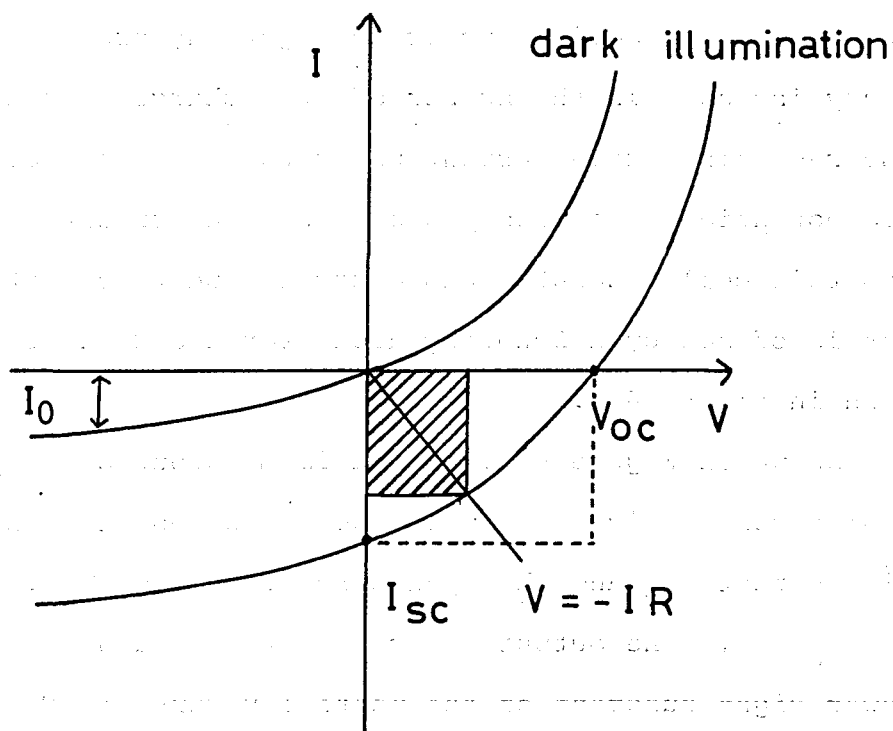
Figure 6-1. Schematic diagram for I-V characteristics of a Schottky device in the dark and under illumination.

6-3. Experimental Procedures

6-3-1. Materials

Poly(3BCMU) and poly(3KAU) samples were used in this
experiment. Films of 0.2-0.3 mm thickness and 2.5 μm
thickness were prepared from $CHCl_3$ solution of
poly(3BCMU)/0.09Mrad and poly(3BCMU)/15Mrad by evaporating
the solvent. Two doping procedures were used: iodine
doping was carried out by exposing poly(3BCMU) as-cast
films to the vapor, while doping with TCNQ, TTF, and their
complex TCNQ/TTF was made by co-casting $CHCl_3$ solution of
the polymer mixed with the dopant.

Poly(3KAU) films were cast from the aqueous solution.

6-3-2. Methods

For measuring time dependent photoconduction, we used
iodine-doped poly(3BCMU)/0.09Mrad film attached to 2-
terminal electrodes placed in a home-made glass cell. The
film was irradiated with a 0.5 mW cm^{-2} white light through
a glass plate, as shown in Figure 6-2-a.

The I-V characteristics of the devices were measured
by a circuit, as shown in Figure 6-2-b. Dry batteries
were used as the sources. The current I through the
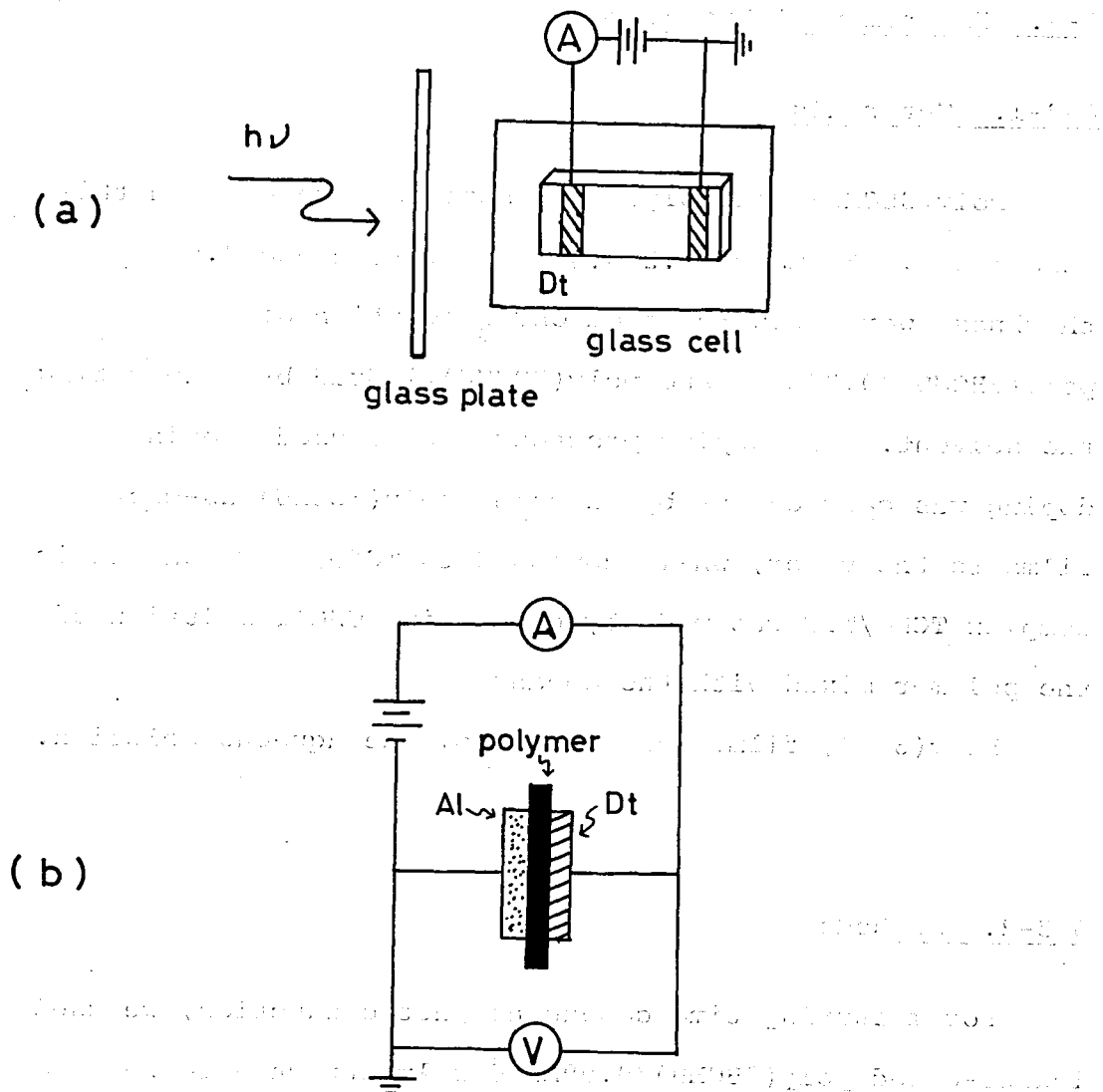circuit was measured by a Keithley 640 Electrometer and the

Figure 6-2. (a) The experimental setup for the photo-
conductivity measurement of doped poly(3BCMU) specimens
and (b) Schematic circuit diagrams for the I-V charac-
teristics measurements.

potential difference V between the devices was recorded by

a Keithley 610 Electrometer.

6-4. Results and Discussion

6-4-1. A simple demonstration of Photoconduction

Figure 6-3 shows time dependence of photocurrent

observed for iodine-doped poly[3BCMU(I_3)$_{0.52}$]. When the

light is off for the specimen under the potential of 1.5 v,

the current is about 0.086 μA. The dark conductivity σ_{dc}

is determined to 8.3 x 10^{-6} Ω^{-1} cm^{-1}. When the specimen

is exposed to white light having from a 0.5 mW cm^{-2} lamp,

the current increases rapidly to the level of 0.11 μA

within a minute, as shown in Figure 6-3. When the light

is off, the current decreases within a minite to the

initial dark current. This photoconduction phenomenon was

reversible and reproducible against the on-and-off of the

white light.

Because the specimen was placed in the special glass

cell and illuminated through a glass plate, the irradiation

with white light gave little thermal energy to the

specimen. This fact was confirmed by monitoring the

constancy of the temperature of the specimen by a copper-

constantan thermocouple during the experiment. Further,

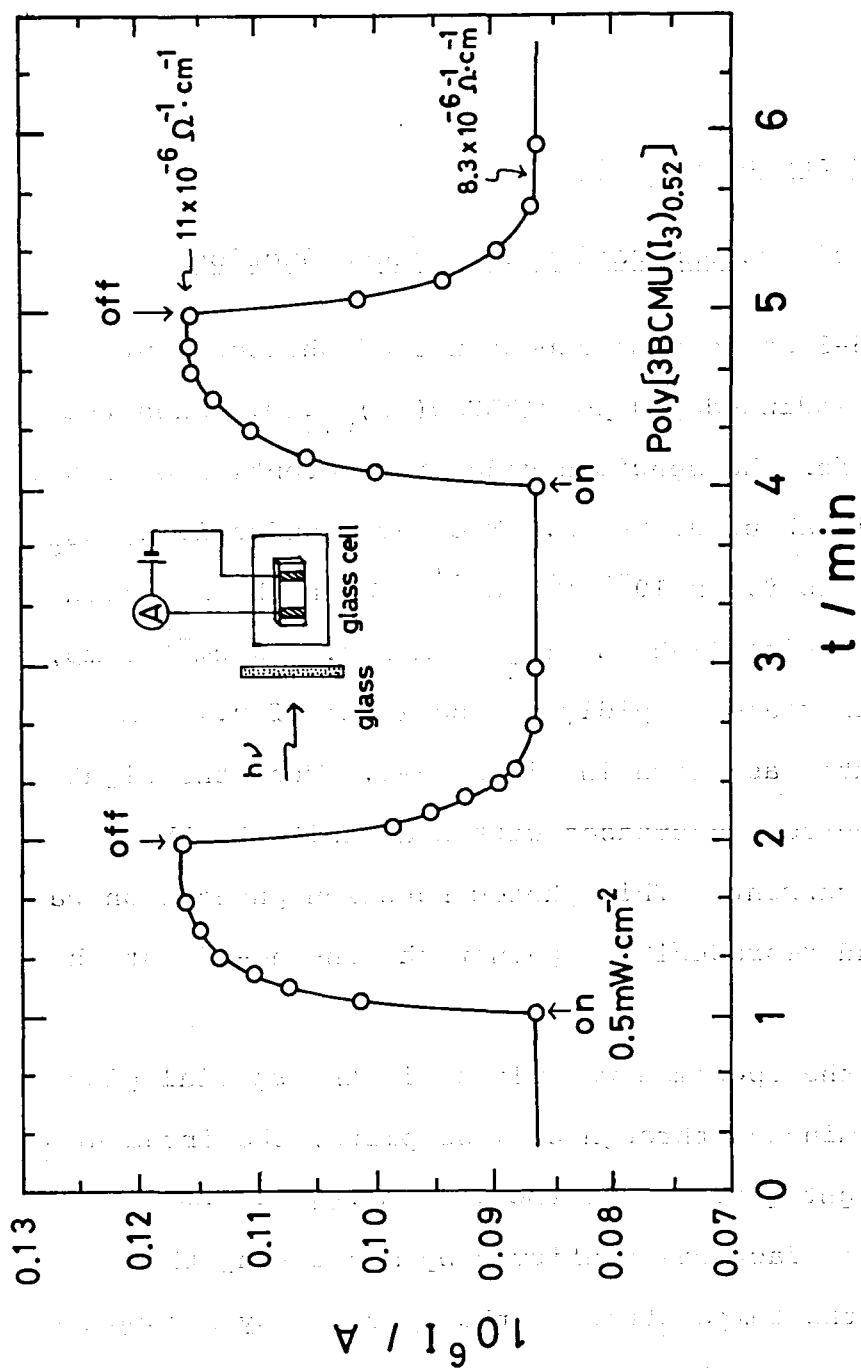the reversibility in the photoconduction suggests that

Figure 6-3. Photoconduction response of poly[3BCMU(I_3)$_{0.52}$] specimen upon turn-on and off of a 0.5 mW cm^{-2} lamp of white light.

the photocurrent is not due to any kinds of chemical reactions.

The photons can interact with the semiconductor in a variety of ways to generate carriers. [F12] The simplest process is the activation of an electrons directly from the valence band to the conduction band to give electron-hole pairs, therby enhancing the concentration of the intrinsic carriers. For this to be possible the photon energy must exceed the band gap and/or the threshold wavelength. The threshold also appears in the absorption spectrum where an absorption edge occurs at the frequency corresponding to the onset of electronic transition across the band gap. Generation of carriers by photon absorption, however, often proceeds in a more complex manner.

Rise and decay times of photoconduction was found to be slow in iodine-doped poly(3BCMU) because of their rather high resistivity and rather numerous trapping levels compared with inorganic semiconductors. It is worthwhile to note that this time dependence can be used to gain information about the conduction mechanism, kinetics and trap distribution in doped poly(3BCMU).

6-4-2. Rectifying Behavior of Schottky Diodes

To make a Schottky diode from doped poly(3BCMU), we employed aluminum Al as the metal electrode. There are three ways to form a Schottky contact between aluminum Al and doped poly(3BCMU): (1) Casting the polymer on Al sheet and then doping the specimen in vapor phase; (2) Compression molding of doped poly(3BCMU) films to Al sheet; and (3) depositing Al on doped poly(3BCMU) films. The last method was employed only in the case of nonvolatile dopants.

A Schottky device with Al and Dotite electrodes is indicated by Dt/poly[3BCMU(I_3)$_Y$]/Al here. The Electrode at the right hand side of the symbol is the cathode and that of the left side is the anode in the forward direction for these devices.

Casting of poly(3BCMU) on Al sheet: Al film was deposited on a slide glass by vacuum evaporation at the pressure of about 10^{-5} torr. On the Al film a thin poly(3BCMU) film of 12 µm thickness was formed by casting from $CHCl_3$ solution and then doped with iodine vapor. Two copper wires were attached with Dotite XC-12 to the Al electrode and to Dotite, as shown in Figure 6-4-a.

Devices of Dt/poly(3BCMU)/Dt, Dt/poly[3BCMU(I_3)$_{0.3}$]/Dt obeyed Ohmic rule on I-V characteristics in the voltage of
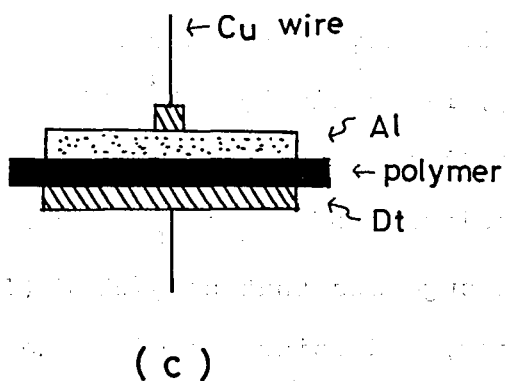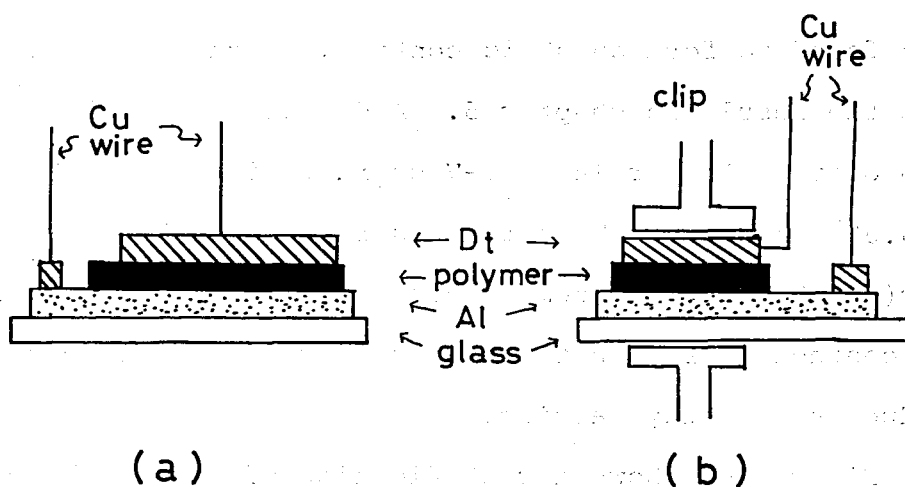
Figure 6-4. Schematic diagrams of Schottky barrier
devices: (a) forming as-cast film on Al sheet;
(b) compressing doped poly(3BCMU) film to Al sheet;
(c) Depositing Al on doped poly(3BCMU).

0.05 V and 7 V, listed in Table 6-1. Dotite electrodes were found to form an ohmic contact. Such a fact coincides with the result in chapter 5. A device of Dt/poly(3BCMU)/Al also obeyed ohmic rule on I-V characteristics in the range of 0.05 V and 7 V. This fact is reasonable because pure poly(3BCMU) is not a semiconductor but an insulator, and the contact surface between insulator and metal does not produce a Schottky barrier.

Figure 6-5 shows a rectification effect exhibited by a device of Dt/poly[3BCMU$(I_3)_{0.38}$]/Al. The forward bias direction of the device is in the case of Al electrode being cathode. Theories on semiconductors show that p-type and n-type Schottky barriers hold the relation of $\phi_{ps} > \phi_m$ and $\phi_{ns} < \phi_m$, respectively. [F13] The work function of Al metal is small compared to those of other metals. Therefore, we have a relation of $\phi_{ps} > \phi_m$ for our Schottky device. This result suggests that poly[3BCMU$(I_3)_{0.38}$] is a p-type semiconductor, and coincides with the conduction mechanism of free-extra holes mentioned in chapter 5. The rectification effect was significantly influenced by repetition of I-V measurements, as shown in Figure 6-5. The reason may be that the fresh aluminum-surface forming the rectification barrier is oxidized by iodine.

Table 6-1. I-V characteristics of poly(3BCMU) semiconductor devices.

Devices	I-V Characteristics
Dt/Poly(3BCMU)/Dt [a]	Ohmic
Dt/Poly[3BCMU(I_3)$_{0.3}$]/Dt [a]	Ohmic
Dt/Poly(3BCMU)/Al [a]	Ohmic
Dt/Poly[3BCMU(I_3)$_{0.38}$]/Al [a]	Schottky
Dt/Poly[3BCMU(I_3)$_{0.25}$]/Al [b]	non-Ohmic
Dt/Poly[3BCMU(TTF/TCNQ)$_{0.068}$]/Dt [c]	Ohmic
Dt/Poly[3BCMU(TTF/TCNQ)$_{0.068}$]/Al [c]	non-Ohmic
Dt/Poly[3BCMU(TTF)$_{0.68}$]/Dt [c]	Ohmic
Dt/Poly[3BCMU(TTF)$_{0.68}$]/Al [c]	Schottky

There are three ways to form a Schottky devices : a) casting, b) compression molding and c) depositing (see the text).
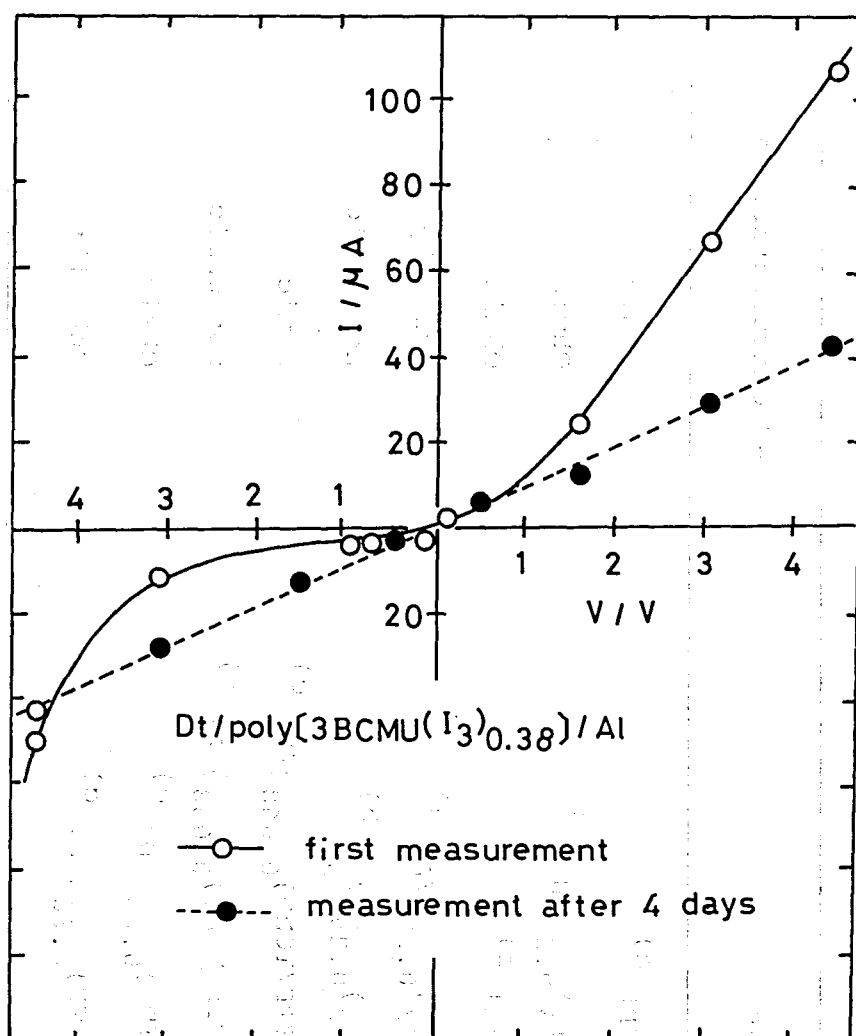
Figure 6-5. The I-V characteristics of a Schottky barrier of $Dt/poly[3BCMU(I_3)_{0.38}/Al]$ device. The dashed line indicates the I-V characteristics of a Schottky device after 4 days.

Compression Molding of Doped poly(3BCMU) to Al sheet:

In order to avoid the oxidation of aluminum by iodine, we
adopt a new procedure in making a Schottky barrier. Namely,
instead of doping of poly(3BCMU) after attaching to Al
film, doped poly(3BCMU) was pressed to Al film.
Experimental procedures were as follows: A poly(3BCMU)
film of 0.15 mm thickness doped with iodine was compressed
at a pressure of 20 kg/cm^2 onto an Al film which was
deposited in advance on a slide glass. Figure 6-4-b shows
a schematic diagram of this device.

The device of Dt/poly[3BCMU(I_3)$_{0.25}$]/Al made by
compression molding showed non-ohmic I-V characteristics
and did not show rectifying behavior. The contact between
doped poly(3BCMU) and Al film made by compression was
insufficient. The I-V curve did not pass the origin.
This device may produce some kinds of electromotive forces,
which can not respond to light. The V_{oc} and I_{sc} were 0.8 V
and 1 μA, respectively.

Depositing Al on Doped Poly(3BCMU): Iodine as dopant was
undesirable for Al electrode, and compressing of doped
specimen to Al film was not satisfactory to achieve a
complete surface contact. As a next step, we attempted
to form a Schottky barrier by using poly(3BCMU) doped
with charge transfer complexes.

The last device shown in Figure 6-4-c was the Al

electrode deposited on one side of a doped poly(3BCMU)
film by vacuum evaporation at about 10^{-5} torr. Dotite was
pasted on the other surface and Cu wires are connected to
form a circuit.

Poly[3BCMU(TCNQ)$_{0.43}$] film showed the conductivity of
only 3×10^{-9} $\Omega^{-1}cm^{-1}$. This value was too low to obtain
a satisfactory Schottky device. Poly[3BCMU(TTF/TCNQ)$_{0.068}$]
film had the conductivity of 3×10^{-5} $\Omega^{-1}cm^{-1}$. Hence,
we prepared a device of Dt/poly[3BCMU(TTF/TCNQ)$_{0.068}$]/Al.
As listed in Table 6-1, this device exhibited non-ohmic
I-V characteristics but did not give a satisfactory
rectifying behavior. On the other hand, a device of
Dt/poly[3BCMU(TTF)$_{0.68}$]/Al exhibited a rectification
characteristics, as shown in Figure 6-6. The device was
rather stable for repetition of I-V measurements, compared
with the device of Dt/poly[3BCMU(I$_3$)$_{0.25}$]/Al.

For doped poly(3BCMU) devices the quality factors n
in Eq. 6-2 was determined from semilogarithmic I-V
plots.[F15] For the devices mentioned above, the value
of n was found larger than 5. The quality factors of an
ideal Schottky diode and those of doped polyacetylene are
one and in the range of 3 and 4,[F7-F10] respectively.
Therefore, the rectification efficiency for the devices
of poly(3BCMU) specimens are not as good as
polyacetylene/Al devices.
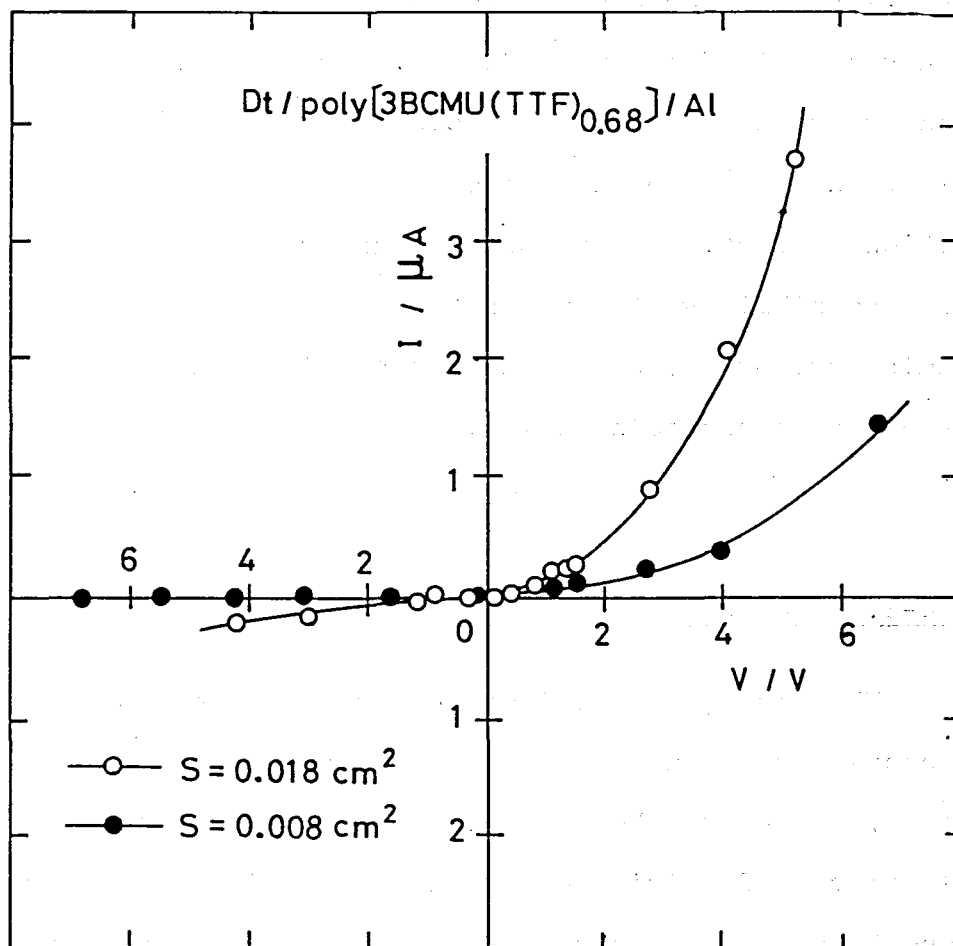
A successful formation of rectification devices,

Fifure 6-6. The I-V characteristics of a Schottky barrier of Dt/poly[3BCMU(TTF)$_{0.78}$]/Al two devices whose contact surface areas are different each other.

although the quality factor was very poor, revealed a superiority of an electronic conduction than an ionic conduction in doped poly(3BCMU), because any ionic conductors having high conductivity do not display electronic semiconductor properties such as the rectification effect. The results obtained suggest that there is a possibility of applying soluble polydiacetylenes to semiconductor devices such as rectification diodes, transistors and solar cells.

6-4-3. Application to Sensors

The employment of inorganic semiconductors for specific sensors have been attempted in recent years. [F16] In some cases, a sensor takes advantage of an abrupt change in electric conductivity due to an change in an enviromental condition. Such sensors need not be limited to inorganic semiconductors but should be extended to polymeric semiconductors.

We attempted to apply poly(3KAU) film as a thermo-sensor. A poly(3KAU) film was placed in a room under controlled temperature, where a commercial air-conditioner was in motion. By applying a potential of 25 V continuously to the specimen, the current through the specimen was recorded on a recorder. Figure 6-7 shows the change in
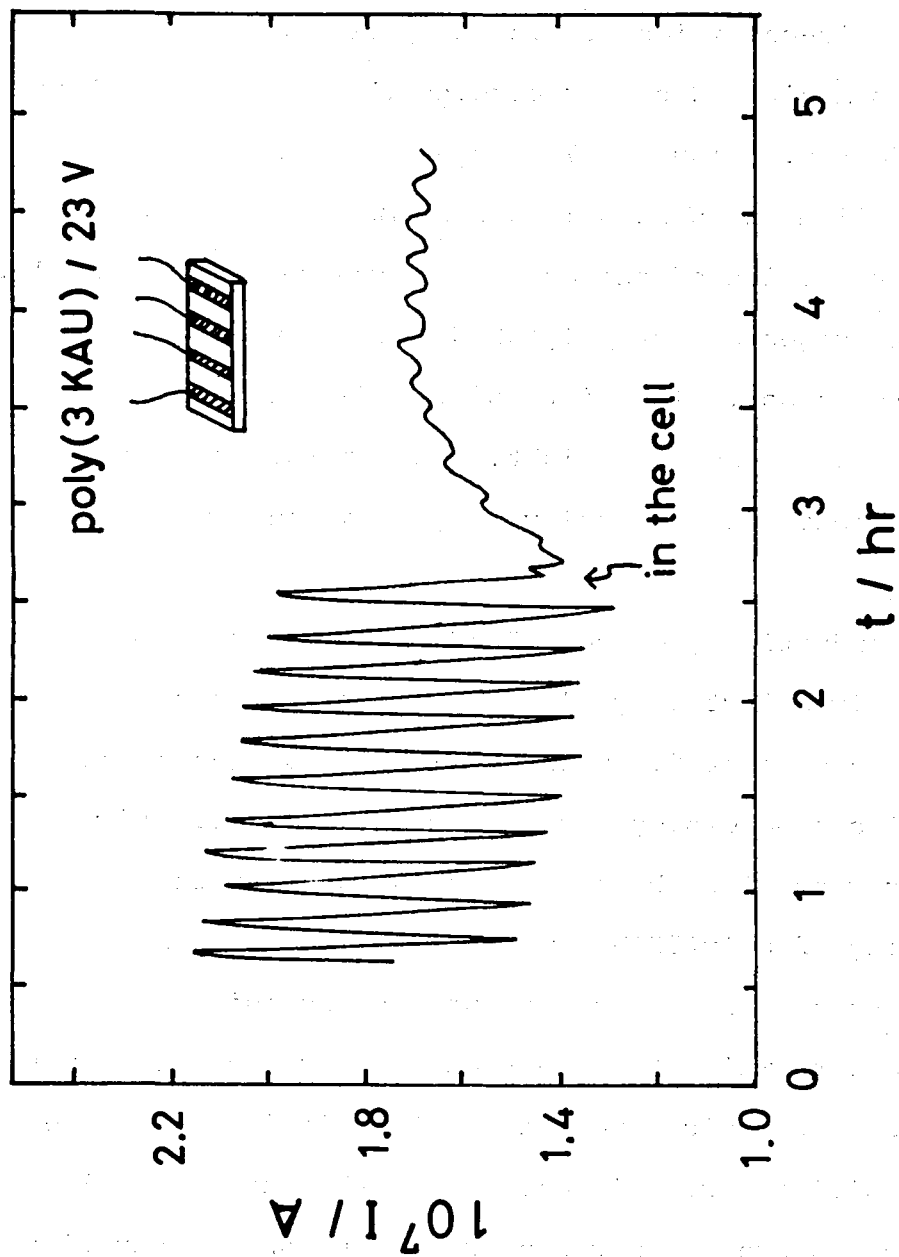
Figure 6-7. The changes in current for poly(3KAU) under a potential of 23 V. The specimen was placed in the room under controlled temperature.

the current versus time. It is seen that the current

runs zigzag across the graph paper. The time-period of

zigzag process coincides with that of the automatic on and

off of the air-conditioner. The temperature fluctuation

in the room monitored by a recording thermometer was less

than one degree. Figure 6-7 also shows that when a

poly(3KAU) film was placed in a home-made special glass

cell, the variation of the current became negligibly small.

The result suggests that poly(3KAU) film may be used as a

temperature sensor. The width of the current of the

current-change decreased slightly with time, presumably

because K^+ ions were gradually purged as mentioned in

chapter 5.

The conductivity of poly(3KAU) specimen was

significantly affected by slight moisture, as already

mentioned in chapter 5. This result also suggests that

poly(3KAU) can be employed as a humidity sensor. If we

can properly combine these factors influencing the

conductivity of poly(3KAU), we can utilize it as a

simulteneous sensor for temperature and humidity.

It is worthwhile to note that polymer sensors do not

require an electronic conduction. Certain ions sometimes

play a significant role in detecting the enviromental

changes, and hence polymer sensors of an ionic conduction

mechanism might be useful in detecting physical, chemical

and biological changes in the environment. Ions migrate

with difficulty in inorganic semiconductors, while they migrate with ease in polymers because inorganic compounds consist of ionic crystals and polymer compounds of molecular aggregates. Therefore polymer sensors might have an advantage over inorganic sensors in certain situations.

6-5.   Conclusion

A certain degree of photoconduction was observed in doped poly(3BCMU). This result suggests that photons interact with semiconductive poly(3BCMU) to generate carriers.

A device of Dt/poly[3BCMU(I_3)$_{0.38}$]/Al exhibited a rectification effect which was significantly influenced by repetition of I-V measurements. Furthermore, iodine-doped poly(3BCMU) was found to be a p-type semiconductor. Dt/poly[3BCMU(TTF)$_{0.68}$]/Al showed a stable rectification characteristics. The quality factor of doped poly(3BCMU) was larger than 5.

Doped poly(nACMU)s have following advantages: (1) the absorption spectrum is close to the solar spectrum, (2) photoconduction is observed and (3) Schottky barriers can be made. Thus, doped poly(nACMU)s might be appliable as solar cell devices.

Poly(3KAU) films exhibited conductivity changes
sensitive to moisture as well as temperature. Although
the conduction mechanism appear to be ionic, poly(3KAU)
films might be used as a multifunctional sensor to monitor
temperature and humidity simultaneously.

References

F1. Shirakawa, H.; Yamabe, T., Eds., "Gohsei Kinzoku (Synthetic Metals)" Kagaku Dojin, Kyoto, 1980.

F2. MacInnes, D, Jr.; Druy, M. A.; Nigrey, P. J.; Nairns, D. P.; MacDiarmid, A. G.; Heeger, A. J. J. Chem. Soc., Chem. Comm,. 1981, 317

F3. Chiang, C. K. Polymer, 1981, 22, 1454.

F4. Se, K.; Ohnuma, H.; Kotaka, T. Macromolecules, 1983, in press.

F5. Tsukamoto, J.; Ohigashi, H. Synthetic Metals, 1982, 4, 177

F6. Shirakawa, H.; Kobayashi, M.; Nagai, A.; Ikeda, S.; Shijime, I.; Konagai, K.; Takahashi, K. Polym. Prep., Jpn., 1979, 28, 467.

F7. Shirakawa, H.; Ikeda, S.; Aizawa, M.; Yoshitake, J.; Suzuki, S. Synthetic Metals, 1981, 4, 43.

F8. Ozaki, M.; Peebles, D. L.; Weinberger, B. R.; Chiang, C. K.; Heeger, A. J.; MacDiarmid, A. G. Appl. Phys. Lett., 1979, 35, 83.

F9. Ozaki, M.; Peebles, D. L.; Weinberger, B. R.; Heeger, A. J.; MacDiarmid, A. G. J. Appl. Phys., 1980, 51, 4252.

E10. Tsukamoto, J.; Ohigashi, H.; Matsumura, K.; Takahashi, A. Jpn. J. Appl. Phys., 1981, 20, L127.

E11. Chiang, C. K.; Heeger, A. J.; MacDiarmid, A. G. Ber. Bunsenges. Phys. Chem., 1979, 83, 407.

F12. Chen, S. N.; Heeger, A. J.; Kiss, Z.; MacDiarmid, A. G. Appl. Phys. Lett., 1980, 36, 96.

F13. Seanor, D. A., Ed., "Electrical Properties of Polymers", Academic Press, New York, 1982.

F14. Blythe, A. R., "Electrical Properties of Polymers", Cambridge Univ. Press., 1979.

F15. Tsubomura, H., "Hikari Denki Kagaku to Enerugi Henkan (Photoelectrochemistry and Energy Conversions)", Tokyo Kagaku Dojin, 1980.

F16. Yamamoto, N.; Tonomura, S.; Matsuoka, T.; Tsubomura, H. Surf. Sci., 1980. 92, 400.

Summary

Four different diacetylenes (R-C≡C-C≡C-R) having 4,6-
decadiyne-1,10-diol-bis(n-butoxy carbonyl methyl urethane)
(3BCMU), 4,6-decadiyne-1,10-diol-bis(ethoxy carbonyl methyl
urethane) (3ECMU), 3,5-octadiyne-1,8-diol-bis(n-butoxy
carbonyl methyl urethane) (2BCMU), and 5,7-dodecadiyne-1,
10-diol-bis(n-butoxy carbonyl methyl urethane) (4BCMU) as
substituents R were synthesized. Their crystallites were
exposed to ^{60}Co-γ ray at various doses to obtain the poly-
(n-methyl-alkoxy-carbonyl-methyl urethane)s [poly(nACMU)s],
respectively, coded as poly(3BCMU), poly(3ECMU), poly(2BCMU),
and poly(4BCMU).

PS-reduced molecular weights, M_n and M_w, of the poly-
(nACMU)s from GPC measurements were about the order of
$0.1 \times 10^6 - 1 \times 10^6$. Non-Newtonian intrinsic viscosities
of $CHCl_3$ and $CHCl_3$/n-hexane solutions of poly(3BCMU) were
compared. The result suggested that poly(3BCMU) assumes
a more extended, planar conformation in a poor solvent
$CHCl_3$/n-hexane than in a good solvent $CHCl_3$ in contrast to
ordinary flexible polymers in poor and good solvents.

The process of polymerization was observed as the
development of blue color. Changes in color of poly(3BCMU)
in $CHCl_3$ and n-hexane were compared. The critical solvent
compositions X_c and X_c' at which yellow-to-blue or blue-to-

yellow changes occurred, respectively, were independent of polymer concentration but varied with molecular weight and temperature. Visible absorption spectra and Raman spectra were compared for yellow $CHCl_3$ and blue $CHCl_3$/n-hexane solution of poly(3BCMU). Intramolecular hydrogen bonds between adjacent urethane moieties were found to be unstable in the solution between X_c and X_c'.

The effects of dopant iodine on the mechanical and electrical properties were examined in detail. The DSC, X-ray diffraction and mechanical studies indicated that poly(nACMU) films were semicrystalline, although the degree of crystallinity are usually low. Raman spectra indicated the presence of iodine in the forms of I_3^- and I_5^- in poly-(nACMU)s. The doping increased the glass transition temperature T_g as much as 27 K. An X-ray diffraction study suggested that the doping mostly occurs in the amorphous region.

The direct-current conductivity σ_{dc} of undoped poly-(nACMU)s was of the order of 10^{-11} $\Omega^{-1}cm^{-1}$, while the doping with iodine enhanced the σ_{dc} by about 10^7 fold. The σ_{dc} of doped poly(nACMU)s was found to obey Ohm's law. The activation energy E_a was virtually unchanged by doping but decreased abruptly at a certain temperature as T was decreased: The E_a in the high and low temperature regions were in the range of 1.07-0.98 eV mol^{-1} and 0.033-0.008 eV mol^{-1}, respectively. The substituent side groups affect-

ed the conductivity very little.

For seven poly(3BCMU) samples, the dependence of σ_{dc} on molecular weight was investigated in detail. The σ_{dc} was proportional to M_n at each dopant concentration Y. The E_a was proportional to M_n^{-1}, and extrapolated to 0.44 eV mol^{-1} at infinitely large M_n.

For single crystalline poly(4BCMU) specimens, the conductivities along the main chain (c'-axis) $\sigma_{/\!/}$ and along the chain stacking direction (b'-axis) $\sigma_{\perp}$ were measured. Also for stretched poly(3BCMU) specimens those in the directions parallel ($\sigma_{/\!/}$) and parpendicular ($\sigma_{\perp}$) to the stretch direction were measured. Anisotropy in the conductivities $\sigma_{/\!/}/\sigma_{\perp}$ of the single crystalline poly(4BCMU) and partially oriented poly(3BCMU) are 6.5 and 4.2, respectively.

All these evidences suggested that the conduction is mainly electronic, involving such processes as activation of charge carriers from dopant to the conjugated backbones of poly(nACMU)s and the transfer of the carriers from one chain to another. Dopant iodine withdraws electrons from the conjugated main chains to become ions. Extra holes produced are charged solitons and polarons. Extra holes may play the dominant role in enhanced conduction. We suggested an empirical formula for the σ_{dc} as a function of Y, M_n and T.

Besides iodine, 7,7,8,8-tetracyanoquinodimethane

(TCNQ), tetrathiafulvalene (TTF) and TCNQ/TTF complex were also tested as dopants. TCNQ and TTF were not effective, but TCNQ/TTF complex was found to be an effective dopant. The conductivity at 18°C of poly(3KAU), a KOH-hydrolyzed poly(3BCMU), was 5×10^{-4} $\Omega^{-1}cm^{-1}$ and its mechanism was ionic.

A certain degree of photoconduction was observed in doped poly(3BCMU). Devices of Dt/poly[3BCMU(I_3)$_{0.38}$]/Al and Dt/poly[3BCMU(TTF)$_{0.68}$]/Al showed a rectification effect. Poly(3KAU) films might be used as a multifunctional sensor to monitor temperature and humidity simultaneously.

List of Publications

The content of this thesis has been or will be published in the following papers and communications:

1. Poly(diacetylene derivative)s: Synthesis and Characteriszation of Poly(3BCMU).

   Se, K.; Ohnuma, H.; Kotaka, T.

   Rept. Progr. Polym. Phys., Japan, 1980, 23, 3.

2. Poly(diacetylene derivative)s: Structure and Electrical Properties of Poly(3BCMU).

   Se, K.; Ohnuma, H.; Kotaka, T.

   Rept. Progr. Polym. Phys., Japan, 1981, 24, 209.

3. Me de miru kohbunshi no kagaku hanno to butsuriteki henka

   Kotaka, T.; Se, K., Ohnuma, H.; Patel, G. N.

   Kagaku, 1981, 36, 811

4. Urethane Substituted Polydiacetylene: Synthesis and Characterization of Poly[4,6-decadiyn-1,10-diol bis(n-butoxy-carbonyl-methyl-urethane)].

   Se, K.; Ohnuma, H.; Kotaka, T.

   Polymer J., 1982, 14 895.

5. Poly(diacetylene derivative)s: Structure and Electrical
    Properties of Some Urethane Substituted Polymers.
    Se, K.; Ohnuma, H.; Kotaka, T.
    Rept. Progr. Polymer. Phys., Japan, 1982, 25, 423.

6. Poly(diacetylene derivative)s: Electrical Conductivity
    of Amorphous and Single Crystalline Poly(4BCMU).
    Ohnuma, H.; Inoue, K.; Se, K.; Kotaka, T.
    Rept. Progr. Polym. Phys., Japan, 1982, 25, 427.

7. Poly(diacetylene derivative)s: Effect of Molecular
    Weight on Conductive Properties of Poly(3BCMU).
    Se, K.; Ohnuma, H.; Kotaka, T.
    Rept. Progr. Polym. Phys., Japan, 1982, 25, 429.

8. Urethane Substituted Polydiacetylenes: Structure and
    Electrical Properties of Poly[4,6-decadiyn-1,10-diol
    bis(n-butoxy-carbonyl-methyl-urethane)].
    Se, K.; Ohnuma, H.; Kotaka, T.
    Macromolecules, 1983, 16, in press.

9. Electrical Conductivity of Oriented Films of Poly[4,6-
    decadiyne-1,10-diol bis(n-butoxy-carbonyl-methyl-
    urethane)].
    Ohnuma, H.; Hasegawa, K.; Se, K.; Kotaka, T.
    Rept. Progr. Polym. Phys., Japan, 1983, 26, in press

10. Urethane Substituted Polydiacetylene: electrical
    Conductivity of Poly[5,7-dodecadiyn-1,12-diol
    bis(n-butoxy-carbonyl-methyl-urethane)] in an
    Amorphous and Single Crystalline Forms.

    Ohnuma, H.; Inoue, K; Se, K.; Kotaka, T.

    Macromolecules, 1983, 16, in press.

11. Electrical Conductivity of Urethane Substituted
    Poly(diacetylene)s: Effect of Substituent Side Groups
    and Molecular Weights

    Se, K.; Ohnuma, H.; Kotaka, T.

    Macromolecules, 1983, submitted

Other Related Papers

1. Dielectric Behavior of Poly(ethylene oxide)s and
   Poly(ethylene oxide)-Polystyrene-Poly(ethylene oxide)
   Block Copolymers.

   Se, K.; Adachi, K.; Kotaka, T.

   Rept. Progr. Polym. Phys., Japan, 1979, 22, 393.

2. Thermal-Depolarization-Current Study of Poly(ethylene
   oxide)-Polystyrene-Poly(ethylene oxide) Block
   Copolymers.

Se, K.; Kotaka, T.

Rept. Progr. Polym. Phys., Japan, 1979, 22, 397.

3. Dielectric Relaxation in Poly(ethylene oxide):

    Dependence on Molecular Weight.

    Se, K.: Adachi, K.; Kotaka, T.

    Polymer J., 1981, 13, 1009.

Acknowledgements

This work has been performed under the direction of Professor Tadao Kotaka, Department of Macromolecular Science, Faculty of Science, Osaka University. The author would like to express his sincere gratitude to Professor Tadao Kotaka for his cordial guidance and discussions, and intimate encouragements throughout his course of study.

Thanks are tendered also to Assistant Professor Hiroshi Ohnuma for his kind guidance and close collaboration throughout the course of this research.

Special thanks are extended to Professor Emeritus Masato Nakagawa and Dr. Masahiko Iyoda, Chemistry Department, Faculty of Science, Osaka University, for the diacetylene synthesis; Professor Koichiro Hayashi and Dr. Sachio Yamamoto, Institute of Scientific and Industrial Research, Osaka University, for the radiation polymerization; Professors Hiroshi Tsubomura and Naoto Yamamoto, Department of Synthetic Chemistry, Faculty of Engineering Science, Osaka University, for the measurements of visible absorption spectra.

The author is greatly indebted to Professors Akira Takahashi and Tadaya Kato, Department of Industrial Chemistry, Faculty of Engineering, Mie University, for the measurement of refractive index increments of colored solutions; Professor Hideki Shirakawa, Institute of

-223-